Fall 2010

Optimization of parameters and study of kinetics in lactulose production by lactose isomerization using strong basic anion exchange resin

Arvind Nanduri

OPTIMIZATION OF PARAMETERS AND STUDY OF KINETICS IN LACTULOSE PRODUCTION BY LACTOSE ISOMERIZATION USING STRONG BASIC ANION EXCHANGE RESIN

by

ARVIND NANDURI

A THESIS

Presented to the Faculty of the Graduate School of the

MISSOURI UNIVERSITY OF SCIENCE AND TECHNOLOGY

In Partial Fulfillment of the Requirements for the Degree

MASTER OF SCIENCE IN CHEMICAL ENGINEERING

2010

Approved by

Dr. Oliver C. Sitton, Advisor
Dr. V. A. Samaranayake
Dr. Neil. L. Book

ABSTRACT

In this work, an experimental design was employed to investigate the effects of different operating conditions on the isomerization of lactose to lactulose by using strong basic anion exchange resin (AMBERLITE-IRA 402). Temperature, resin/lactose mass ratio and pH were considered to be the three factors affecting the conversion of lactose. Box-Behnken design was then used to optimize the operating conditions for maximum response and also to study the various interaction and main effects of the factors. The analysis of variance (ANOVA) of the experimental data showed a high correlation coefficient R^2 (0.99) and a low root mean square error (2.84) values for the second order regression model for the experimental design, indicating the good predictive nature of the model. The results gave an operating condition of temperature = 80.8^0C, resin/lactose mass ratio = 0.371 and pH = 10.3 for maximum response.

A kinetic model was deduced on the basis of Langmuir-Hinshelwood-Hougen-Watson formulation and the experimental data was later fit to the model by using least square approximation to estimate the activation energy (E_a), pre-exponential factor (A_0) and the adsorption coefficient (K_1). The effect of resin bead diameter was also studied and the results indicated that the bead diameter of the as-received resin is sufficiently small to eliminate internal diffusion resistances. The parameter estimation resulted in an activation energy of E_a= 19.5 $\frac{\text{kJ}}{\text{mole of lactose}}$ and pre-exponential factor of A_0 = 4.91 x 10^7 $\frac{1}{\text{hr}}$ at pH = 9, A_0 = 7.69 x 10^7 $\frac{1}{\text{hr}}$ at pH = 10 and A_0 = 13.3 x 10^7 $\frac{1}{\text{hr}}$ at pH = 11.

ACKNOWLEDGEMENTS

This thesis would have been well-nigh impossible without the support and guidance of my advisor, Dr. Oliver C. Sitton. I would like to forward my deepest gratitude to my advisor for motivating me with his perpetual energy and enthusiasm in research. In addition, he has always been accessible to help me with my research.

I would like to thank Dr. Neil Book and Dr. V. A. Samaranayake for being on my thesis committee. In particular, I was delighted to interact with Dr. V. A. Samaranayake by attending his classes and his insights to statistical analysis and experimental design helped me immensely in my research.

I would like to thank Bhatia, Unni, Kande, Rama, Nikhare, Ekta, Kothari and Aumi for their friendship and support. In particular, I would like to thank Sindhu Marella for her friendship, love and emotional support for the past five years.

I am indebted to my father, Dr. Pratap Nanduri, mother, Mrs. Radha Nanduri, and my brother, Aditya, for their unconditional love and support through the thick and thin of my life.

Last but not least, thank you God for giving me a wonderful life.

TABLE OF CONTENTS

Page

LIST OF FIGURES

Figure Page

LIST OF TABLES

Table Page

NOMENCLATURE

Symbol	Description
A_0	Pre-exponential factor (1/hr)
C_{As}	Surface concentration of the species A (gmoles/dm^3)
D_e	Effective diffusivity (dm^2/sec)
E_a	Activation energy (k J/g)
K_1	Adsorption equilibrium constant of lactose
K_3	Desorption equilibrium constant of lactulose
k_2	Surface reaction rate constant $\left(\frac{\text{g of lactose}}{\text{L hr}}\right)$
R_0	Total number of active sites on AMBERLITE IRA-402 resin
R_a	Total number of active sites in 1 g of AMBERLITE IRA-402 resin $\left(\frac{\text{g equivalents}}{\text{g of resin}}\right)$
L	Concentration of lactose (g/L)
Lu	Concentration of lactulose (g/L)
L_i	Initial concentration of lactose (g/L)
L_f	Final concentration of lactose (g/L)
M_A	Actual rate of the reaction
n	Overall reaction order
$-r_A'$	Rate of disappearance of A per unit area of the catalyst surface (gmoles A/m^2.sec)
$-r_L$	Rate of disappearance of lactose per unit volume (g/L.hr)
r_{Lu}	Rate of generation of lactulose per unit volume (g/L.hr)
S_a	Surface area per unit mass of catalyst (m^2/g)

w	Weight of AMBERLITE IRA-402 used for isomerization (g)
ρ	Density (g/cm^3)
η	Internal effectiveness factor
Φ	Thiele modulus
λ	Dimensionless distance (r/R)
φ	Dimensionless concentration (C_A/C_{As})

1. INTRODUCTION

The annual cheese production in the United States is approximately 8 billion pounds (Malinda, 2010). The liquid remaining after curdling milk with rennet or acid in the beginning steps of cheese manufacture is whey. The dairy industry produces approximately 9 pounds of whey for each pound of cheese produced. The whey contains lactose, proteins and several glycoproteins. There is considerable incentive to separate the whey stream into its sugar and protein fractions for sale into human and animal feeds. For a number of years the industry produced purified lactose and whey proteins from these materials for sale into a developing market for nutritional foods. Whey proteins are a main staple in the nutritional supplements market and demand a premium price. The disaccharide, lactose (4-O-β-D-galactopyranosyl-D-glucose), is both a human and animal feed material. A significant number of the world's population suffers from lactose intolerance due to a metabolic inefficiency to hydrolyze lactose to glucose and galactose which are easily absorbed into the blood stream. This limits the use of lactose in a number of nutritional supplements. The price for lactose is quite low in comparison to whey protein; lactose constitutes a disposal cost particularly from low concentration permeate streams (Tatdao Paseephol, Darryl M. Small, Frank Sherkat, 2007).

More recent research and market development show enhanced nutritional benefits from specific proteins, glycoproteins and sugars found in whey. Several specific whey proteins indicate the ability to lower blood pressure (Alan B. Boscoe, Charles R. Listow, 2008). Other specific proteins appear to stimulate insulin release for the treatment of type 2 diabetes (B. Ahren, P. J. Havel, G. Pacini, K. Cianflone, 2003). Several sugars derived

from lactose appear to enhance the formation of beneficial microflora in the human gut (Schumann, 2002). Lactulose (4-O-β-D-galactopyranosyl-D-fructose) is a non-absorbable sugar that increases the water content and volume of the stool in the gut, thereby aiding severe cases of constipation. Certain beneficial bacteria in the gut can metabolize lactulose to short chain fatty acids like lactic and acetic acids, which lower the gut pH thereby converting free ammonia to non-absorbable ammonium ion. This is the primary treatment for hepatic encephalopathy. Because of the potential revenue from these products, the dairy industry is adapting to produce specific purified proteins and specialized carbohydrates, like lactulose, from its whey streams. Lactulose production from lactose is one focus because of the increasing applications as a pharmaceutical for the treatment of chronic constipation and as a prebiotic food additive (Schumann, 2002). Continued consumption of lactulose may select for the beneficial bacteria in the gut microflora.

Alkaline treatment of lactose causes the isomerization of the glucose moiety of lactose to the fructose moiety in lactulose via the Lobry de Bruyn–Alberda van Ekenstein transformation employing either homogeneous or heterogeneous catalysts. Calcium hydroxide (Montgomery and Hudson,1930), sodium hydroxide (Dendene, Guihard, Nicolas and Bariou, 1994; De Haar and Pluim, 1991; Deya and Takahashi, 1991; Nagasawa, Tomita, Tamura, Obayashi, and Mizota, 1974; Zokaee, Kaghazchi, Soleimani, and Zare, 2002a; Zokaee, Kaghazchi, Zare, and Soleimani,2002b), potassium hydroxide and carbonate (Nagasawaet al., 1974), magnesium oxide (Carobbi, Miletti, and Franci, 1985), tertiary amines (Parrish, 1970), borates (Carubelli, 1970; Hicks, 1981; Kozempel

and Kurantz,1994; Kozempel, McAloon, and Roth, 1997; Krumbbolz and Dorscheid, 1991; Mendicino, 1960; Zokaee et al., 2002a; Zokaee et al., 2002b), and sodium aluminate (Carobbi and Innocenti, 1990; Guth and Tumerman, 1970; Tumerman and Guth, 1974; Zokaee et al., 2002a, 2002b) have been employed as homogeneous catalysts to obtain lactulose. Zeolites (Shukula, Verykios, and Mutharasan, 1985) and sepiolites have been proposed as heterogeneous catalysts for lactose isomerization into lactulose (de laFuente, Jua´rez, de Rafael, Villamiel, and Olano, 1999; Troyano, de Rafael, Martinez-Castro and Olano, 1996; Villamiel, Corzo, Foda, Montes, and Olano, 2002). Most of these processes cause a high level of undesirable side products, which are difficult to remove from lactulose syrup. For industrial production, degradation products should be avoided or at least kept to a minimum. The presence of monosaccharide and lactose is especially undesirable for medical purposes and requires an additional separation step.

A recent work includes an approach which uses strong anion exchange resins as heterogeneous catalyst (Lodygina A. D, Evdokimov I. A, Ryabtseva S. A, Lodygin A. D and Abakumov N. N, 2005; Russian patent 2101358). This approach eliminates the removal of the homogeneous catalyst in a downstream processing step and may offer more precise control of the residence time, which may lead to reduced degradation products. This work aims to extend the previous work and develop a kinetic model describing the isomerization of lactose to lactulose using a strong anion exchange resin as catalyst.

1. BACKGROUND

The sections below give an overview of the lactose isomerization mechanism, the molecular transport issues associated with a heterogeneous catalyst and the kinetic model used for the reaction.

2.1 CHEMISTRY OF LACTULOSE PRODUCTION

In alkaline media, the isomerization of lactose (Figure 2.1) to lactulose (Figure 2.2) follows the mechanism of Lobry de Bruyn-van Ekenstein (Mohammed Aider and Damien de Halleux, 2007). The Lobry de Bruyn-van Ekenstein transformation proceeds through an enediol intermediate of the aldose or ketose having hydrogen at the α-carbon (Momcilo Miljkovic, 2010). The α-carbon in the glucose moiety of lactose can be seen in Figure. The C-H bond on the α-carbon breaks easily in alkaline media leading to its isomerization to fructose. The enediol intermediate occurs when a double bond forms between carbons 1 and 2 in the glucose moiety during the transformation as shown in Figure 2.3. The enediol intermediate, Figure 2.4, then undergoes rearrangement, Figure 2.5, to form lactulose. The general reaction would be $\text{Lactose} + OH^- \rightleftharpoons \text{Enediol} \rightleftharpoons \text{Lactulose}$. The reaction requires proton acceptors during lactose isomerization and this is achieved by having an alkaline medium. The pretreated strong anion exchange resin AMBERLITE IRA-402 will provide proton acceptors in the form of hydroxyl (OH^-) ions during the isomerization. The hydroxyl ion on the resin would be replenished by the water molecule generated in the enediol formation step, Figure 2.5. The cleavage of the α-carbon and hydrogen bond would be faster at high pH values leading to high reaction

rates. High pH values of the reaction medium would also help in replenishing the hydroxyl ion on the resin to complete the catalytic reaction cycle.

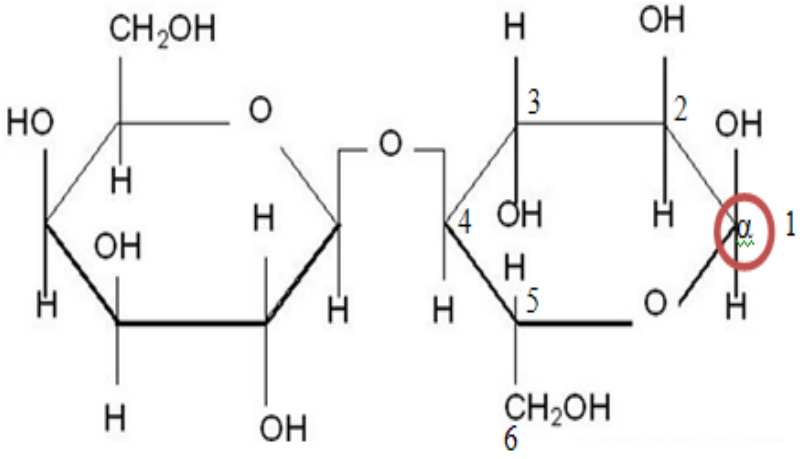

Figure 2.1. Schematic Representation of the Lactose Molecule.

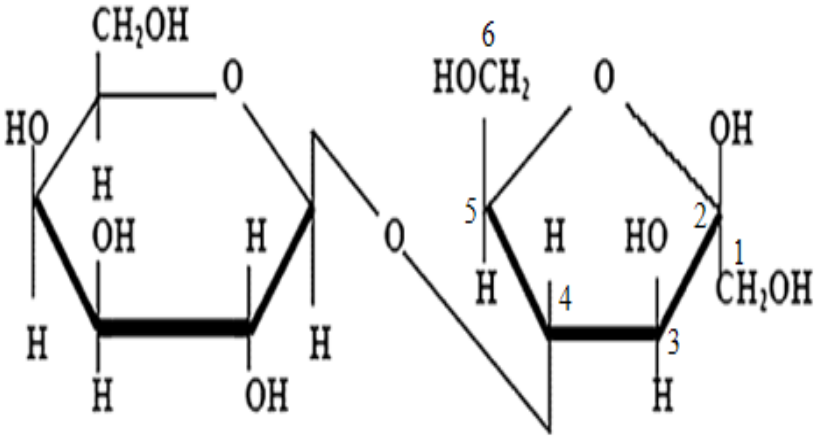

Figure 2.2. Schematic Representation of the Lactulose Molecule.

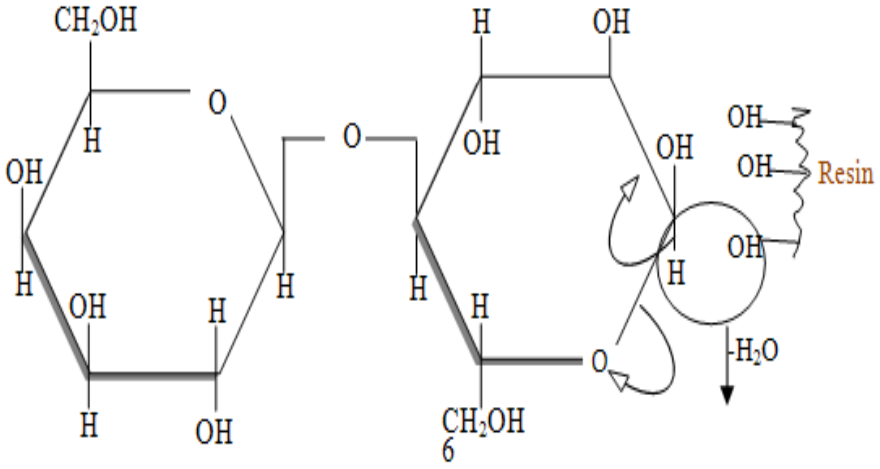

Figure 2.3. Formation of the Enediol Intermediate.

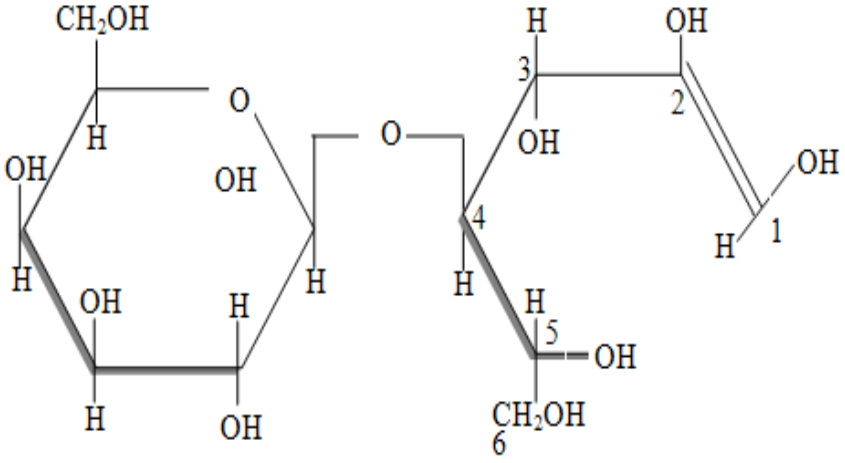

Figure 2.4. Schematic Representation of the Enediol Intermediate.

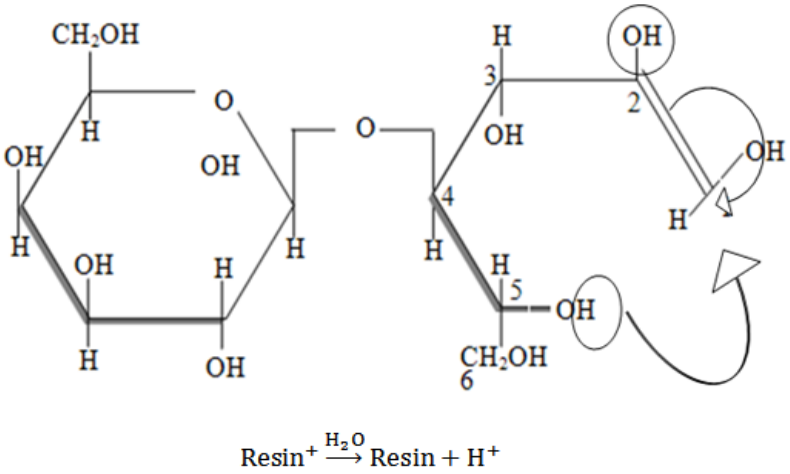

Figure 2.5. Schematic Representation of the Rearrangement in the Enediol Intermediate and Completion of the Catalytic Cycle.

2.2 DIFFUSION RESISTANCES IN HETEROGENEOUS CATALYTIC REACTIONS

During the isomerization reaction, the lactose molecules experience external and internal diffusion resistance in the presence of the resin. The lactose molecules initially have to diffuse from the bulk phase to the surface of the catalyst. If the concentration of lactose in the bulk phase is C_b and on the surface of the catalyst is C_{As}, then the external diffusion resistance causes a gradient between these two concentrations. This resistance could be eliminated if the conditions on the catalyst surface are the same as that in the bulk phase. This is achieved by creating turbulence, using a stirrer, in the medium. Figure 2.6 and Figure 2.7 show the external diffusion resistance experienced by the lactose and lactulose molecules. Similarly, the lactose and lactulose molecules experience internal diffusion resistance while diffusing both into and out of the catalyst pore. Figure 2.8 and

Figure 2.9 show the internal diffusion resistance experienced by the lactose and lactulose molecules.

It is highly essential to eliminate the internal and external diffusion resistances as the rate of reaction will contain the effects of the mass transfer parameters, which is not desired (Maryam Mohagheghi, Gholamreza Bakeri, Maryam Saeedizad, 2007). The internal effectiveness factor (η) and the Thiele modulus (Φ) are two dimensionless numbers that capture the effects of these resistances (H. Scott Fogler 2001).

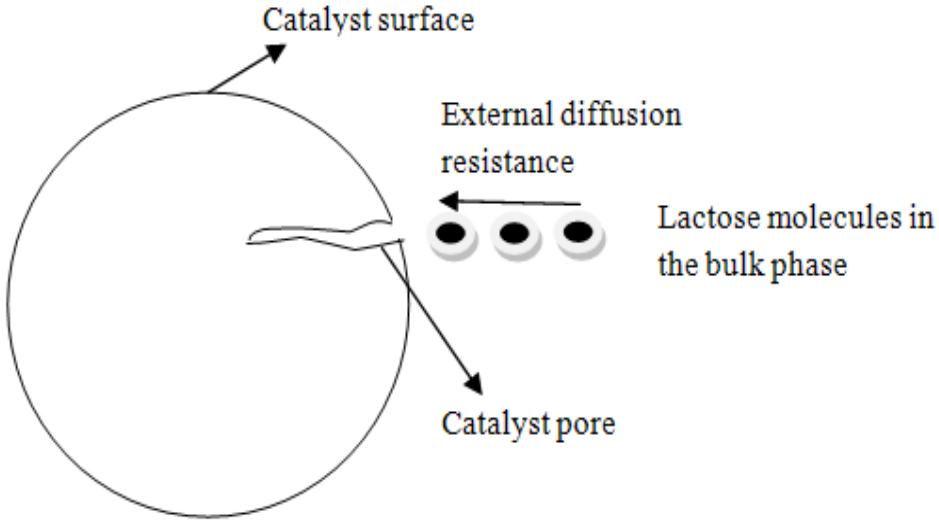

Figure 2.6. Schematic Representation of Adsorption of the Lactose Molecules onto the Catalyst Surface from Bulk Phase.

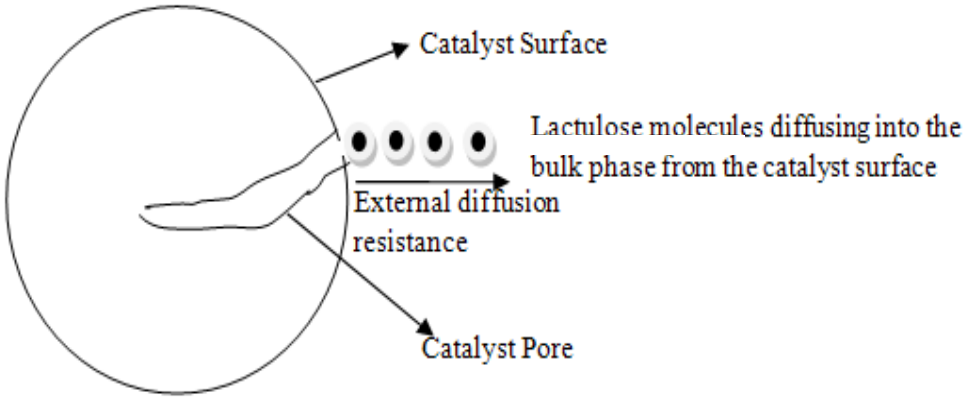

Figure 2.7. Schematic Representation of Diffusion of the Lactulose Molecules into the Bulk Phase.

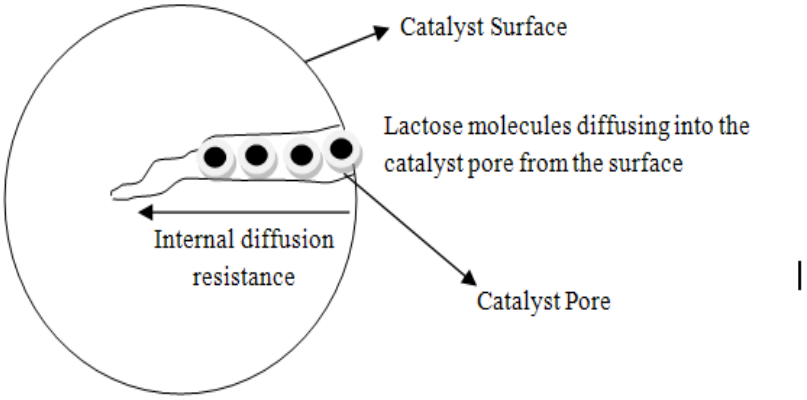

Figure 2.8. Schematic Representation of Diffusion of the Lactose Molecules through the Catalyst Pore.

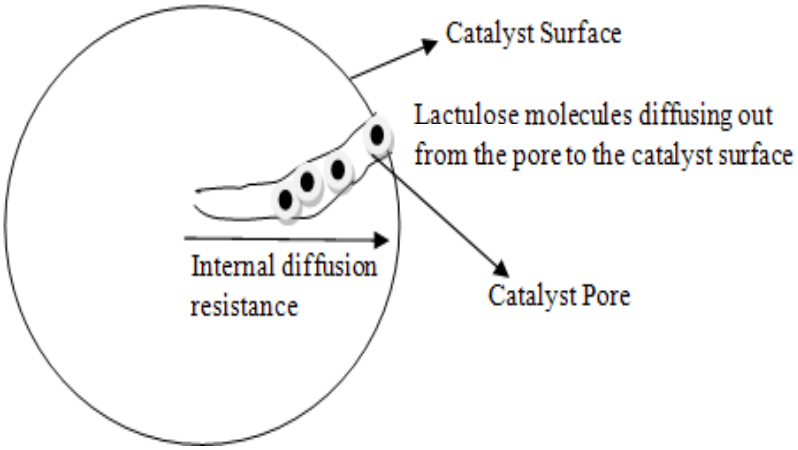

Figure 2.9. Schematic Representation of Diffusion of the Lactulose Molecules from the Catalyst Pore to the Surface.

The Thiele modulus compares the ratio of the surface reaction rate to the rate of diffusion through the catalyst and the effectiveness factor compares overall reaction rate to the overall rate if the intraparticle lactose concentration is the same at all points and equal to the surface concentration (H. Scott Fogler 2001). The Thiele modulus and the effectiveness factor are given by Equation (1) to Equation (4).

$$\Phi_n^2 = \frac{K_n C_{As}^{n-1} \rho_p S_a R^2}{D_e} = \frac{\text{Surface Reaction}}{\text{Diffusion rate}} \tag{1}$$

$$\text{Thiele modulus} = \Phi_n = \sqrt{\Phi_n^2}$$

$$\Phi_n = R\sqrt{\frac{K_n C_{As}^{n-1} \rho_p S_a}{D_e}} \tag{2}$$

The Thiele modulus for a first order reaction is

$$\Phi_1 = R\sqrt{\frac{K_1 \rho_p S_a}{D_e}} \tag{3}$$

$$\eta = \frac{\text{Actual overall rate of the reaction}}{\text{Rate of the reaction that would result if the entire interior surface were exposed to the external pellet conditions}} \tag{4}$$

For a first order reaction on a spherical catalyst, the effectiveness factor is (H. Scott Fogler 2001)

$$\eta = \frac{M_A}{-r_{As}(\text{mass of catalyst})} \tag{5}$$

First, consider the denominator

$$\text{rate} = (\text{rate per unit area})(\text{surface area})$$

$$= (\text{rate per unit area})\left(\frac{\text{surface area}}{\text{mass of catalyst}}\right)(\text{mass of catalyst})$$

$$= (k_1 C_{As})(S_a)\left(\frac{4}{3}\pi R^3 \rho_p\right)$$

$$= -r_{As}(\text{mass of catalyst})$$

At steady state, the overall reaction rate (M_A) is equal to the total molar flow of the reacting species into the catalyst pore as shown below:

$$M_A = 4\pi R W_{Ar} \tag{6}$$

$$\text{where } W_{Ar} = -D_e \frac{dC_A}{dr} = \text{Molar flux}$$

By using the transformations $\varphi = \frac{C_A}{C_{As}}$ and $\lambda = \frac{r}{R}$ (H. Scott Fogler 2001)

$$M_A = 4\pi R D_e C_{As} \frac{d\varphi}{d\lambda} \text{and } \varphi = \frac{1}{\lambda}\left(\frac{\sinh\Phi_1\lambda}{\sinh\Phi_1}\right) \tag{7}$$

Differentiating the above equation at $\lambda = 1$ yields

$$M_A = 4\pi R D_e C_{As}(\Phi_1 \coth\Phi_1 - 1) \tag{8}$$

Combining the above equations:

$$\eta = \frac{M_A}{-r_{As}(\text{mass of catalyst})} = \frac{4\pi R D_e C_{As}}{K_1 C_{As} S_a \rho_P \frac{4}{3}\pi R^3}(\Phi_1 \coth\Phi_1 - 1)$$

$$= 3\frac{1}{K_1 S_a \rho_P R^2/D_e}(\Phi_1 \coth\Phi_1 - 1)$$

$$\eta = \frac{3}{\Phi_1^2}(\Phi_1 \coth\Phi_1 - 1) \tag{9}$$

When the Thiele modulus is large (≈30) then the diffusion rate limits the overall reaction. Equation (9) gives the relationship between the internal effectiveness factor and the Thiele modulus assuming a first order reaction and a spherical catalyst pellet. Figure 2.10 shows a plot between the effectiveness factor (η) as a function of the Thiele modulus

(Φ) for a first order reaction on a spherical catalyst surface (H. Scott Fogler 2001). The reaction system becomes reaction-rate limited for small values of the Thiele modulus. At these conditions the effectiveness factor approaches 1. The Thiele modulus would attain low values for small catalyst radius or small catalyst surface area and low reaction rate constant.

The overall reaction rate can be increased by decreasing the radius of the catalyst pellet, increasing the reaction temperature, increasing the concentration of the reactants, increasing the internal surface area of the pellet or by increasing stirring in the reaction medium.

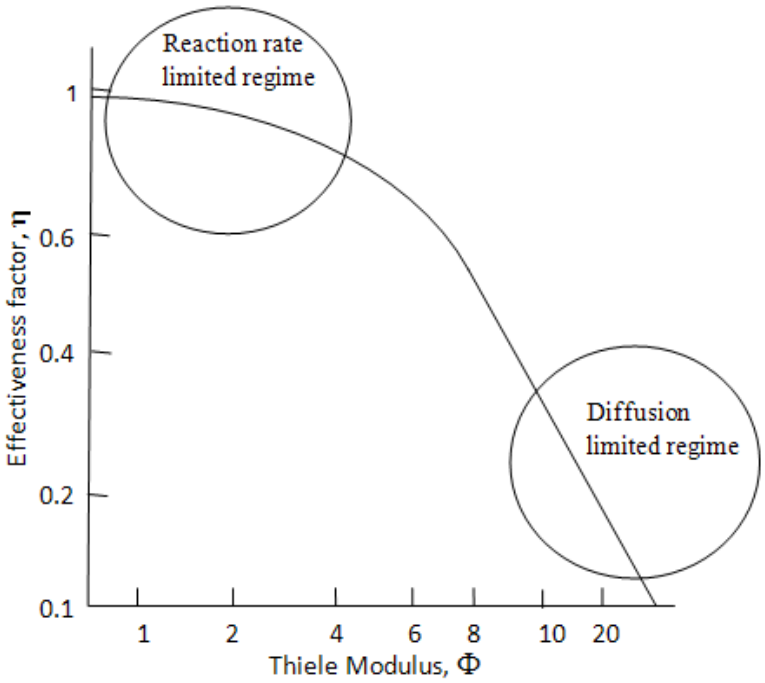

Figure 2.10. Effectiveness Factor Plot for 1st Order Kinetics on a Spherical Catalyst Particle (H. Scott Fogler 2001).

The external diffusion resistance shown in Figure 2.6 and Figure 2.9 can be minimized by creating turbulence in the medium with the help of a stirrer; however, the internal diffusion resistance depends on the internal effectiveness factor (η) and the Thiele modulus (Φ) as shown in Figure 2.10. The Weisz-Prater criterion (H. Scott Fogler 2001) was developed to estimate the reaction and internal diffusion limited regimes. This criterion could be deduced from the effectiveness factor for a first order reaction on a spherical catalyst pellet as shown in Equation (10) and Equation (11) (H. Scott Fogler 2001).

$$\eta\,\Phi_1^2 = 3(\Phi_1\coth\Phi_1 - 1) \tag{10}$$

For the Weisz-Prater parameter, $C_{WP} = \eta\,\Phi_1^2 = \frac{\text{Observed reaction rate}}{\text{Diffusion rate}}$

however:

$$\eta = \frac{-r_A'(obs)}{-r_{As}'} \quad \text{and} \quad \Phi_1^2 = \frac{-r_{As}'\rho_p R^2}{D_e C_{As}}$$

Substituting η and Φ_1^2 in Equation (10) gives

$$C_{wp} = \frac{-r_A'(obs)\rho_p R^2}{D_e C_{As}} \tag{11}$$

When $C_{wp}<<1$, the reaction would have negligible internal diffusion limitations and this could be achieved at low values of the resin bead diameter. This work measures the effect of the resin bead diameter on lactose isomerization.

2.3 KINETIC MODEL

A reaction catalyzed by a solid catalyst will have different steps:

a) Transport of reactant molecules from the bulk phase to the fluid-solid interface,

b) Transport of the molecules from the solid surface into the pores (if the catalyst is porous),

c) Reaction of the molecules at the active sites (surface reaction),

d) Transport of the products from the pores to the catalyst surface (desorption step),

e) Transport of the products from the catalyst surface into the bulk phase.

Each of the above steps, except for the surface reaction, is assumed to be in equilibrium. It is also assumed that the catalyst surface is homogeneous allowing monolayer adsorption and the adsorbed species do not interact with the neighboring molecules. These assumptions are reasonable in gas adsorption but may not hold well in the case of liquid systems (Seungman Sohn, Dongsu Kim 2004).

The Langmuir-Hinshelwood-Hougen-Watson model (LHHW) is the most effective formulation used to derive single site catalytic reaction rate expressions (James J. Carberry, 1976). The LHHW model assumes the following steps:

Step 1: $\mathrm{L\ (lactose)} + \mathrm{R\ (resin)} \overset{K_1}{\Leftrightarrow} (\mathrm{L} * \mathrm{R})$ ADSORPTION

Step 2: $(\mathrm{L} * \mathrm{R}) \underset{k_{-2}}{\overset{k_2}{\rightleftharpoons}} (\mathrm{Lu} * \mathrm{R})$ SURFACE REACTION

Step 3: $(\mathrm{Lu} * \mathrm{R}) \overset{K_3}{\Leftrightarrow} \mathrm{Lu(lactulose)} + \mathrm{R}$ DESORPTION

A surface reaction controlled model can be derived by considering the surface reaction as the rate determining step (Step 2). Equation (12) gives the rate of formation of lactulose and the rate of consumption of lactose.

$$r_{Lu} = -r_L = k_2 (L * R) - k_{-2} (Lu * R) \quad (12)$$

All steps except that controlling the overall rate will exist in equilibrium.

$$\text{Step 1: } \frac{(L * R)}{L\,R} = K_1 \quad (13)$$

$$\text{Step 3: } \frac{(Lu * R)}{Lu\,R} = K_3 \quad (14)$$

Substituting the adsorbed species concentrations in Equation (12) using Equation (13) and Equation(14)

$$r_{Lu} = -r_L = K_1\, k_2\, R \left\{ L - \left(\frac{K_3}{K_{eq}} \right) Lu \right\} \quad (15)$$

where L and Lu are the concentrations of lactose and lactulose and the overall experimental equilibrium constant K_{eq} is defined as $K_{eq} = \frac{k_2}{k_{-2}}$. If R_0 is the total concentration of active sites and R is the concentration of unoccupied sites then the free site concentration balance is given by Equation (17). R_L and R_{Lu} are the active site occupancy of lactose and lactulose.

$$R_0 = R + R_L + R_{Lu} \quad (16)$$

$$R_0 = R + (L * R) + (Lu * R) \tag{17}$$

Substituting the adsorbed species concentration into Equation (17)

$$R_0 = R + K_1 L R + K_3 Lu R$$

Hence,

$$R = \frac{R_0}{(1 + K_1 L + K_3 Lu)} \tag{18}$$

or

$$\frac{R}{R_0} = \frac{1}{(1 + \sum k_i X_i)} \tag{19}$$

Equation (19) is the Hougen – Watson formulation where $\frac{R}{R_0}$ is the fraction of total sites which are unoccupied. The number of sites occupied by lactose and lactulose are given by Equation (20) and Equation (21).

$$\frac{(L * R)}{R_0} = \frac{L R K_1}{R_0} = \frac{K_1 L}{(1 + \sum k_i X_i)} \tag{20}$$

$$\frac{(Lu * R)}{R_0} = \frac{Lu R K_3}{R_0} = \frac{K_3 Lu}{(1 + \sum k_i X_i)} \tag{21}$$

The relationship between the Hougen - Watson and Langmuir - Hinshelwood formulations is given by Equation (22)

$$\frac{R}{R_0} = 1 - \theta_{total} \tag{22}$$

θ_{total} = Total coverage

$$\theta_{total} = 1 - \frac{R}{R_0}$$

Using Equation (19) gives

$$\theta_{total} = \frac{\sum k_i X_i}{(1 + \sum k_i X_i)} = \theta_1 + \theta_2 + \theta_3 + \cdots = \theta_L + \theta_{Lu} \tag{23}$$

$$\theta_L = \frac{K_1 L}{(1 + K_1 L + k_2 Lu)} \tag{24}$$

$$\theta_{Lu} = \frac{K_3 Lu}{(1 + K_1 L + k_2 Lu)} \tag{25}$$

Substituting Equation (18) in Equation (15) yields

$$r_{Lu} = -r_L = \frac{R_0 K_1 k_2}{(1 + K_1 L + K_3 Lu)} \left\{ L - \left(\frac{K_3}{K_{eq}} \right) Lu \right\} \tag{26}$$

Assuming that desorption of the lactulose molecule into the bulk phase from the pore is very fast then K_3 can be negligible. This assumption is valid in the absence of external and internal diffusion resistances and the experimental runs were performed after eliminating these resistances. By considering the above assumption, Equation (26) becomes the simplified rate equation.

$$r_{Lu} = \frac{K_1 k_2 R_0 L}{(1 + K_1 L)} \tag{27}$$

Let 'w' represent the weight of the resin used for the reaction. Then the number of active sites (R_0) would be w*R_a (R_a is the number of active sites per gram of resin) and Equation (27) becomes

$$r_{Lu} = -r_L = \frac{K_1 k_2 R_a w L}{(1 + K_1 L)} \tag{28}$$

The differential form of the rate equation is given by Equation (29)

$$-\frac{dL}{dt} = \frac{K_1 k_2 R_a w L}{(1 + K_1 L)} \tag{29}$$

The reaction constant k_2 can be expanded using the Arrhenius equation as shown in Equation (30).

$$k_2 = A_0 e^{\left(\frac{-E_a}{RT}\right)} \tag{30}$$

By substituting Equation (30) into Equation (29) the rate equation now becomes

$$-\frac{dL}{dt} = \frac{K_1 A_0 e^{\left(\frac{-E_a}{RT}\right)} R_a w L}{(1 + K_1 L)} \tag{31}$$

Substituting

$$a = A_0 e^{\left(\frac{-E_a}{RT}\right)} R_a w \text{ and, } b = K_1 \tag{32}$$

Yields

$$-\frac{dL}{dt} = \frac{abL}{(1+aL)}$$

$$\frac{(1+aL)}{abL} dL = -dt \tag{33}$$

Integrating Equation (33) between the limits $L = L_0$ to L and $t = 0$ to t gives

$$\frac{1}{ab}\int_{L_0}^{L} \frac{1}{L} dL + \frac{1}{b}\int_{L_0}^{L} dL = \int_{0}^{t} -dt$$

$$\frac{1}{ab} \ln\left(\frac{L}{L_0}\right) + \frac{1}{b}(L - L_0) = -t \tag{34}$$

By using Equation (32) the integrated analytical expression is

$$\frac{1}{K_1 A_0 e^{\left(\frac{-E_a}{RT}\right)} R_a w} \ln\left(\frac{L}{L_0}\right) + \frac{1}{K_1}(L - L_0) = -t \tag{35}$$

Equation (35) provides a good proposed model to estimate the parameters K_1, A_0 and E_a using a measured lactose concentration-time profile and the least-squares approximation method.

3 MATERIALS AND METHODS

3.1 MATERIALS

AMBERLITE IRA-402 (Cl form) (Sigma Chemical Company), styrene/divinyl benzene copolymer with trimethyl amine functional group, is the strong anion exchange resin which was used for the isomerization reaction.

D-lactose monohydrate powder (Fisher Chemicals) was used to prepare the lactose solution. Analytical reagent grade 98.7% sodium hydroxide and 37.4% hydrochloric acid (Fisher chemicals) were used to prepare the solutions, for pH adjustments. Pure water of 18 mega-ohm resistivity, produced by using Milli-Q-ultrapure water purification system, was used for all solutions.

3.2 ANALYTICAL DETERMINATIONS

This section describes the procedure for operating the liquid chromatograph.

3.2.1 Analyzing Samples on the Liquid Chromatograph. Sugars were analyzed using a Phenomenex Rezex-RCM ion exchange column in calcium form on an Agilent HP 1090 high performance liquid chromatograph (HPLC) running Chemstation A.03 software. The mobile phase was Milli-Q water (18 mega-ohm resistivity) at 0.6 mL/min flow rate. The column temperature was controlled at 85^0C. The detector was an Agilent 1037 refractive index detector operated at 40^0C. The injection size was 10 µL for all samples. Figure 3.1 shows the Method and Run Control screen of the ChemStation software.

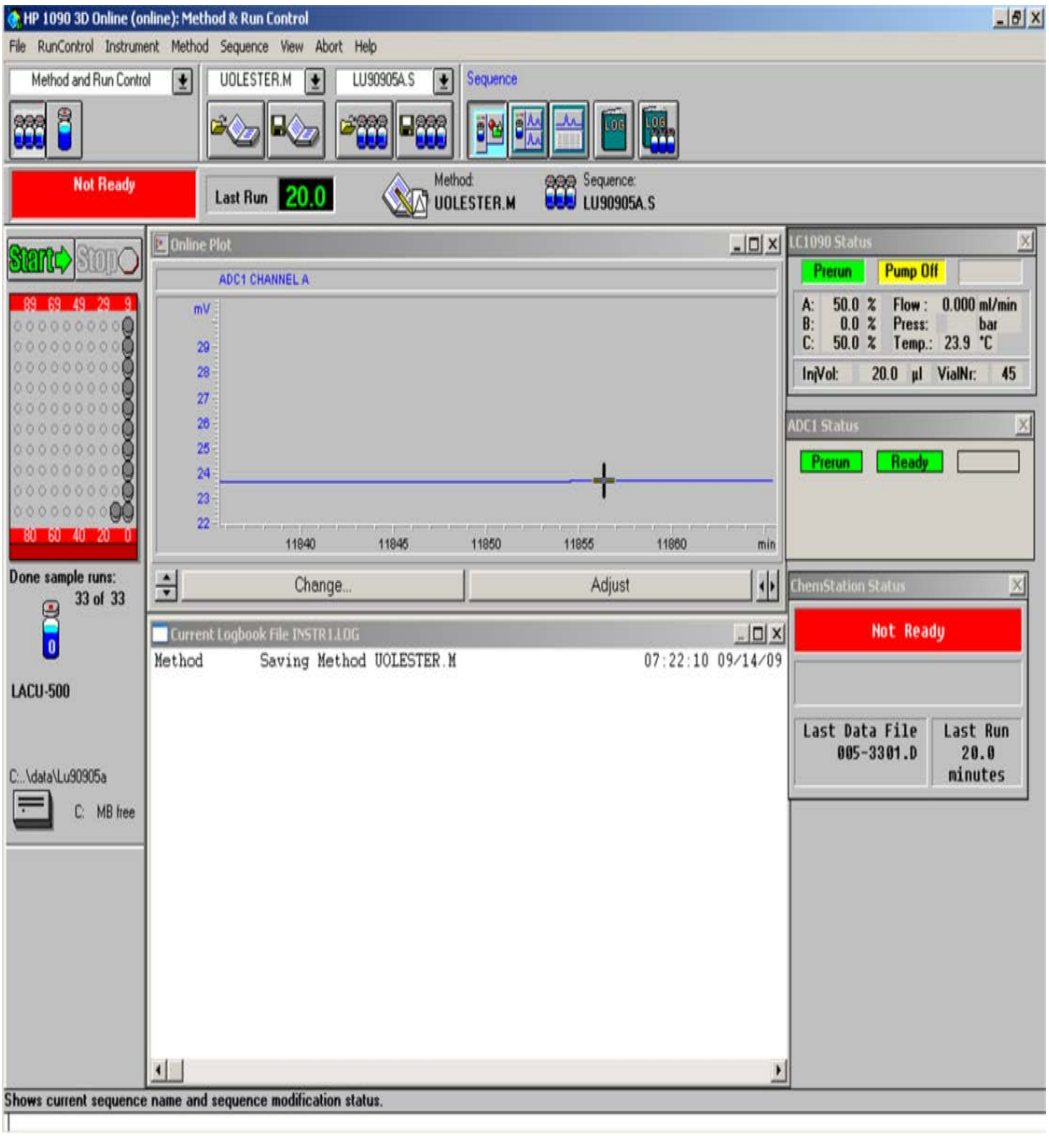

Figure 3.1. Snapshot of the ChemStation Main Screen.

A. Loading Samples

1. Place the sample vials into the magazine holders. Each magazine holds ten vials. Vial zero is the front vial and vial 9 is the back vial. The back end of the magazine contains a ridge whereas the front end of the magazine is smooth.

2. Place the magazine into the autosampler. Be sure the ridged end of each magazine points to the back of the autosampler.

3. Note the location of each sample vial in the autosampler tray. The numbering is from 0 to 99 with zero being the first vial in the rightmost magazine.

B. Defining the Sequence

A sequence file contains the information instructing the instrument to analyze a particular sample using a specified method a specified number of times. The sequence consists of setting parameters and defining a sample table.

C. Sequence Parameters

Figure 3.2 shows the Sequence Parameters screen.

1. From the Main Menu, click on Sequence | Sequence Parameters.

2. Enter the operator's name into the Operator Name field.

3. In the Subdirectory field, enter UOYYMMDD as the name of the subdirectory that holds the data files for this set of analyses. Substitute the two-digit number of the current year (10) for YY, the two-digit number of the current month for MM and the two-digit number of the current day for DD. The software asks if you want to create the subdirectory if it does not exist. If this message does not appear then the subdirectory already exists and most likely contains data files from a previous analysis. If you choose to re-use this subdirectory then the software will overwrite the data files destroying the original information.

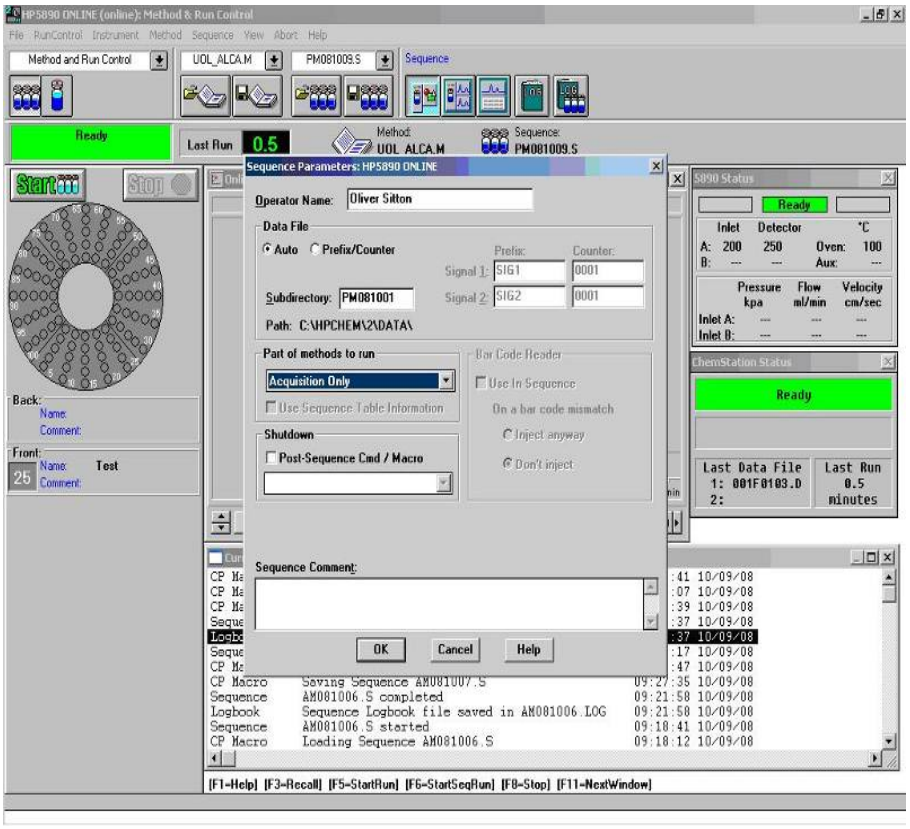

Figure 3.2. Snapshot of the Sequence Parameters Screen.

4. In the *Part of methods to run* area, select Acquisition only from the drop-down list. The software performs the analyses and acquires the data, but does not analyze or generate reports.

5. Click OK when finished.

D. Sequence Table

Figure 3.3 shows the Sequence Table screen.

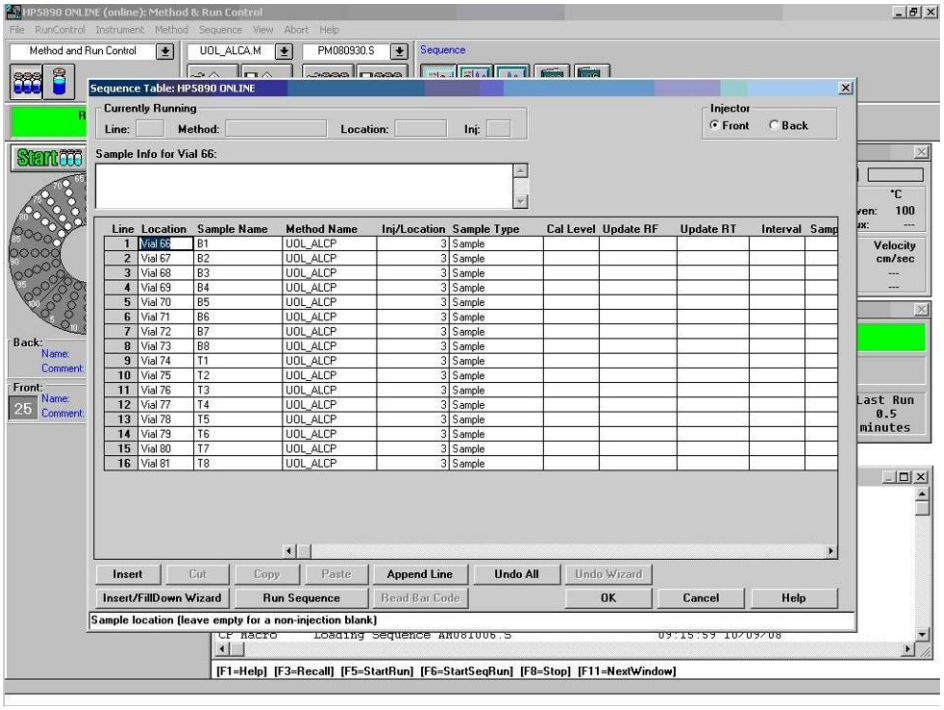

Figure 3.3. Snapshot of the Sequence Table Screen.

1. From the Main Menu select Sequence | Sequence Table.

2. In the Location field, type in the number of the vial containing the sample for analysis.

3. In the Sample Name field, type in the name of the sample contained in the specified vial.

4. In the Method Name field, select RCNLACU from the drop down list. This contains the instrument operating parameters for this analysis.

5. In the Inj/Location field, enter the number of injections for the sample. Two injections is a typical entry.

6. In the Sample Type field, select Sample from the drop-down list.

7. Repeat steps 2 to 6 for all samples in the set.

8. Click OK when finished.

E. Saving the Sequence

1. From the Main Menu select Sequence | Save Sequence As.

2. In the File Name field, type in the same name specified as the subdirectory name.

3. Click OK when finished.

F. Running a Sequence

Run the sequence to actually analyze the samples. From the Main Menu, select Run Control | Run Sequence.

G. Print the Analysis Reports

To generate a report for each sample analysis, you need to run the sequence with reporting parameters.

1. From the Main Menu, click on Sequence | Sequence Parameters.

2. In the *Part of methods to run* area, select Reprocessing Only from the drop-down list. The software analyzes the data for each sample in the Sample Table and generates a report with the results.

3. Click OK when finished.

4. From the Main Menu, select RunControl | Run Sequence.

3.2.2 Calibration Method. Standard solutions of lactose and lactose monohydrate (lactose•H_2O) were prepared for the calibration procedure as given in Table 3.1 Serial dilutions listed in Table 3.2 were then prepared using the standard solutions and analyzed using the HPLC procedure described above. A calibration solution containing approximately 40g/L of lactose and 40g/L of lactulose was run with each sample set and used to update the response factors.

Table 3.1. Standard Solutions for HPLC Calibration.

Component	Standard Solution	Molecular Weight (g/mol)	Amount (g)	Volume (ml)	Concentration (g/L)
Lactulose	A	342.3	0.401	10	40.1
Lactose•H_2O	B	360.3	0.443	20	44.3

Table 3.2. Serial Dilutions for HPLC Calibration.

Serial Dilution	Vial	Volume of A (µL)	Volume of B (µL)	Lactose (g/L)	Lactulose (g/L)
LACU-500	0	500	0	0	40.1
LACU-450	1	450	50	4.21	36.1
LACU-400	2	400	100	8.42	32.1
LACU-350	3	350	150	12.6	28.1
LACU-300	4	300	200	16.8	24.1
LACU-250	5	250	250	21.0	20.1
LACU-200	6	200	300	25.3	16.0
LACU-150	7	150	350	29.5	12.0
LACU-100	8	100	400	33.7	8.02
LACU-050	9	50	450	37.9	4.01
LACU-000	10	0	500	42.1	0

The samples were then analyzed in a completely randomized order and each analysis was replicated three times. The HPLC data is given in Appendix B, Table B.1. Figure 3.4 shows a typical chromatogram. Figure 3.5 shows the calibration curves for lactose and lactulose for the three replicates.

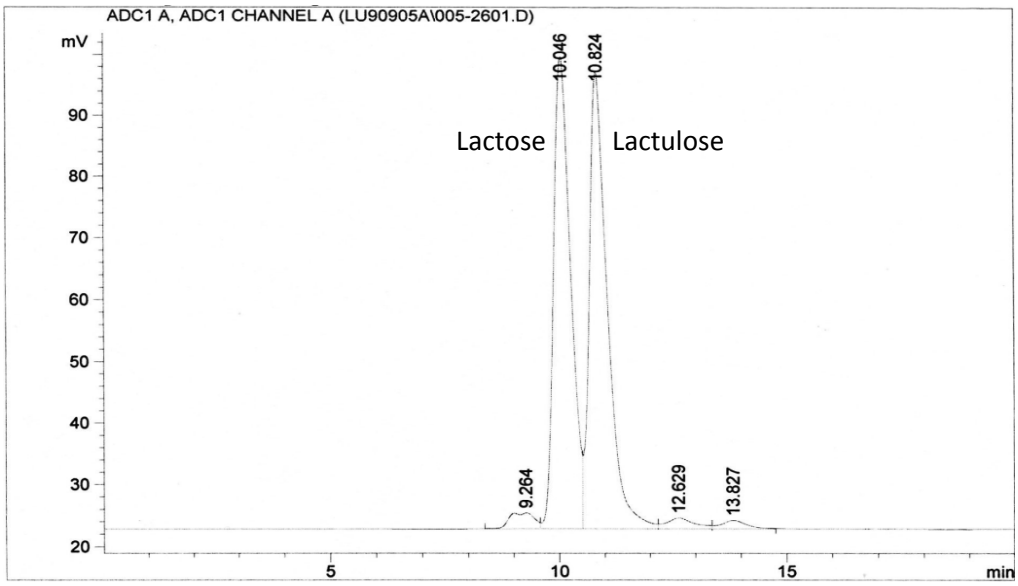

Figure 3.4. HPLC Chromatograph for Lactose (21 g/L) and Lactulose (20.1 g/L).

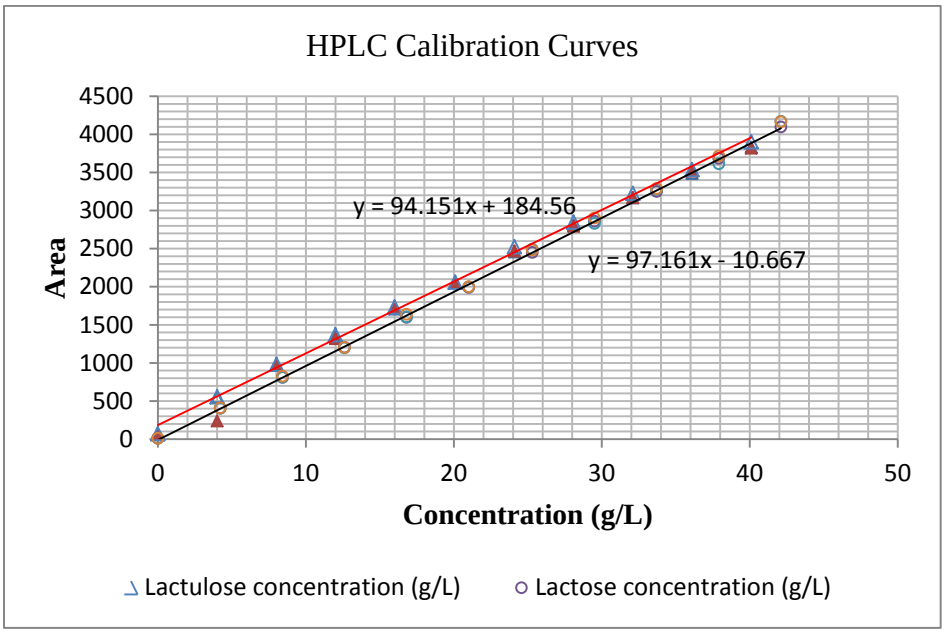

Figure 3.5. HPLC Calibration Curves for Lactose and Lactulose Concentrations for the Three Replicates.

Figure 3.6 and Figure 3.7 show the plots of the residuals for the lactose and lactulose calibrations respectively. This shows that the errors are randomly and independently distributed. Figure 3.8 and Figure 3.9 show the normal probability plots for the residuals. These plots indicate that the residuals are normally distributed as the points form a near linear pattern. Figure 3.6, Figure 3.7, Figure 3.8 and Figure 3.9 verify the constant variance and normality assumptions made for the ANOVA analysis.

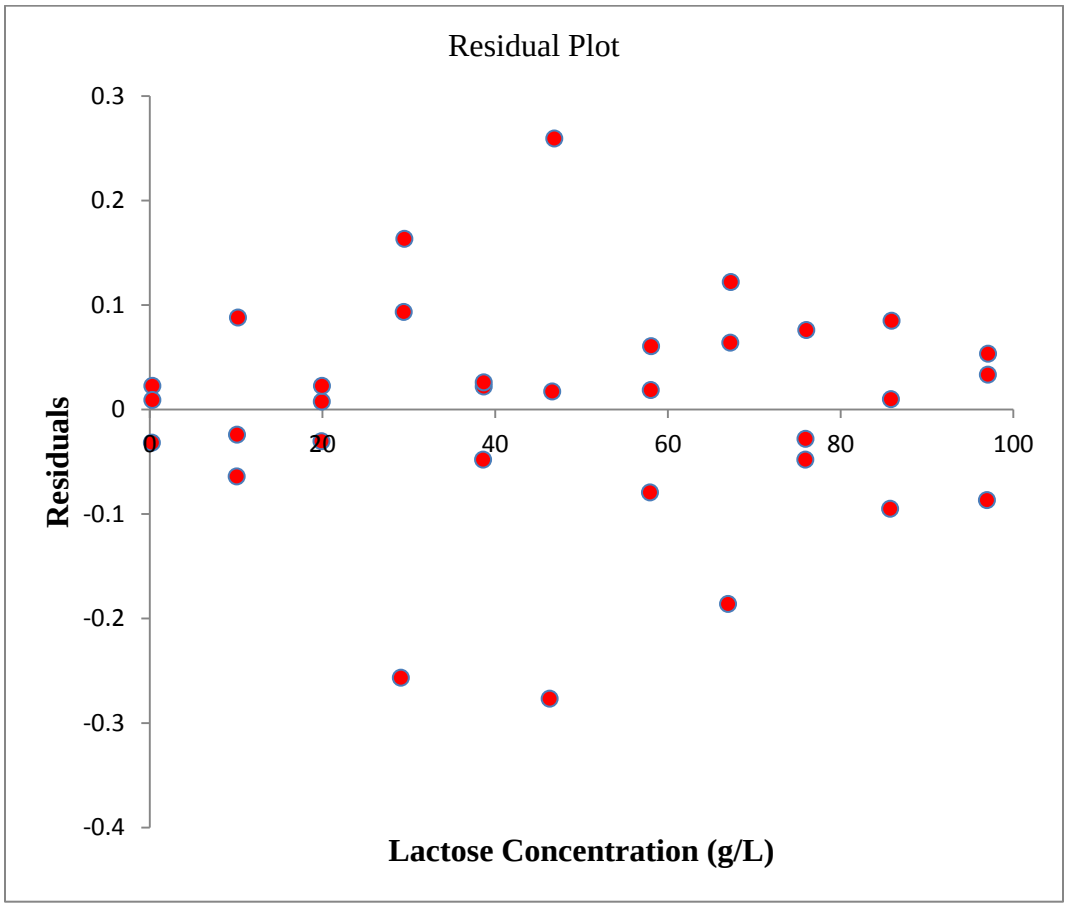

Figure 3.6. Variation of Residuals at Each Lactose Concentration (g/L).

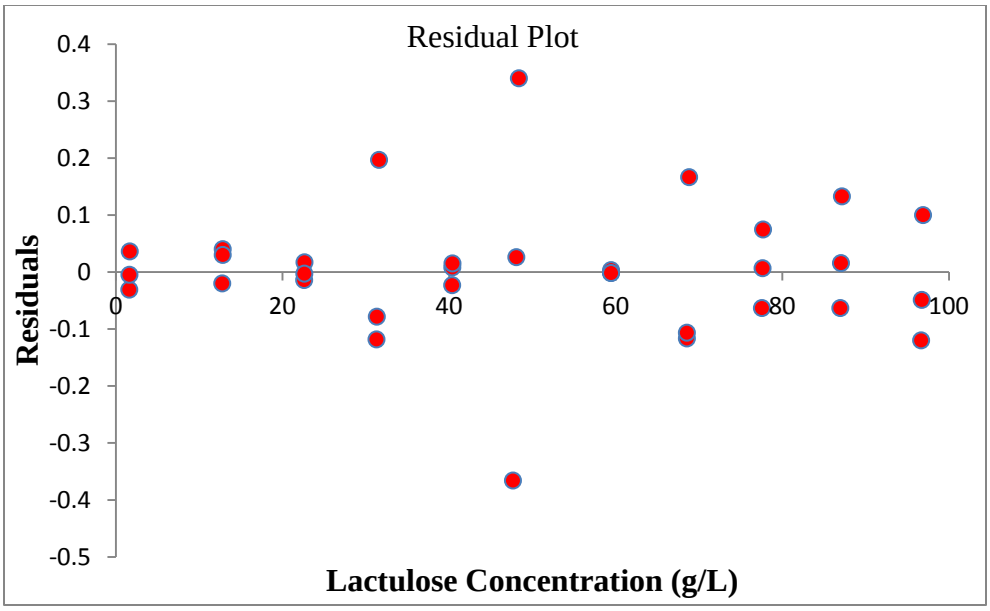

Figure 3.7. Variation of Residuals at Each Lactulose Concentration (g/L).

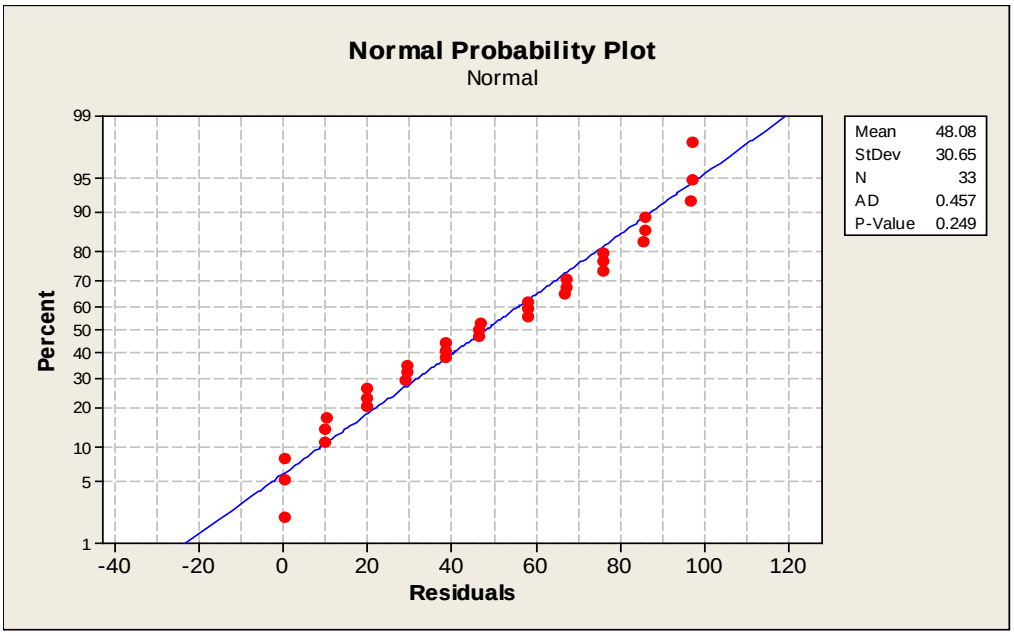

Figure 3.8. Normal Probability Plot for Lactose Calibration.

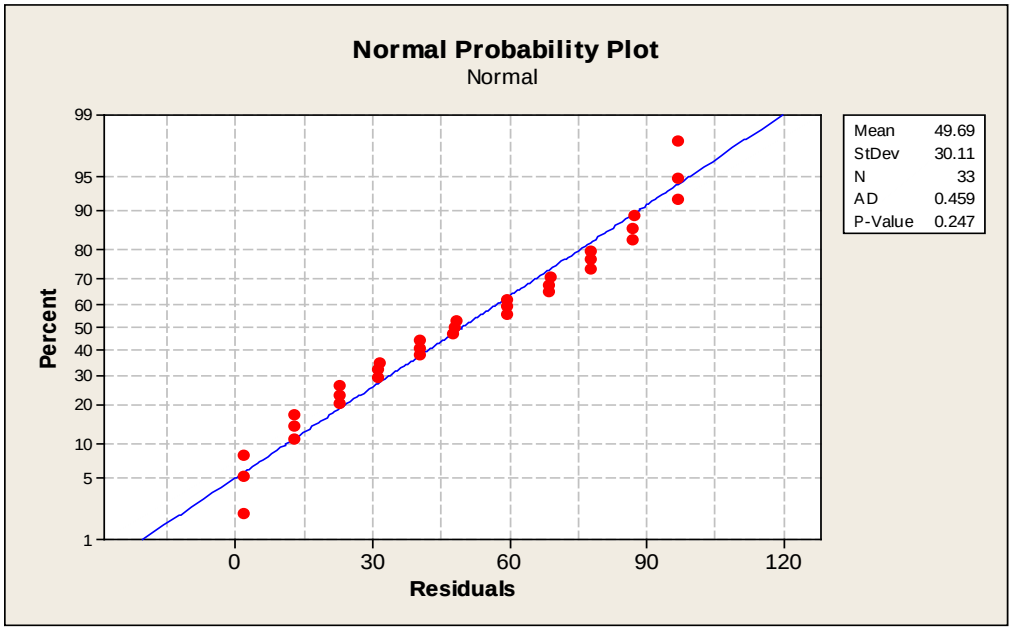

Figure 3.9. Normal Probability Plot of Residuals for Lactulose Calibration.

The analysis of variance tables, Table 3.3 and Table 3.4, demonstrate that the models for both lactose and lactulose calibration data are highly significant ($P < 0.0001$)

Table 3.3. ANOVA Table for Lactose Calibration.

Source of Variation	Degrees of Freedom	Sum of Squares	Mean Square	F value	P Value
Treatments	1	59358067	59358067	50027	< 0.0001
Residuals	31	36782	1187		
Lack of Fit	9	7437	826.3	0.619	0.768
Pure Error	22	29345	1334		
Total	32	59394849			

Table 3.4. ANOVA Table for Lactulose Calibration.

Source of Variation	Degrees of Freedom	Sum of Squares	Mean Square	F value	P Value
Regression	1	57819100	57819100	8003	< 0.0001
Residuals	31	223962	7225		
Lack of Fit	9	47742	5305	0.662	0.733
Pure Error	22	176221	8010		
Total	32	58043062			

3.3 TREATMENTS, PROCEDURES AND PRELIMINARY TESTS

The sections below give an overview of the isomerization reaction procedure, pretreatment of the resin and, optimization of resin bead diameter, stirrer speed and reaction time.

3.3.1 Isomerization Reaction Procedure. The reactions in the experimental design were carried out in sample vials of 9 mL capacity placed in a slotted aluminum block that was maintained at the required temperature. The reactions during the pretreatment step were carried out in 100 mL flasks using an oil bath to maintain the required temperature. The lactose solutions of specific concentrations were prepared by adding required amounts of lactose to a 100 mL volumetric flask and making up the solution to 100.0 mL with Milli-Q water. The solution was then heated to approximately 50^0C with constant stirring until the lactose powder was completely dissolved. The

lactose solution was then cooled before adjusting the pH to the required value for the reaction. For each of the main experimental runs 100.0 mL of 300.0 g/L lactose solution was prepared. Five mL aliquots of the lactose solution was added to a reaction vial and allowed to reach the required temperature. The resin was added only after the lactose solution in the vial reached the required temperature. During the reaction, samples of 20μL were collected by using a 50μL syringe and then were diluted with 500μL Milli-Q water using a 100-1000 μL micro pipette for subsequent HPLC analysis.

3.3.2 Pretreatment of AMBERLITE IRA-402 (Cl form). The strong anion exchange resin ABERLITE IRA-402 was received in its chloride form and would be inactive if used for the isomerization of lactose as such. This is mainly due to the absence of hydroxyl ions (OH^-). The chloride ions in the resin were replaced by hydroxyl ions through pretreatment with sodium hydroxide (NaOH) solution. Three batches of resin, each weighing 2.5 g, were taken and treated with 50 mL of 0.99M NaOH solution for 3, 4 and 8 hours respectively in a flask with constant stirring. A 500.0 mL aliquot of 100.0 g/L lactose solution was prepared and four, 100 mL batches of the solution were each mixed with 1 g of resin pretreated for 0, 3, 4 and 8 hours respectively at 95^oC for 300 minutes. After the reaction, samples were taken and analyzed for lactulose production. Figure 3.10 shows the amount of lactulose produced for each pretreated resin. The results show that the amount of lactulose formed is essentially the same for pretreatment times greater than 4 hours. A pretreatment time of 6 hours was chosen for all subsequent tests. The experimental data is given in Table B.2 in Appendix B.

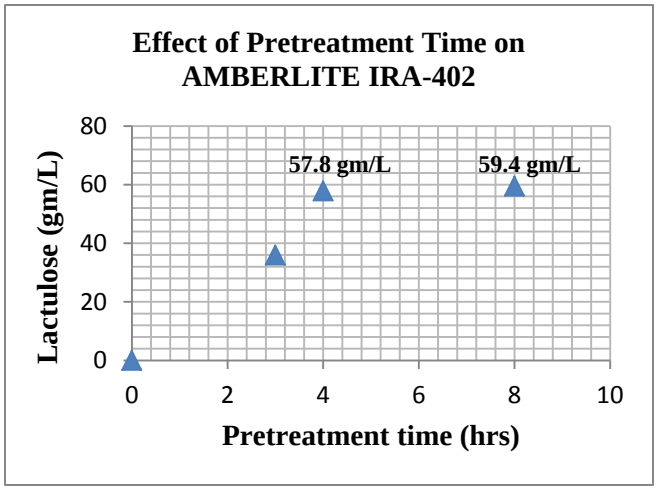

Figure 3.10. Effect of Pretreatment Time on AMBERLITE IRA-402.

3.3.3 Study of Volume Effect on Stirrer Speed, Optimization of Resin Bead Diameter and Determination of Total Reaction Time. Approximately 60 g of pretreated, dried AMBERLITE IRA-402 resin particles were ground and run through US standard sieves of 20, 25, 35, 45 and 100 mesh sizes. Table 3.5 lists the particle size distribution.

Table 3.5. Particle Size Distribution of Ground Resin.

Size distribution	Weight (g)
-20 +25	24.3
-25 +35	11.0
-35 +45	9.53
-45 +100	11.3
-100	1.73
Total	57.9

A. Study of Volume Effect on Stirrer Speed

The maximum stirrer speed setting on the reactor is 7 and it is important to study the reaction volume effect on the setting to eliminate the external diffusion effect. The amount of turbulence created in the reaction medium at a constant stirrer speed setting would change with the reaction volume. It is not appropriate to carry out the experiments at the maximum setting with 9 mL reaction volume (capacity of the reaction vial) as there could be significant external diffusion resistance. Reaction volumes of 5 mL and 3 mL were chosen to be studied at the maximum stirrer speed setting of 7. The -20 to +25 size of the resin was used for the study. Lactose solution of concentration 400.0 g/L was prepared and two samples of 5 mL and 3 mL were used for the reaction at stirrer speed setting of 7 for 5 hours. Samples of 20 µL were taken every 1 hour, diluted then analyzed by HPLC. The reaction conditions for both reaction volumes are given in Table 3.6.

Table 3.6. Reaction Conditions to Study the Volume Effect on Stirrer Speed.

Concentration of the lactose solution (g/L)	400.0	
Volume of lactose solution in the vial # 1 and vial # 2 (mL)	5	3
Reaction temperature (^{0}C)	90	90
Resin/lactose ratio ($\frac{\text{g of resin}}{\text{g of lactose}}$)	0.1	0.1
Weight of resin used for the reaction in vial # 1 and vial # 2 (g)	0.2	0.12
Resin size	-20 +25	-20+25
pH of the lactose solution	9	9
Stirrer speed setting	7	7

The experimental data for both the tests is given in Table B.3 in Appendix B. Figure 3.11 shows the concentration profiles of lactulose with two replicates for each experimental run.

The results show that the amount of lactulose produced for the reaction volumes of 5 mL and 3 mL is the same at stirrer speed setting of 7. The external diffusion effects were eliminated as the production of lactulose was not affected by changing the reaction volumes at the maximum stirrer speed setting. A reaction volume of 5 mL and stirrer speed setting of 7 were used for the subsequent experimental runs.

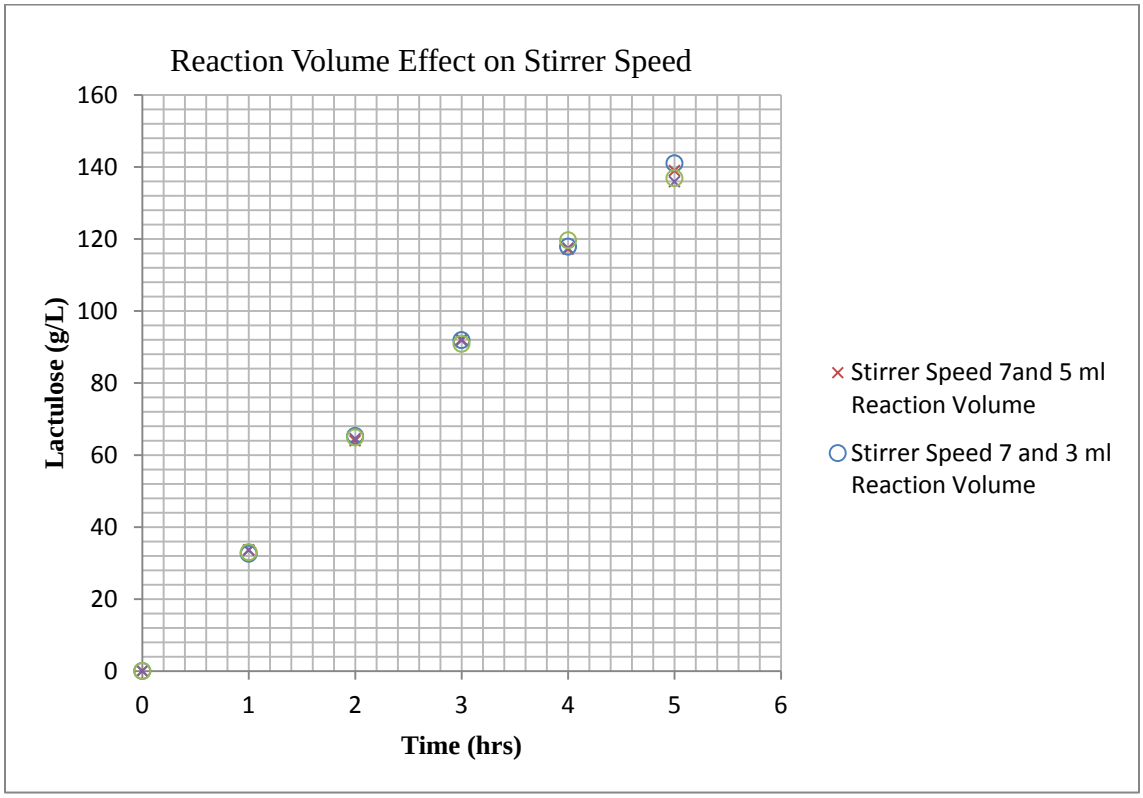

Figure 3.11. Graph Showing the Effect of Reaction Volume on Stirrer Speed.

B. Optimization of the Resin Bead Diameter

The -20 to +25 and the -45 to +100 size fractions were used to study the effect of bead diameter on the internal diffusion rate. To prepare the lactose solution, 40 g of lactose powder was placed in a 100.0 mL volumetric flask and a solution of volume 100.0 mL was made using Milli-Q water with constant stirring at approximately 50^{o}C. The pH of the solution was then adjusted to 9 using a bench top pH meter (Accumet model 50, Fisher Scientific). An aliquot of 5.0 mL of lactose solution was placed into each of two 9 mL vials and allowed to reach a temperature of 90 °C at a stirrer speed setting of 7 (maximum). A 0.2 g amount of the -20 to +25 and the -45 to +100 fractions of resin were then added to the vials. Table 3.7 shows the test conditions used for the two sizes of resin.

The reaction was carried out for 5 hours. Samples of 20 µL were taken every 1 hour, diluted then analyzed by HPLC. Figure 3.12 shows the comparison of lactulose concentration for the two different resin sizes. The plot shows that the amount of lactulose produced was the same for both size fractions. This proves that the bead diameter of the as-received resin is sufficiently small to eliminate internal diffusion resistances. To ensure the kinetic experiments used a uniform resin particle size the resin beads of the -20 to +25 size fractions were then used in the subsequent experimental runs. The experimental data collected is given in Table B.4, Appendix B.

Table 3.7. Test Conditions for Different Resin Sizes.

Concentration of the lactose solution (g/L)	400.0	
Resin size	-20 +25	-45+100
Reaction temperature (^{0}C)	90	90
Resin/lactose ratio ($\frac{\text{g of resin}}{\text{g of lactose}}$)	0.1	0.1
Weight of resin used for the reaction (g)	0.2	0.2
Volume of lactose solution in the vial (mL)	5	5
pH of the lactose solution	9	9
Stirrer speed setting	7	7

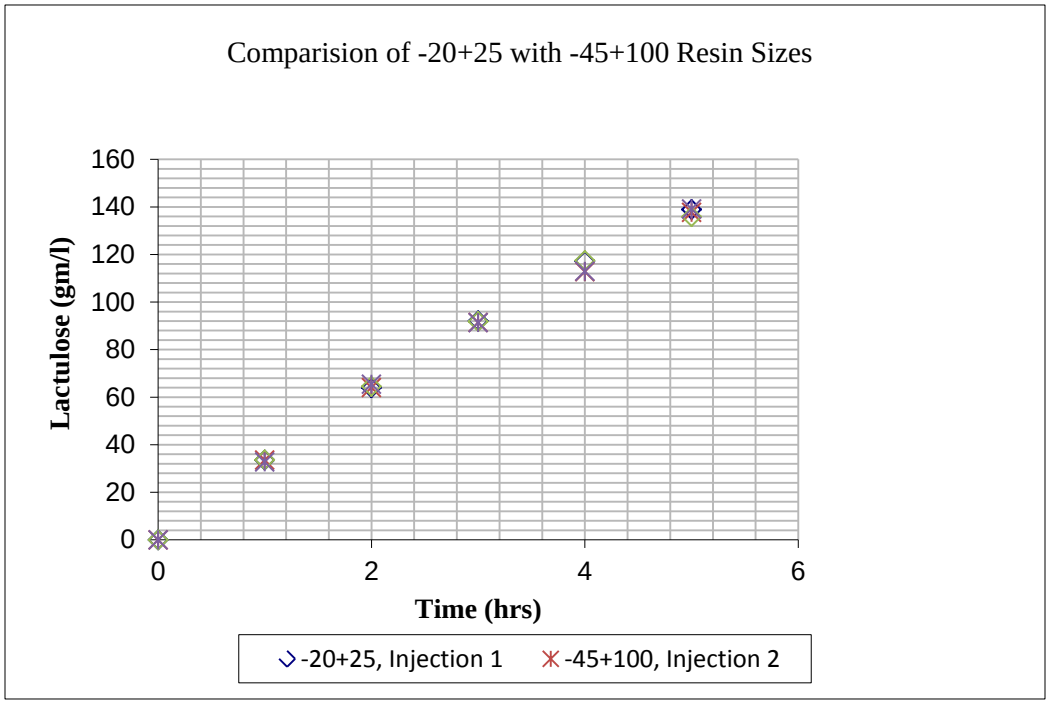

Figure 3.12. Comparison of Resin Sizes for 5 hrs of Reaction Time.

C. Determination of Total Reaction Time

The reaction time was optimized to achieve appreciable conversion. A 100.0 mL volume of 300.0 g/L lactose solution was prepared using the procedure explained in Section 3.3.1 and the pH was adjusted to 9. An aliquot of 5mL of lactose solution was then placed in the 9 mL reaction vial containing a magnetic stirrer. The vial was then placed in the slotted aluminum block and the temperature was maintained at 90^{o}C. The reaction conditions are given in Table 3.8. The resin was added after the lactose solution reached 90^{0}C.

Table 3.8. Reaction Conditions to Achieve Appreciable Conversion.

Concentration of the lactose solution (g/L)	300.0
Volume of lactose solution in the vial(mL)	5
Reaction temperature (^{0}C)	90
Resin/lactose ratio ($\frac{\text{g of resin}}{\text{g of lactose}}$)	0.3
Weight of resin used for the reaction (g)	0.45
Resin size	-20+25
pH of the lactose solution	9
Stirrer speed setting	7

The reaction was carried out for 18 hours and samples of 20µL were taken for every 1 hour and then were diluted with 500µL of Milli-Q water for HPLC analysis. Each sample analysis was replicated twice. Table 3.9 lists the concentrations of lactose, lactulose and the percent lactose conversion. Figure 3.13 shows the concentration profiles of lactose and lactulose for each replicate analysis. Figure 3.14 is the profile of lactose conversion. From

Table 3.9 it can be observed that the conversion of lactose is more than 96% after 12 hours of reaction time. The remaining experimental runs were conducted for a total of 12 hours of reaction time with samples taken each hour.

Table 3.9. Experimental Data for Initial Test to Determine Overall Reaction Time.

Time (Hrs)	Injection	Lactose (g/L)	Lactulose	Conversion %
0	1	326	0	0
1	1	237	84.2	27.3
2	1	183	151	44.0
3	1	132	199	59.6
4	1	97.4	233	70.1
5	1	73.7	249	77.3
6	1	54.8	273	83.2
7	1	40.9	280	87.4
8	1	29.3	294	90.9
9	1	22.0	297	93.2
10	1	16.5	317	94.9
11	1	12.4	322	96.2
12	1	8.84	314	97.3
13	1	6.56	326	97.9
14	1	4.99	326	98.5
15	1	3.58	331	98.9
16	1	2.78	323	99.1
17	1	2.03	332	99.4
18	1	1.52	327	99.5
0	2	331	0	0
1	2	248	82.6	25.0
2	2	177	144	46.6
3	2	130	195	60.6
4	2	101	230	69.5
5	2	71.7	245	78.3
6	2	53.3	268	83.9
7	2	41.3	286	87.5
8	2	29.9	292	90.9
9	2	22.5	297	93.2
10	2	16.3	318	95.1
11	2	11.8	308	96.4
12	2	9.11	314	97.2

Table 3.9 (Contd). Experimental Data for Initial Test to Determine Overall Reaction Time.

13	2	6.58	314	98.0
14	2	4.95	322	98.5
15	2	3.68	324	98.9
16	2	2.66	331	99.2
17	2	2.04	326	99.4
18	2	1.47	315	99.6

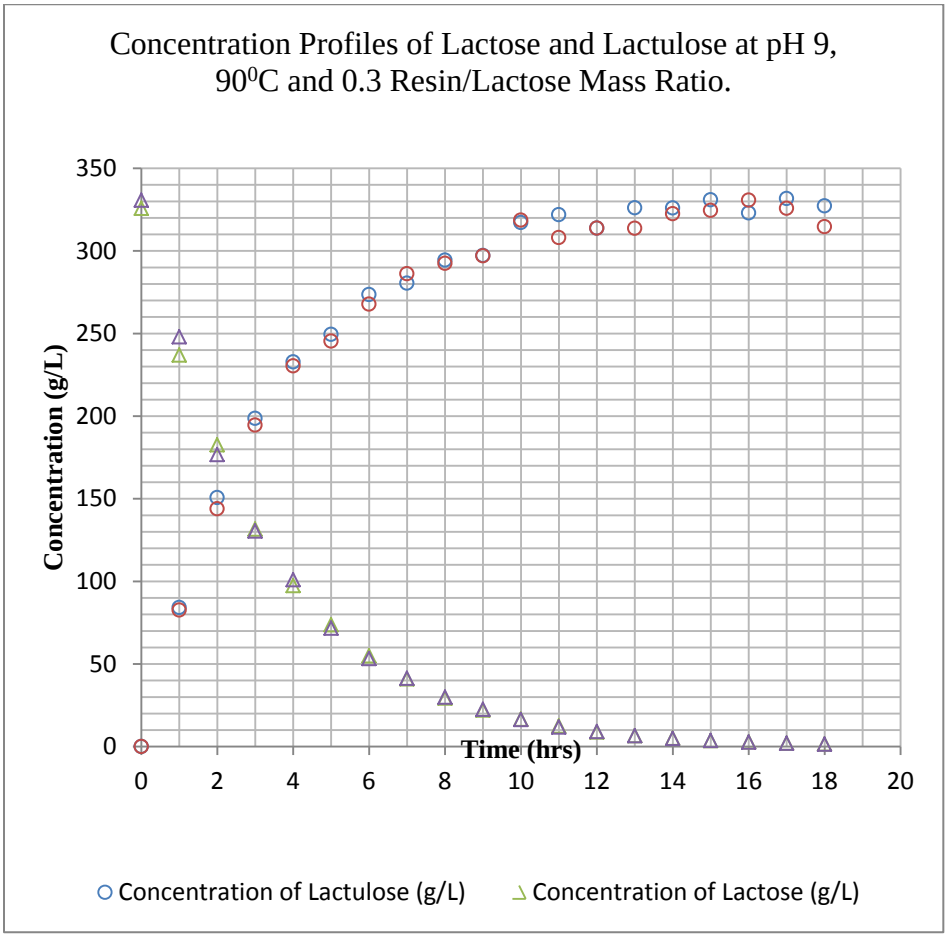

Figure 3.13. Lactose and Lactulose Concentration Profile for the Initial Test at pH 9, 90^0C and 0.3 Resin/Lactose Mass Ratio.

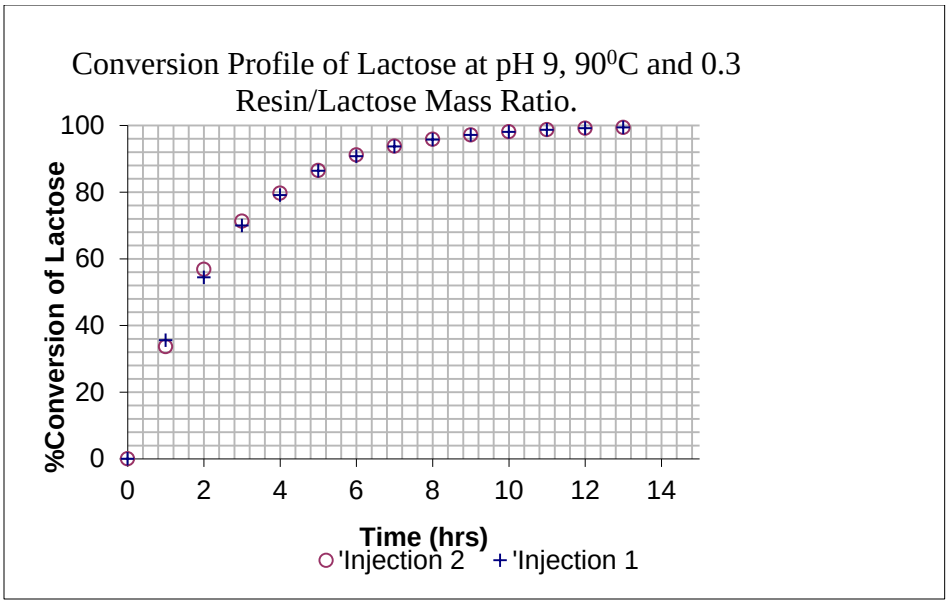

Figure 3.14. Lactose Conversion Profile for the Initial Test at pH 9, 90^{0}C and 0.3 Resin/Lactose Mass Ratio.

3.3.4 Measurement of pH. The pH of the lactose solution was measured using a bench top pH meter (Accumet model 50, Fisher Scientific). The pH meter was calibrated using buffer solutions of pH 4.0, 7.0 and 10.0 before each use.

3.3.5 Measurement of the Number of Active Sites in AMBERLITE IRA-402. A 1 gm sample of -20 +25 AMBERLITE IRA-402 resin particles were pretreated with 150 mL of 0.987 M NaOH solution for 6 hours. After the pretreatment, the resin particles were vacuum filtered and the remaining NaOH solution was titrated with 0.374 M HCl solution using phenolphthalein as the indicator. Table 3.10 shows the titration and pretreatment data. The sample calculation for the number of active sites is given in Appendix A. The weight of NaOH utilized by the resin is given by Equation (36).

$$w_2 = (\frac{M_2 * 150 * 40}{1000}) - w_1 \quad (36)$$

where

w_1 = Weight of NaOH left in the solution after pre-treatment = $\frac{(m_2 * 150 * 40)}{1000}$

m_2 = Molarity of the NaOH sample after pre-treatment = $\frac{(v_1 * M_1)}{v_2}$

The number of equivalents of NaOH used by the resin was calculated to be $0.116 \frac{\text{g equivalents}}{\text{g of resin}}$ as shown in Appendix A. Hence, the total number of active sites in 1 g of AMBERLITE-IRA 402 resin = $R_a = 0.116 \frac{\text{g equivalents}}{\text{g of resin}}$.

Table 3.10. Titration Data for Active Sites Calculation.

Molarity of the HCl solution (M_1)	0.374 M
Molarity of the NaOH solution (M_2)	0.987 M
Volume of NaOH used for pre-treatment (V)	150.0 Ml
Volume of NaOH sample (v_2)	30.0 Ml
Volume of HCl used for titration (v_1)	17.1 mL
Weight of -20 +25 resin beads (W)	1.00 g

3.4 STATISTICAL ANALYSIS

JMP®7.0.1 and SAS were used to carry out the statistical analysis of the experimental data. Microsoft Excel 2007 was used to fit the reaction data to the kinetic model.

4 EXPERIMENTAL DESIGN

Response surface designs are generally used when the object of the experiment is to determine the effect of each variable on the response and to ascertain globally optimum conditions. The Box-Behnken design is one response surface design, which does not require tests at extremes in the variable values since the treatment combinations fall at the mid points of the edges. Replicating the center point allows one to estimate the experimental error. The present experiment has three factors: reaction temperature (T), pH and the resin to lactose ratio (ratio). Each of the factors has three levels as shown in Table 4.1, where a "-" indicates the low value, a "+" indicates the high value and a "0" indicates the central value of each factor. The response variable is the percentage conversion of lactose and is calculated as given in Equation (37).

$$\text{Conversion} = \frac{L_i - L_f}{L_i} * 100 \tag{37}$$

Where L_i and L_f are the initial and final concentrations of lactose. Table 4.1 shows the values selected in these experiments.

Table 4.1. Levels of the Experimental Factors.

Factor	Coded values		
	-	0	+
Reaction temperature (T)	70^0C	80^0C	90^0C
pH of the Lactose solution (pH)	9	10	11
Resin to lactose ratio (mass ratio)	0.1	0.3	0.5

The design for a three-factor experiment with each factor having three levels gives 15 treatment combinations with three replications at the center point. Table 4.2 shows the completely randomized treatment combinations for a Box-Behnken design for the experiment using JMP®7.0.1.

Table 4.2. Treatment Combinations Generated Using a Box-Behnken Design.

Run Order	Pattern	T	Ratio	pH
1	+ 0 -	90	0.3	9
2	0 0 0	80	0.3	10
3	- 0 -	70	0.3	9
4	0 - +	80	0.1	11
5	- 0 +	70	0.3	11
6	0 - -	80	0.1	9
7	+ 0 +	90	0.3	11
8	- + 0	70	0.5	10
9	+ - 0	90	0.1	10
10	+ + 0	90	0.5	10
11	0 + +	80	0.5	11
12	0 + -	80	0.5	9
13	0 0 0	80	0.3	10
14	- - 0	70	0.1	10
15	0 0 0	80	0.3	10

5 RESULTS AND DISCUSSION

The concentration profiles of lactose and lactulose and the lactose conversion profiles for the experimental runs are shown in Figure 5.1 through Figure 5.28. The profiles for the center point replicates are shown in Figure 5.3 and Figure 5.4 to prove the reproducibility of the data. The experimental data for the runs is given Appendix C.

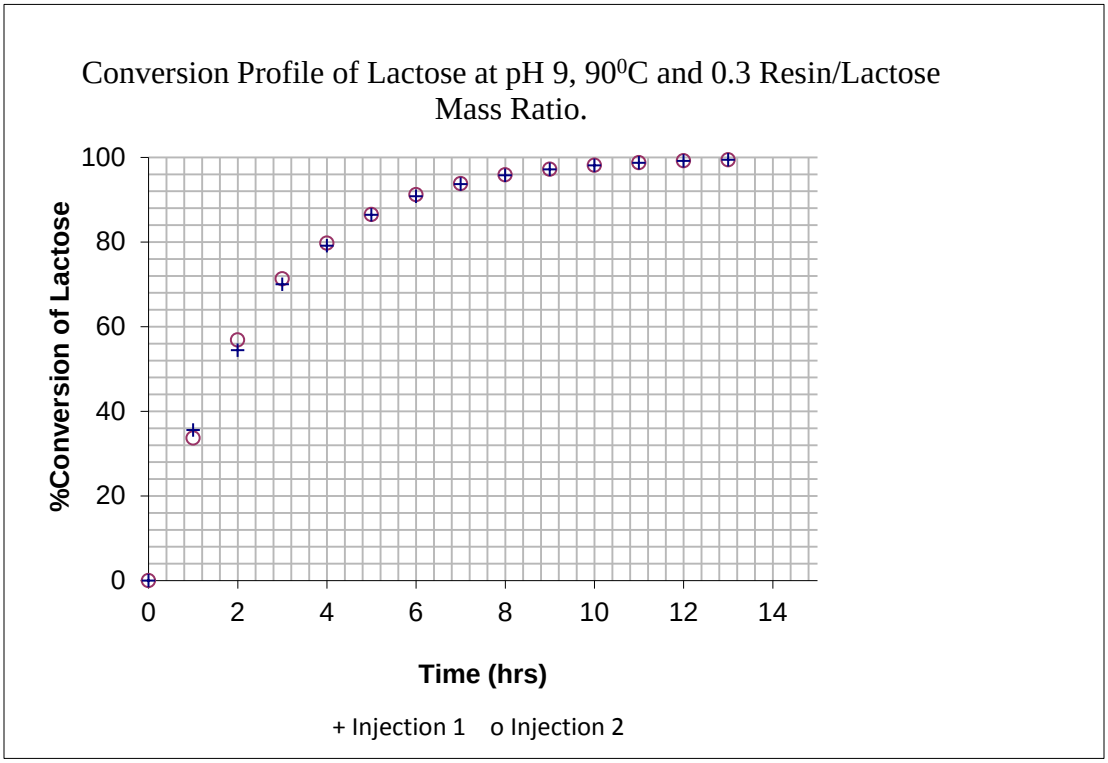

Figure 5.1. Conversion Profile at pH 9, 90^{0}C and 0.3 Resin/Lactose Ratio.

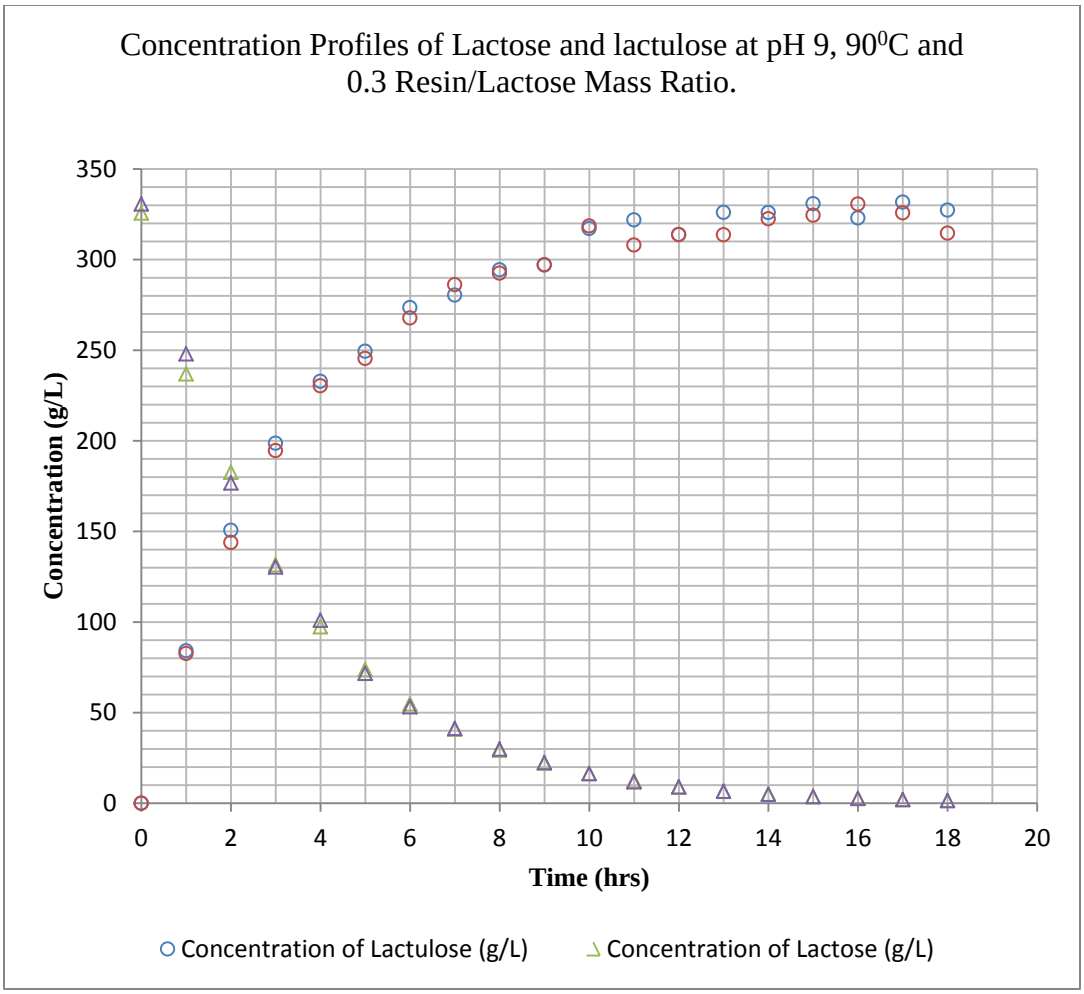

Figure 5.2. Lactose and Lactulose Concentration Profiles at pH 9, 90^{0}C and 0.3 Resin/Lactose Ratio.

Figure 5.3 and Figure 5.4 show the conversion of lactose and concentration profiles for the three replicates at the center point. The plots clearly indicate the reproducibility of data as the variation between the conversion, lactose and lactulose concentration data for the replicates is low. The ANOVA analysis of the data gave an RMSE of 2.83.

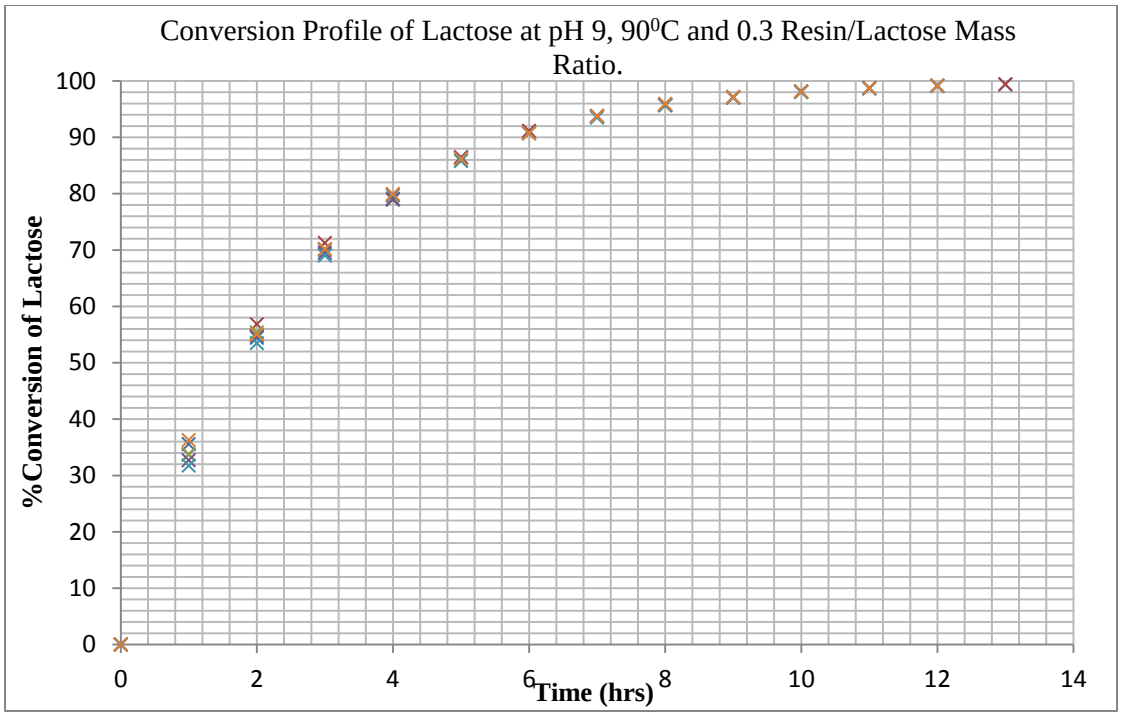

Figure 5.3. Conversion Profiles for the Center Point Replicates at pH 10, 80^{0}C and 0.3 Resin/Lactose Ratio.

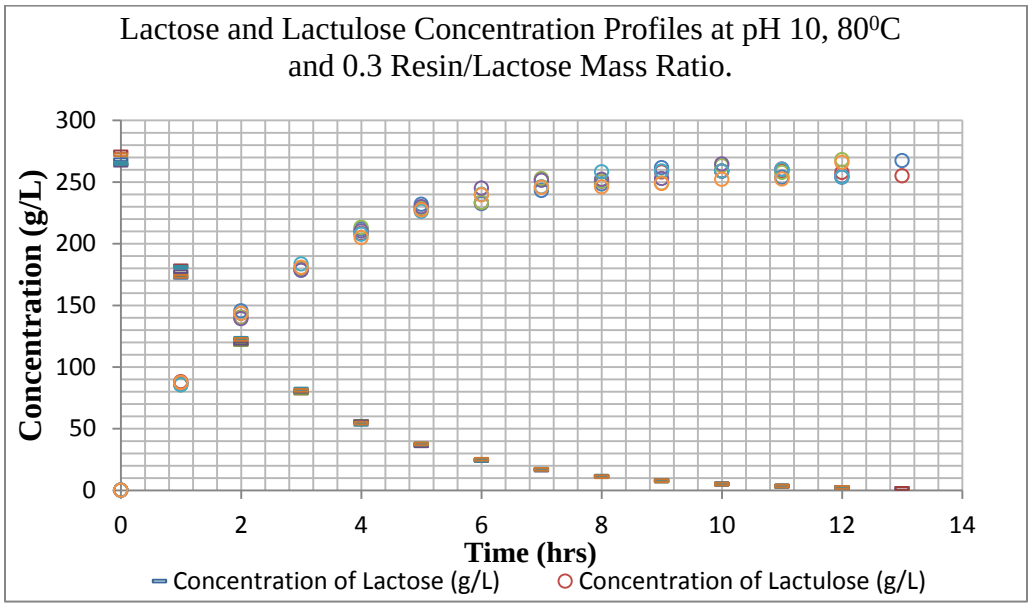

Figure 5.4. Lactose and Lactulose Concentration Profiles for all the Center Point Replicates at pH 10, 80^{0}C and 0.3 Resin/Lactose Ratio.

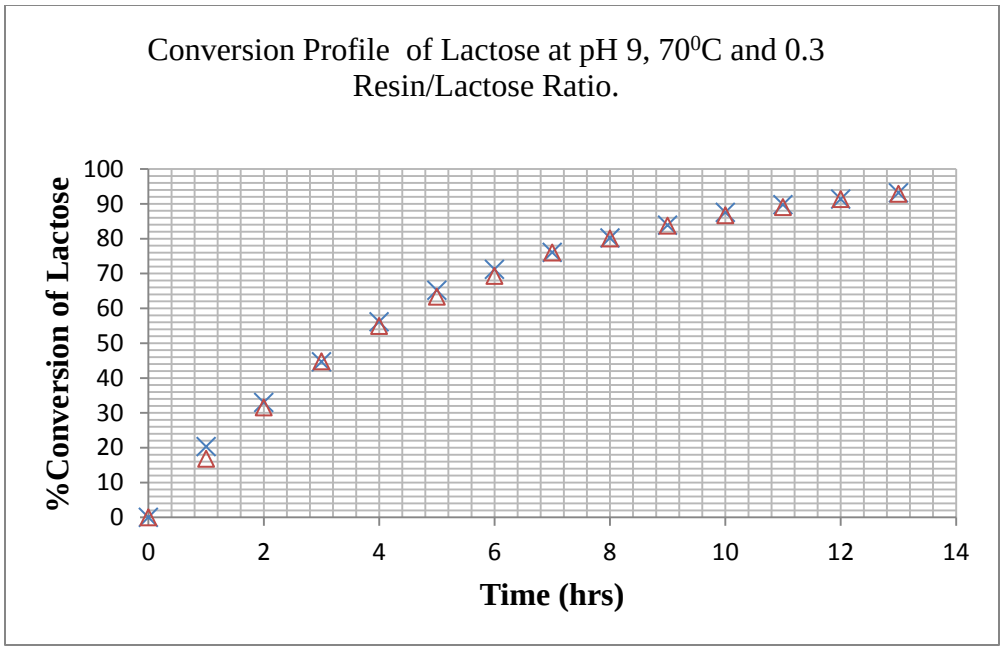

Figure 5.5. Conversion Profile of Lactose at pH 9, 70^{0}C and 0.3 Resin/Lactose Ratio.

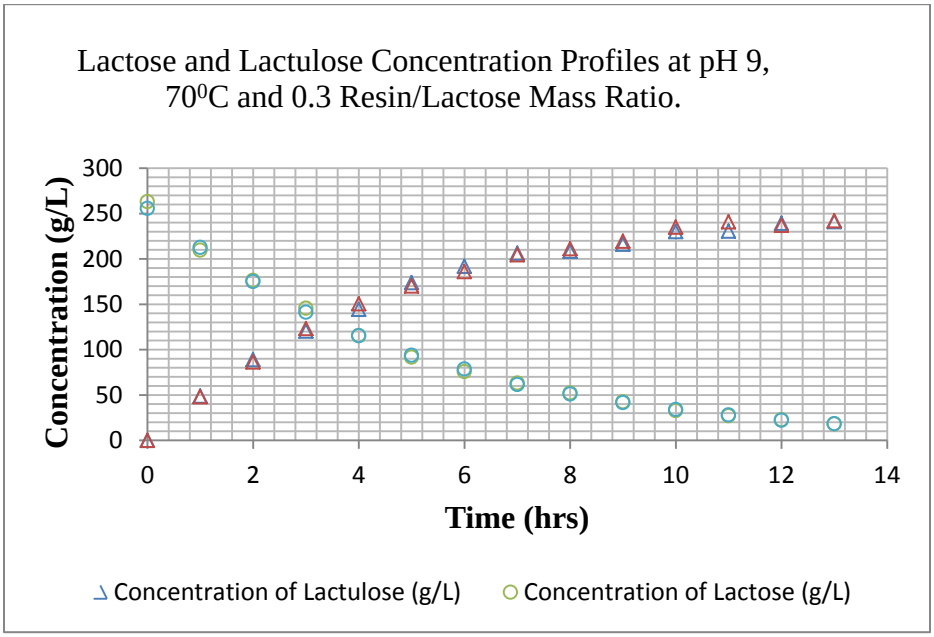

Figure 5.6. Lactose and Lactulose Concentration Profiles at pH 9, 70^{0}C and 0.3 Resin/Lactose Ratio.

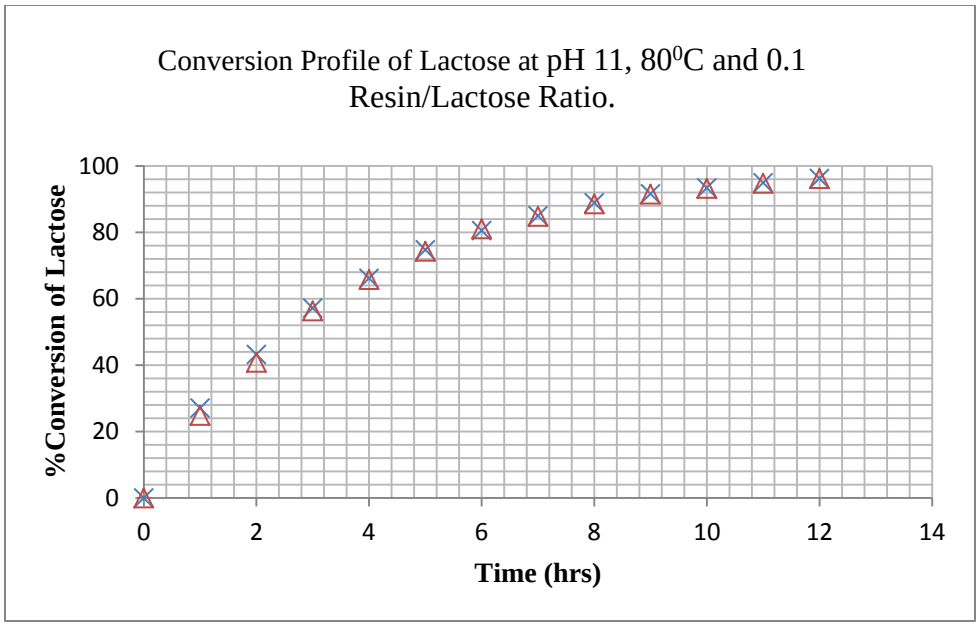

Figure 5.7. Conversion Profile of Lactose at pH 11, 80^0C and 0.1 Resin/Lactose Ratio.

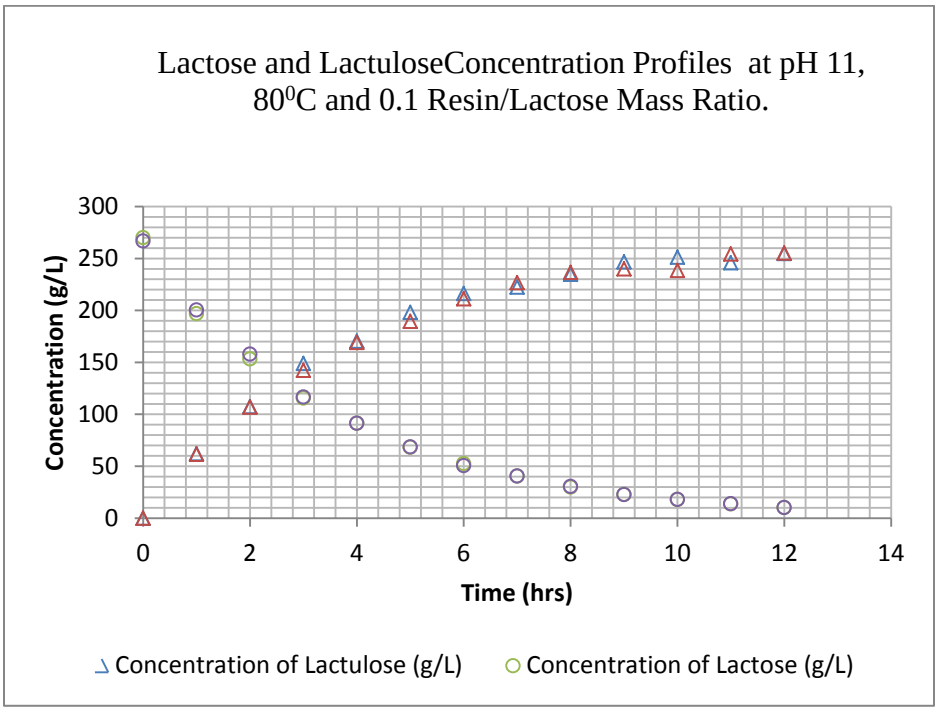

Figure 5.8. Lactose and Lactulose Concentration Profiles at pH 11, 80^0C and 0.1 Resin/Lactose Ratio.

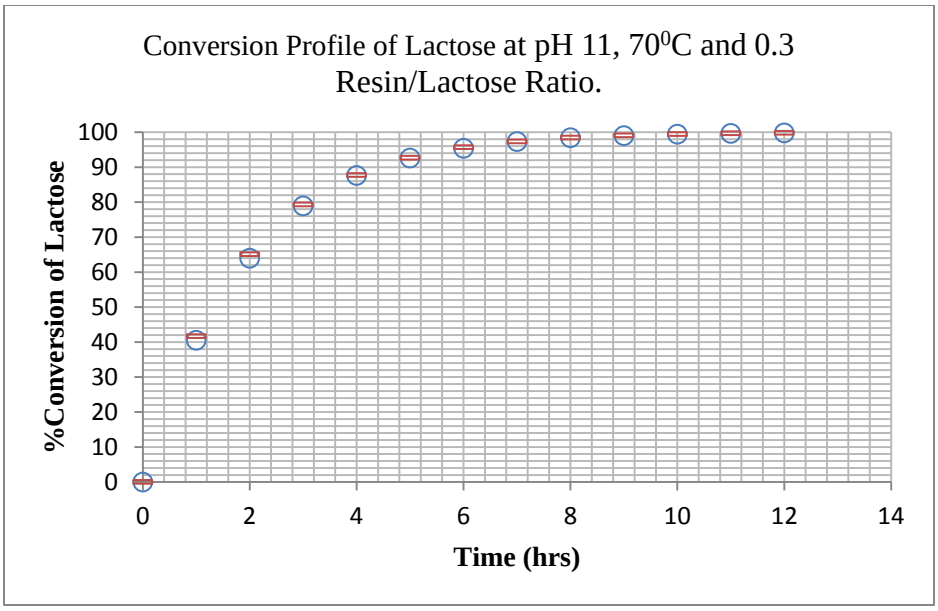

Figure 5.9. Conversion Profile of Lactose at pH 11, 70^{0}C and 0.3 Resin/Lactose Ratio.

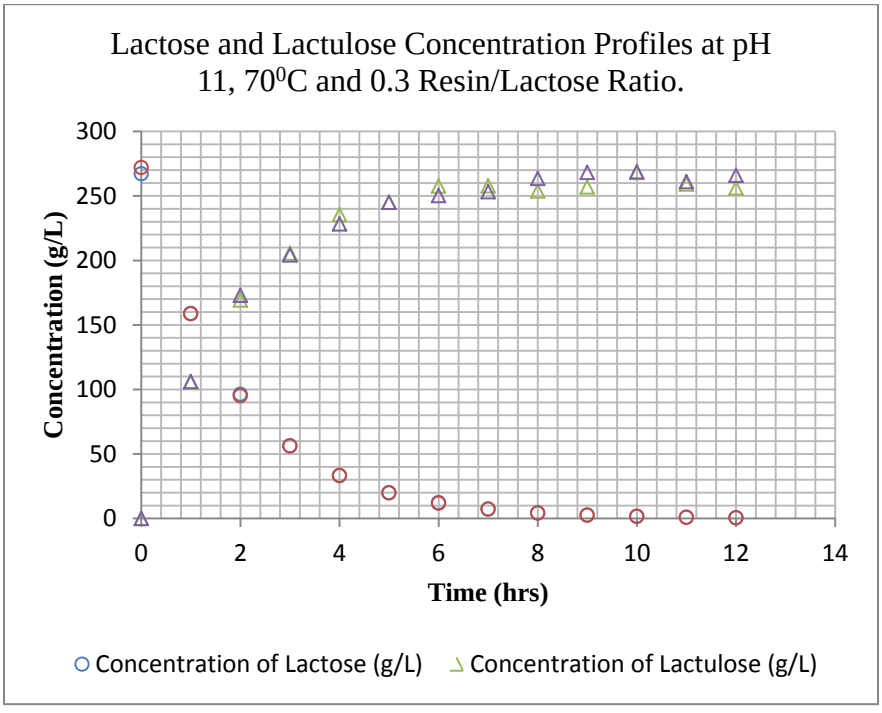

Figure 5.10. Lactose and Lactulose Concentration Profiles at pH 11, 70^{0}C and 0.3 Resin/Lactose Ratio.

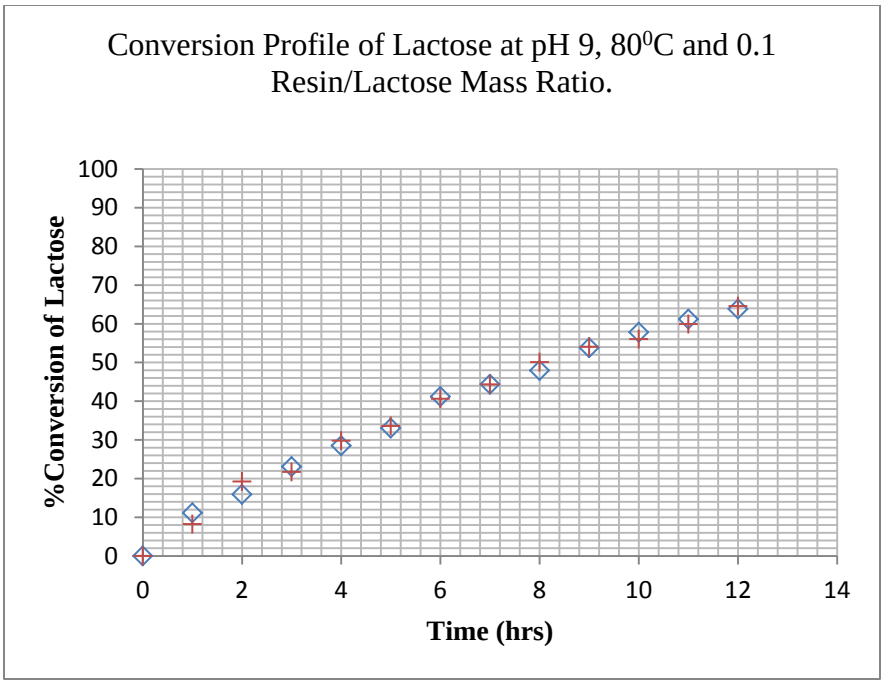

Figure 5.11. Conversion Profile of Lactose at pH 9, 80^{0}C and 0.1 Resin/Lactose Ratio.

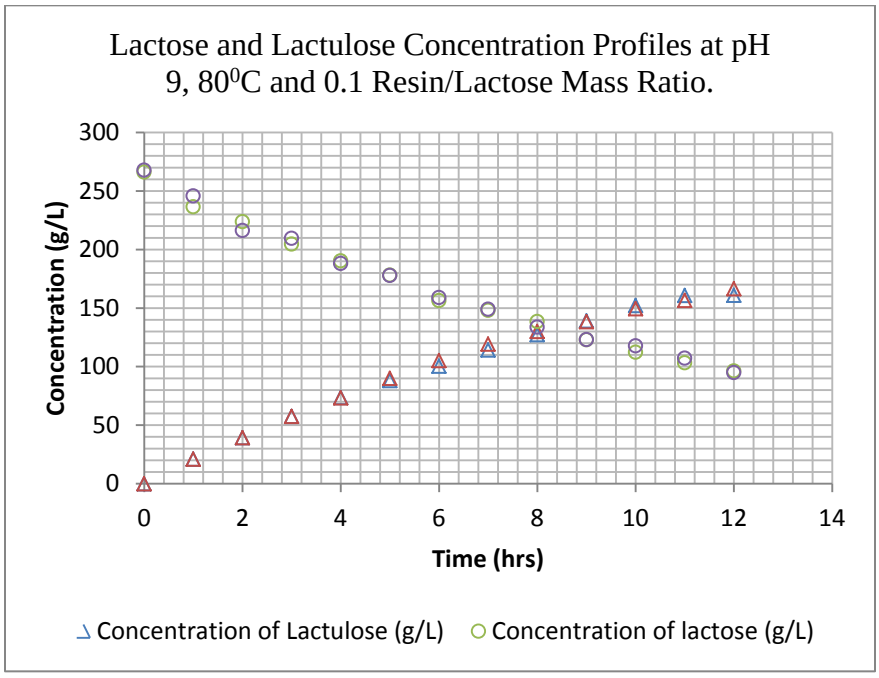

Figure 5.12. Lactose and Lactulose Concentration Profiles at pH 9, 80^{0}C and 0.1 Resin/Lactose Ratio.

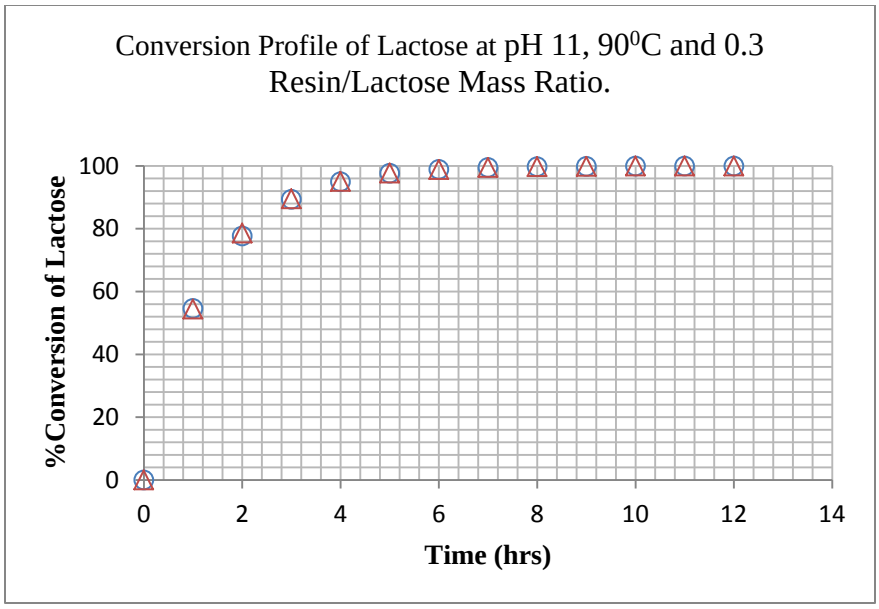

Figure 5.13. Conversion Profile of Lactose at pH 11, 90^0C and 0.3 Resin/Lactose Ratio.

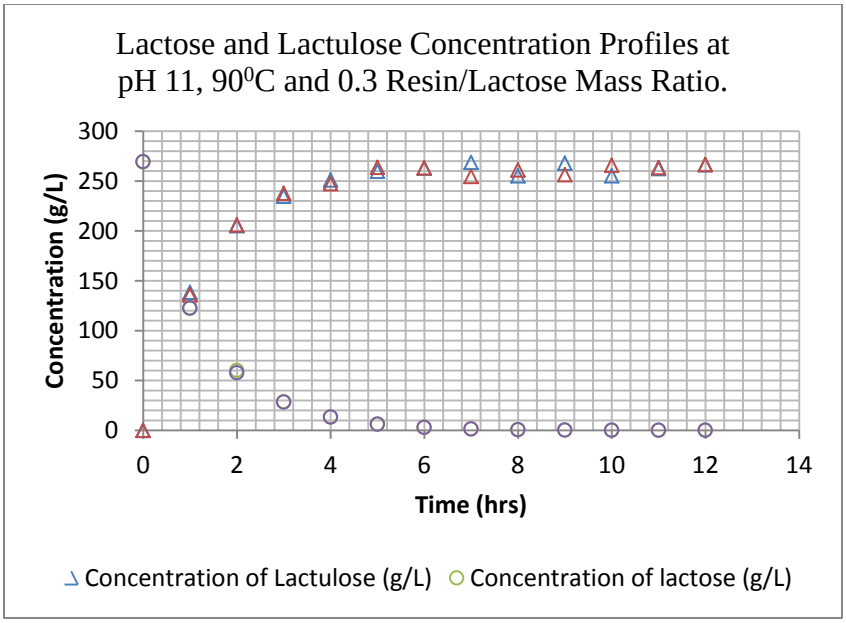

Figure 5.14. Lactose and Lactulose Concentration Profiles at pH 11, 90^0C and 0.3 Resin/Lactose Ratio.

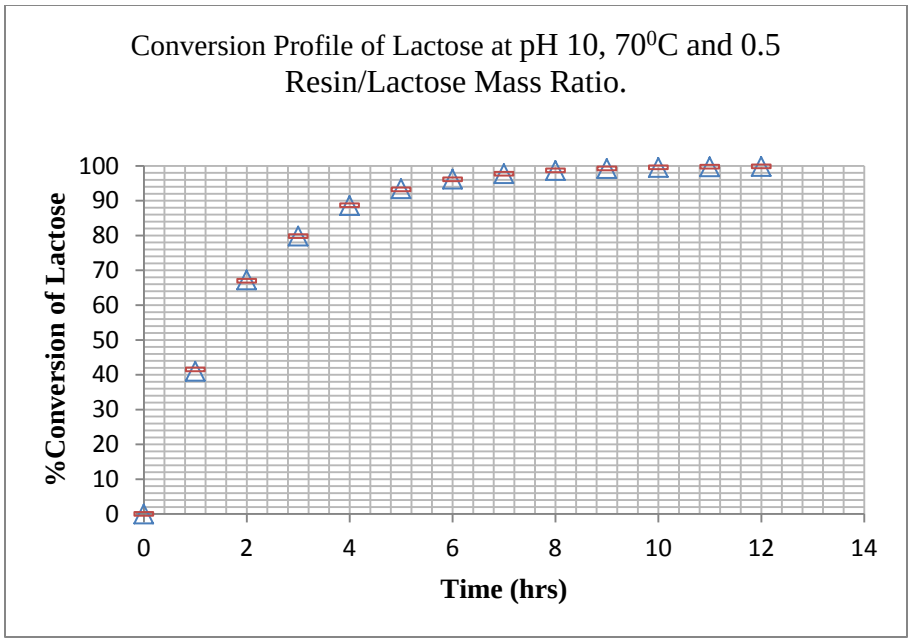

Figure 5.15. Conversion Profile of Lactose at pH 10, 70^{0}C and 0.5 Resin/Lactose Ratio.

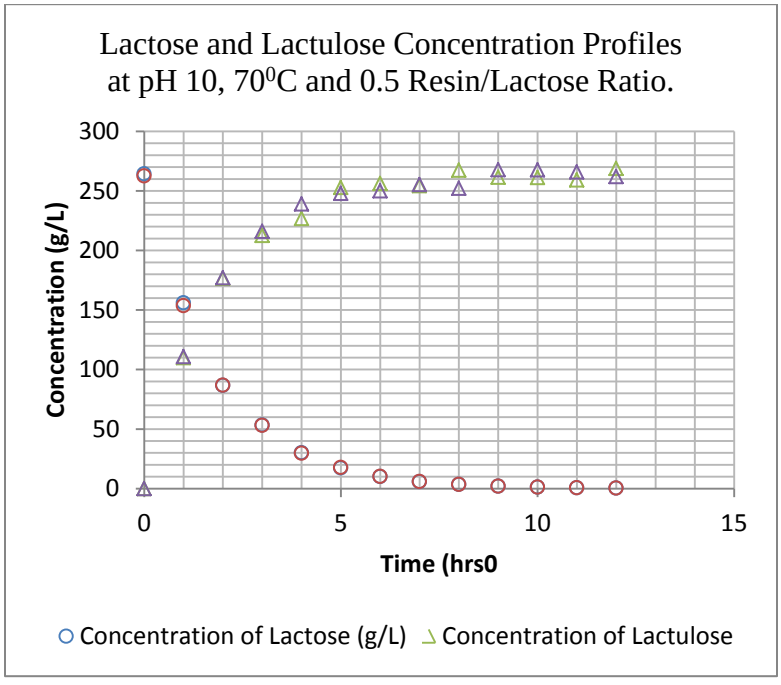

Figure 5.16. Lactose and Lactulose Concentration Profiles at pH 10, 70^{0}C and 0.5 Resin/Lactose Ratio.

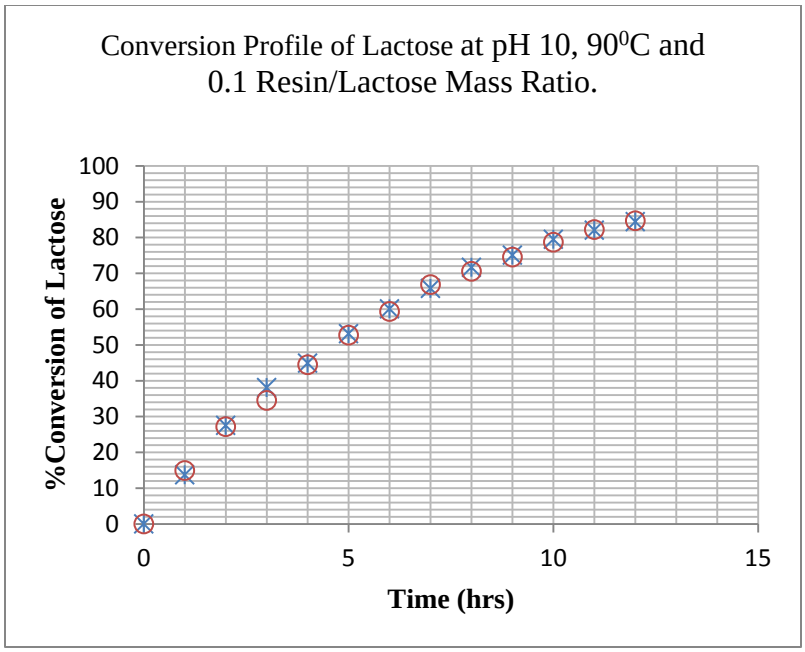

Figure 5.17. Conversion Profile of Lactose at pH 10, 90^0C and 0.1 Resin/Lactose Ratio.

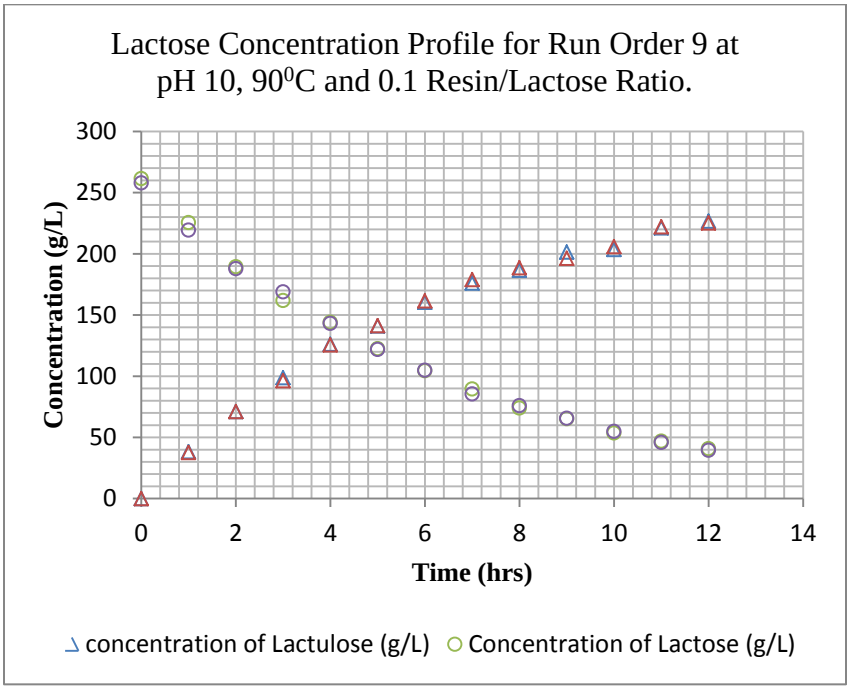

Figure 5.18. Lactose Concentration Profile for Run Order 9 at pH 10, 90^0C and 0.1 Resin/Lactose Ratio.

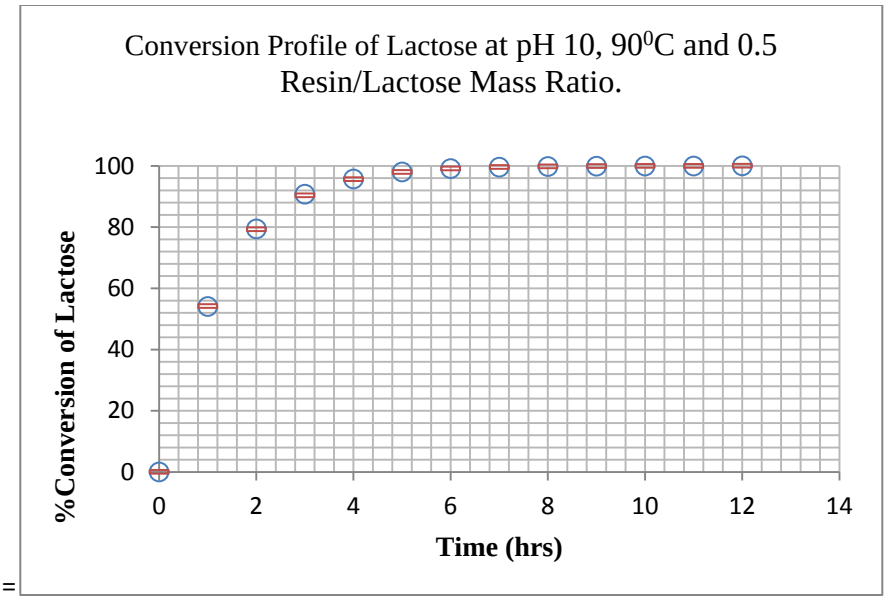

Figure 5.19. Conversion Profile of Lactose at pH 10, 90^{0}C and 0.5 Resin/Lactose Ratio.

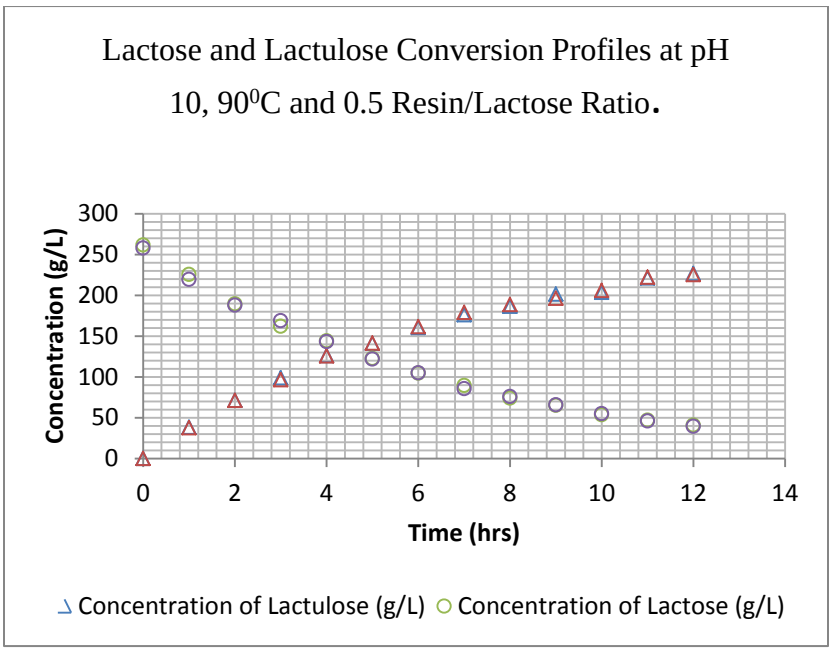

Figure 5.20. Lactose and Lactulose Conversion Profiles at pH 10, 90^{0}C and 0.5 Resin/Lactose Ratio.

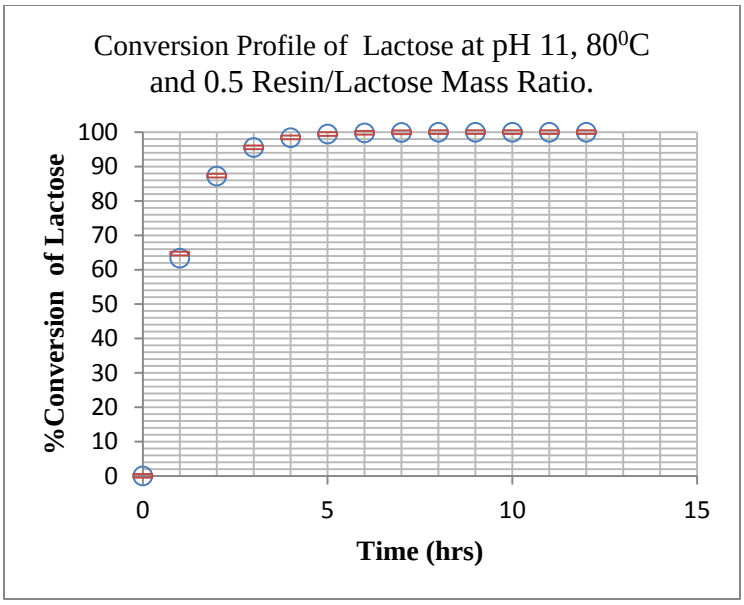

Figure 5.21. Conversion Profile of Lactose at pH 11, 80^{0}C and 0.5 Resin/Lactose Ratio.

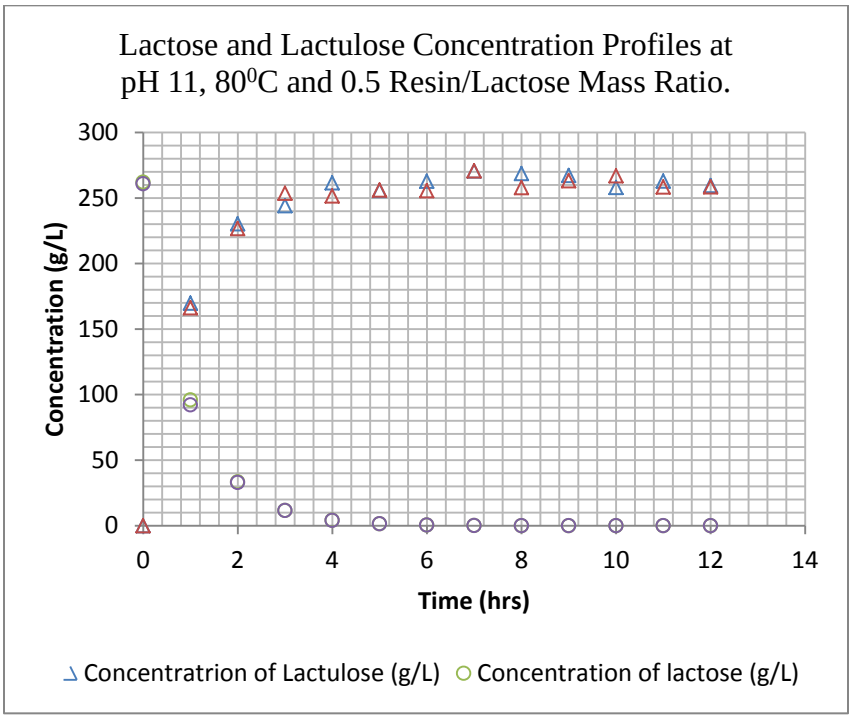

Figure 5.22. Lactose and Lactulose Concentration Profiles at pH 11, 80^{0}C and 0.5 Resin/Lactose Ratio.

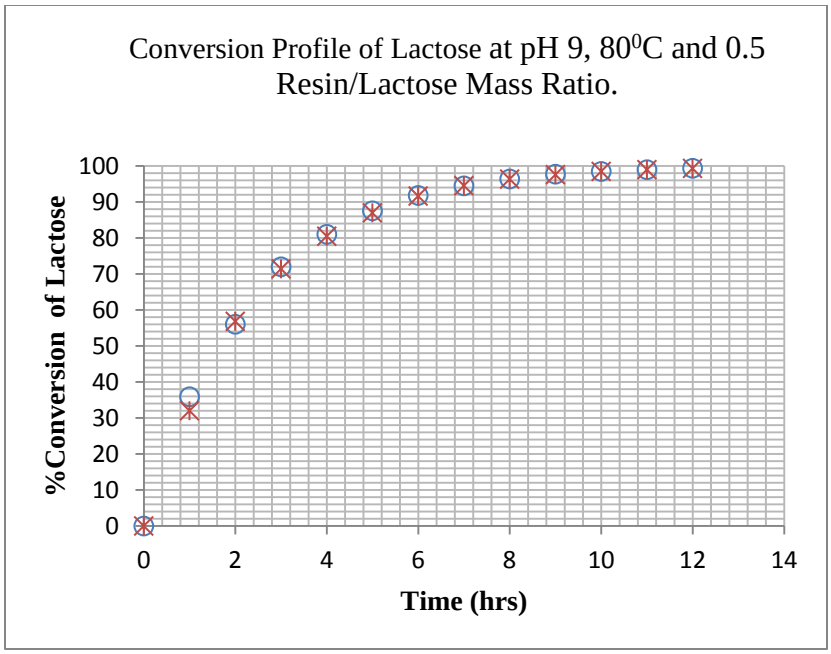

Figure 5.23. Conversion Profile of Lactose at pH 9, 80^{0}C and 0.5 Resin/Lactose Ratio.

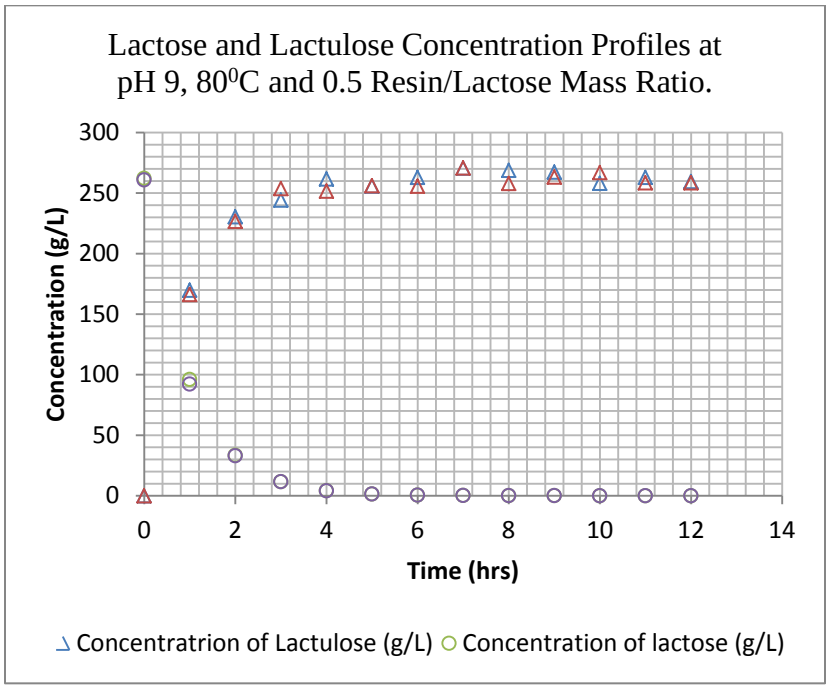

Figure 5.24. Lactose and Lactulose Concentration Profiles at pH 9, 80^{0}C and 0.5 Resin/Lactose Ratio.

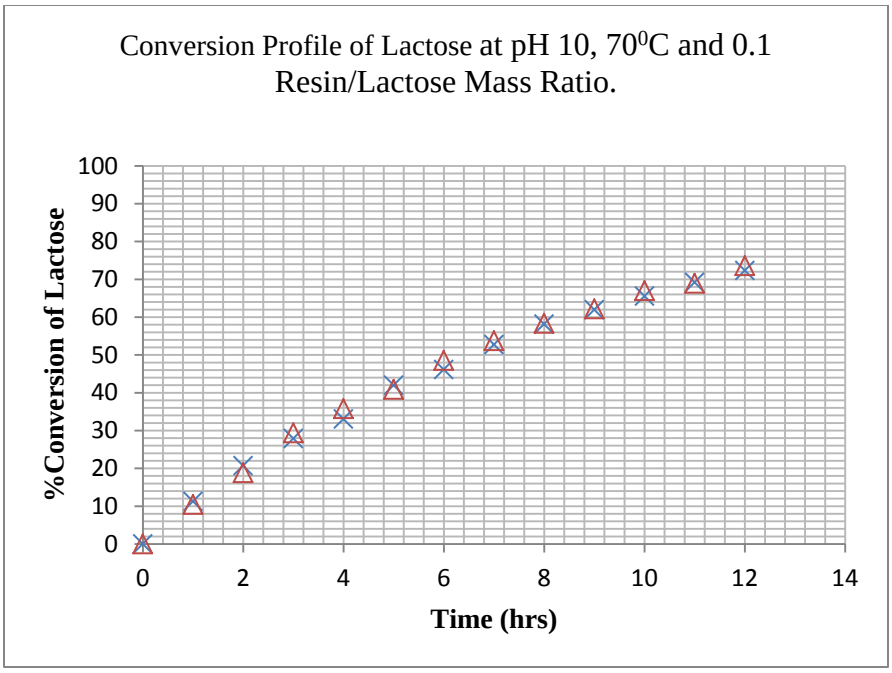

Figure 5.25. Conversion Profile of Lactose at pH 10, 70^{0}C and 0.1 Resin/Lactose Ratio.

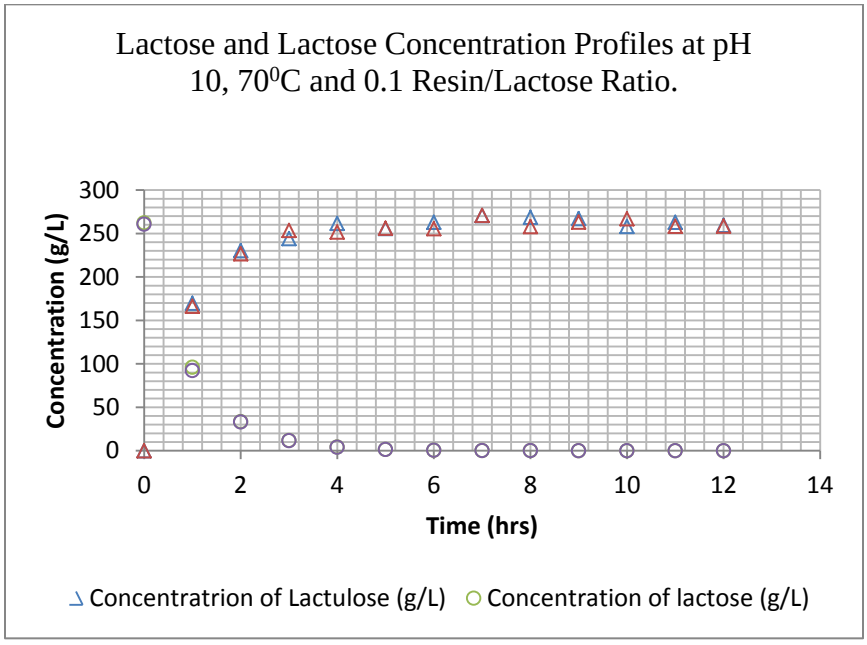

Figure 5.26. Lactose and Lactose Concentration Profiles at pH 10, 70^{0}C and 0.1 Resin/Lactose Ratio.

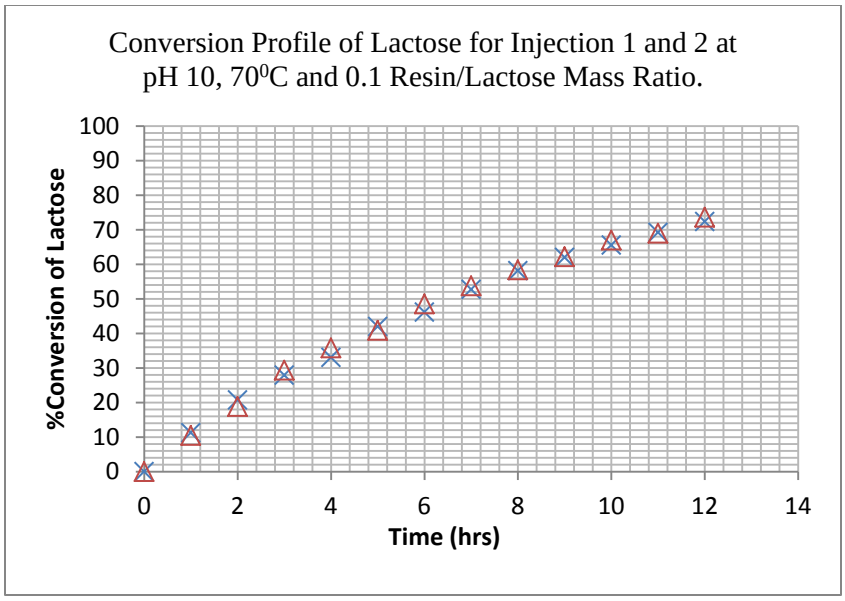

Figure 5.27. Conversion Profile of Lactose at pH 10, 70^{0}C and 0.1 Resin/Lactose Ratio.

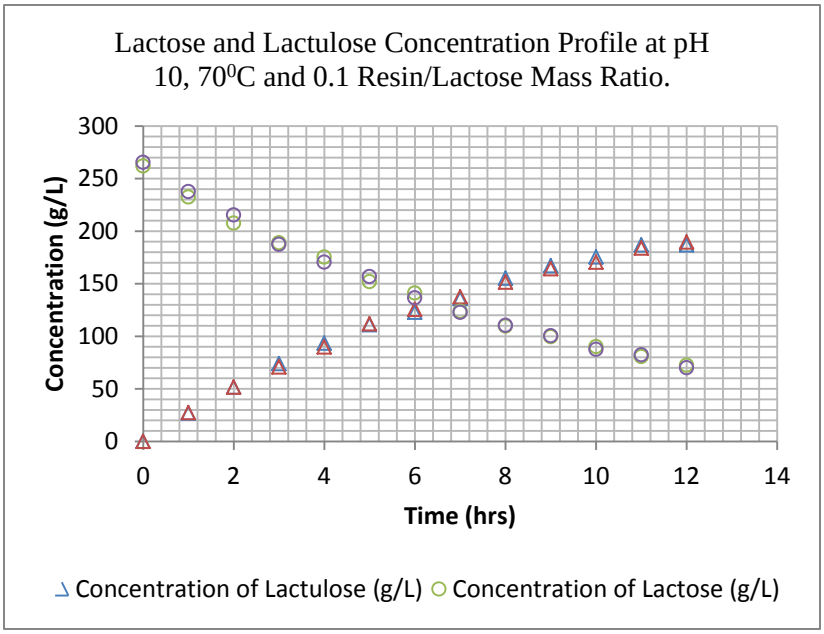

Figure 5.28. Lactose and Lactulose Concentration Profile at pH 10, 70^{0}C and 0.1 Resin/Lactose Ratio.

The treatment combinations were run with a total reaction time of 12 hrs but statistical analyses used the 7 hr conversion as the response variable. This is due to the near complete conversion of lactose for a number of the experimental runs. The data for 12 hrs of reaction time was used to estimate the parameters in the kinetic model. Table 5.1 shows the mean conversion in each experimental run at 7 hrs of reaction time.

JMP®7.0.1 was used to analyze the main experimental design. The analysis uses a full second order model in the factors. Figure 5.29 shows a plot of the residuals at the various conversion levels. The plot shows that the errors are randomly and independently distributed. Figure 5.30, shows a normal probability plot of the residuals. The plot indicates that the data is normally distributed as the points in the plot form a near linear pattern. Figure 5.29 and Figure 5.30 verify the constant variance and normality assumptions made for the ANOVA analysis. Table 5.2 is the ANOVA table for the experimental data. All relevant hypotheses are tested in a logical order at a significance level of 0.05

Table 5.1. Calculated Response for Each Treatment Combination at 7 hrs of Reaction Time.

Run Order	Pattern	T	Ratio	pH	Conversion
1	+ 0 -	90	0.3	9	87.4
2	0 0 0	80	0.3	10	93.7
3	- 0 -	70	0.3	9	76.0
4	0 - +	80	0.1	11	84.9
5	- 0 +	70	0.3	11	97.3
6	0 - -	80	0.1	9	44.3
7	+ 0 +	90	0.3	11	99.5

Table 5.1 (Contd). Calculated Response for Each Treatment Combination at 7 hrs of Reaction Time.

8	- + 0	70	0.5	10	97.7
9	+ - 0	90	0.1	10	66.3
10	+ + 0	90	0.5	10	99.6
11	0 + +	80	0.5	11	99.9
12	0 + -	80	0.5	9	94.4
13	0 0 0	80	0.3	10	93.7
14	- - 0	70	0.1	10	53.3
15	0 0 0	80	0.3	10	93.6

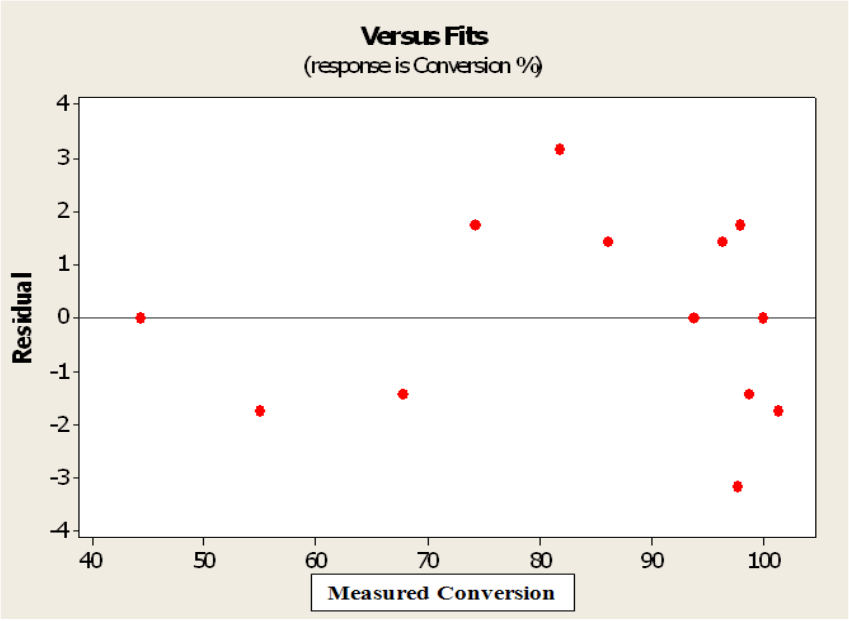

Figure 5.29. Variation of Residuals at each Conversion.

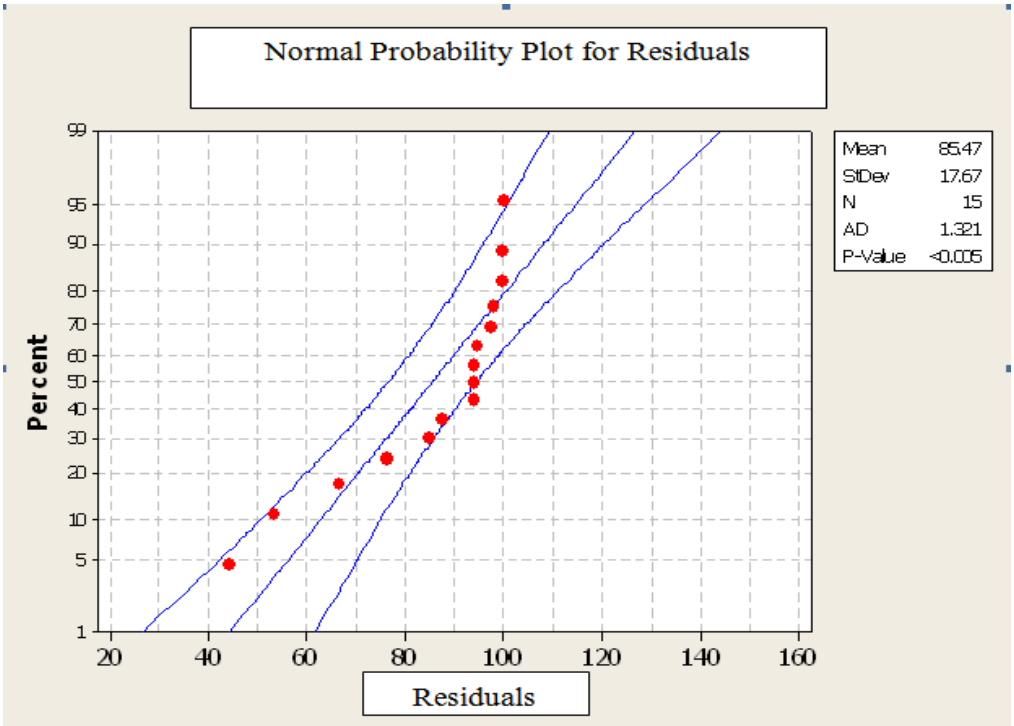

Figure 5.30. Normal Probability Plot for Residuals.

The analysis of variance, Table 5.2, demonstrates that the model is highly significant (P=0.0001). The correlation coefficient (R^2) gives information about the explained variance (variance between two groups due to the experimental variable) in the data but it does not give information about the unexplained variance (variance within the group). The root mean square error (RMSE) encapsulates the standard deviation of the unexplained variance and the low value (RMSE = 2.84) shows the good prediction ability of the model. The low pure error (0.008) also reinforces the model's good predictive nature. The coefficients are calculated and tested for their significance using JMP®7.0.1. The main effects, interaction effects and the respective coefficients are given in Table 5.3.

Table 5.2. ANOVA Table for the Experimental Design.

Source	Degrees of Freedom	Sum of Squares	Mean Square	F Ratio	Prob > F
Model	9	4328	481	59.7	0.0001
Total error	5	40.3	8.06		
Lack of fit	3	40.3	13.4	3390	0.0003
Pure Error	2	0.008	0.004		
Total	14	4369			
R^2	0.991				
RMSE	2.84				

Table 5.3. Effects Test and Coefficient Estimates.

Term	Coefficient	Estimate	Std Error	Prob > F
Intercept	β_0	93.6894	1.6389	< 0.0001
Temp (X_1)	β_1	3.5639	1.00362	0.0164
Resin/Lactose (X_2)	β_2	17.86478	1.00362	< 0.0001
pH (X_3)	β_3	9.914636	1.00362	0.0002

Table 5.3 (Contd). Effects Tests and Coefficient Estimates.

Temp*Resin/Lactose	β_{12}	-2.80457	1.41933	0.1051
Resin/Lactose*pH	β_{23}	-8.76939	1.41933	0.0016
Temp*pH	β_{13}	-2.32212	1.41933	0.1628
Temp*Temp	β_{11}	-2.6457	1.477288	0.1333
Resin/Lactose*Resin/Lactose	β_{22}	-11.81228	1.477288	0.0005
pH*pH	β_{33}	-0.967775	1.477288	0.5413

From Table 5.3, the P values of β_0, β_1, β_2, β_3, β_{23} and β_{22} are statistically significant indicating that temperature (X_1), resin/lactose mass ratio (X_2), pH (X_3), and the resin/lactose*pH interaction effect (X_2*X_3) are each significant ($P<0.05$). Figure 5.31 shows the interaction profiles. It can be observed from the figure that there is no significant Temperature*resin/lactose and Temperature*pH interactions as the plots are parallel to each other. On the other hand the interaction profile shows that there is significant resin/lactose*pH interaction. These results are also supported by the effects test results shown in Table 5.3. By using only the significant coefficients from Table 5.3, Equation (38) would be the second degree model explaining the percentage conversion of lactose as a function of the variables temperature (X_1), resin/lactose mass ratio (X_2) and pH (X_3).

$$\% \text{ Conversion } = 93.6894 + 3.5639X_1 + 17.86478X_2 + 9.914636X_3 - 8.769398X_2X_3 - 11.81228X_2^2 \quad (38)$$

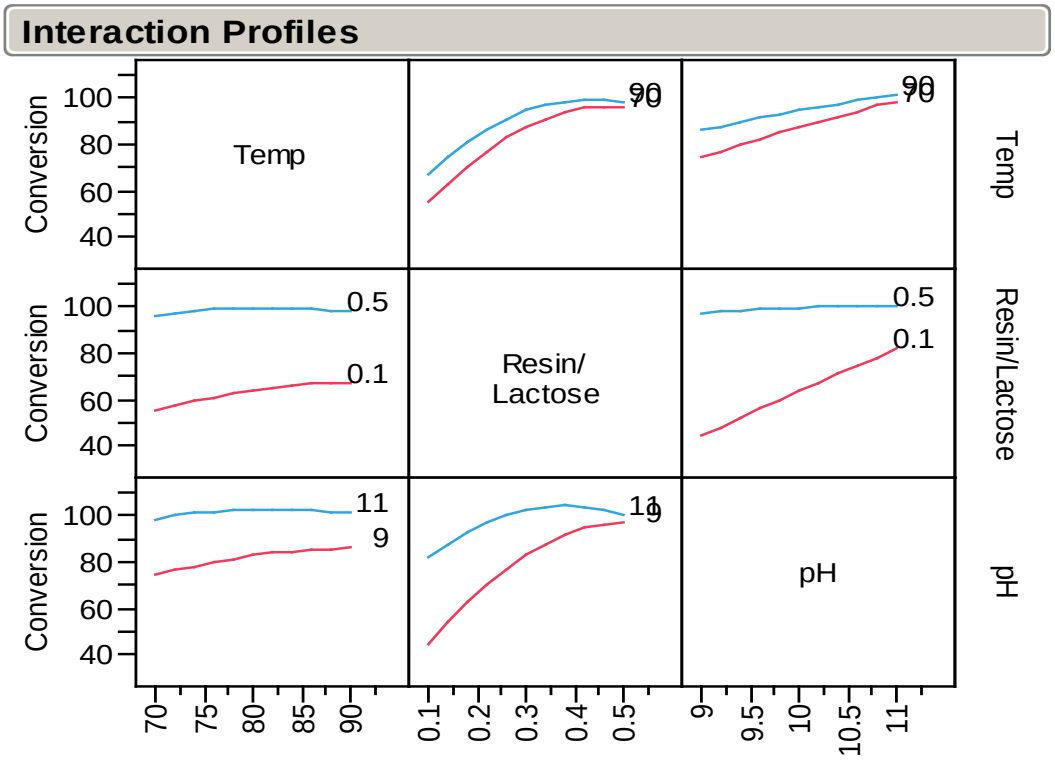

Figure 5.31. Interaction Effect Profiles.

Figure 5.32 shows the main effects plot for lactose conversion. Although each factor is significant, it can be observed from the plots that temperature does not affect the conversion as much as the other factors. The small slope of the main effect plot for temperature indicates that the response does not considerably change by varying temperature at constant values of the other factors. The larger slopes associated with the resin/lactose and pH main effect plots

indicate a stronger influence on conversion over temperature. Temperature is still considered in the model as it was statistically significant at $\alpha = 0.05$.

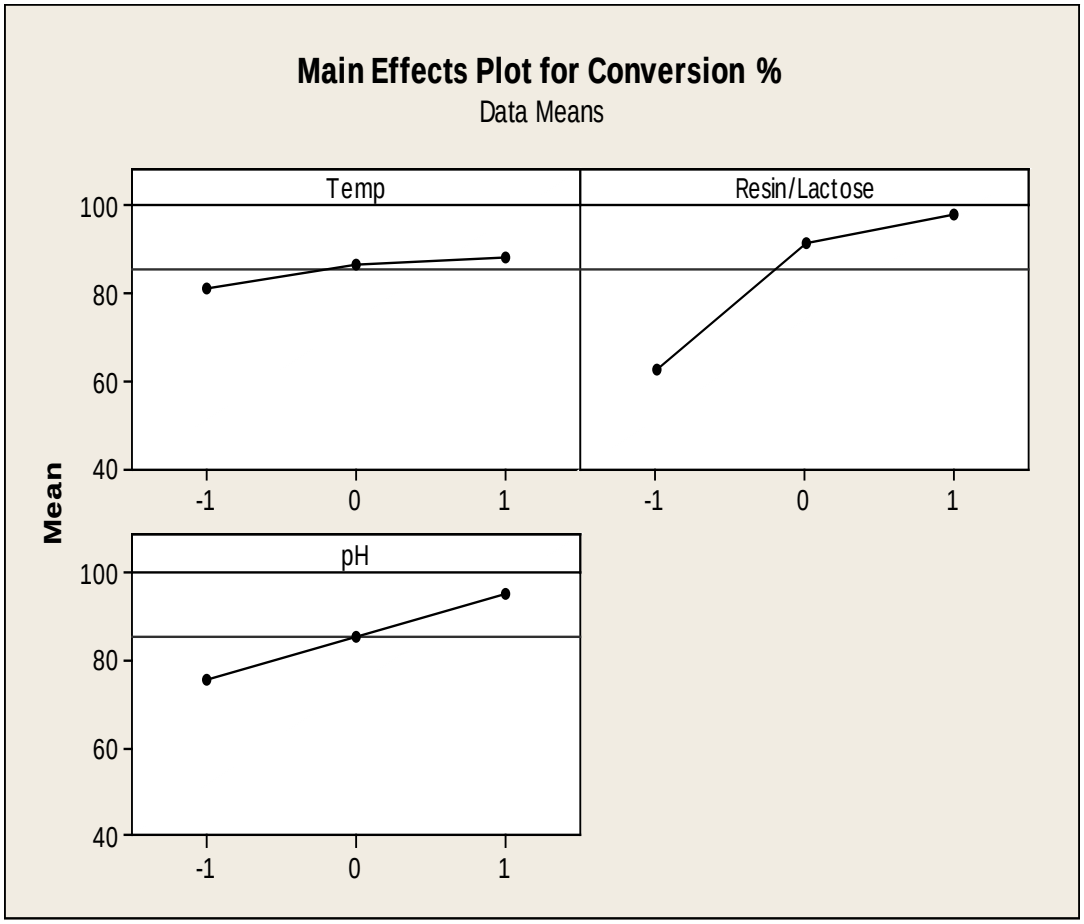

Figure 5.32. Main Effects Plot.

Figure 5.33, Figure 5.34 and Figure 5.35 show the response surface plots at each temperature. The response surfaces were plotted using MATLAB and the code is given in Appendix D. The temperature effect is clearly evident from the surface plots as the major area of the surface at $T=90^0C$ falls within the range of 80% to 100% of conversion.

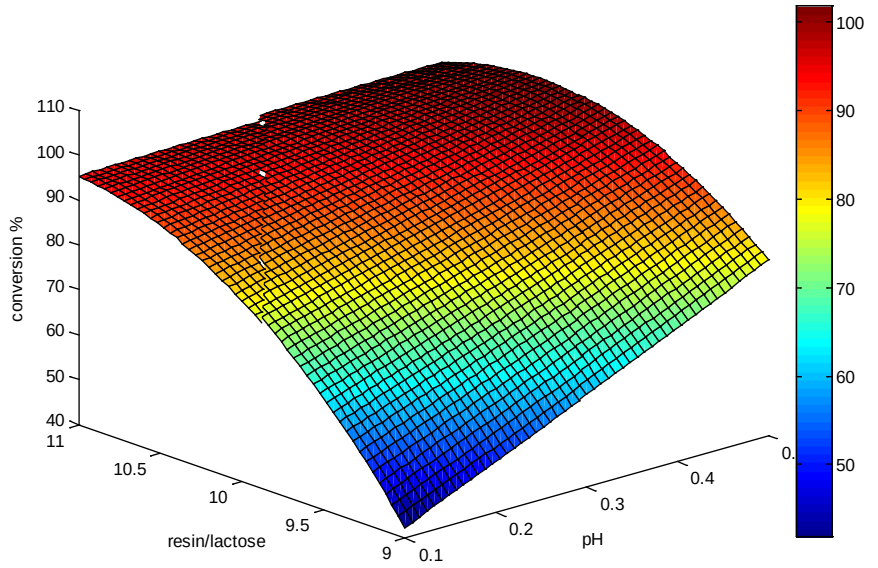

Figure 5.33. Response Surface for Conversion at 70^0C.

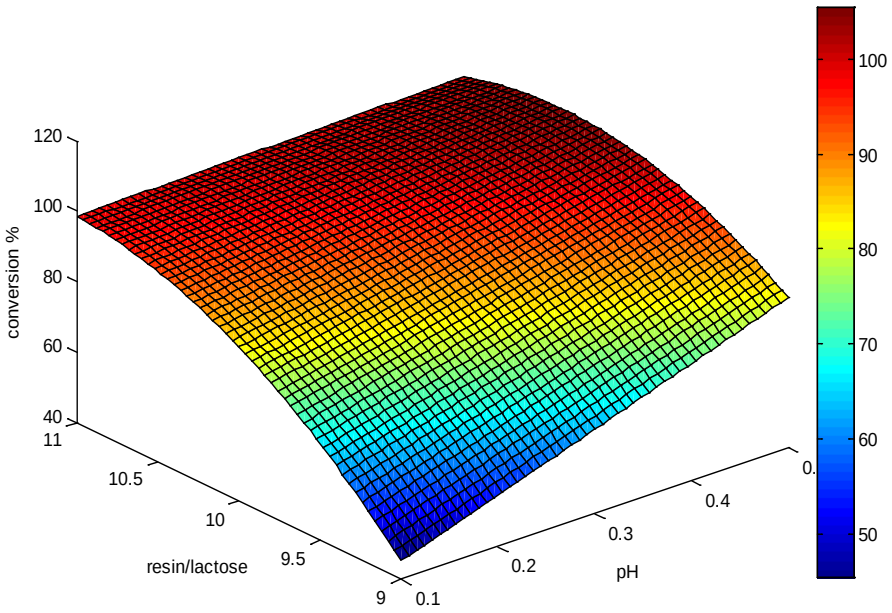

Figure 5.34. Response Surface for Conversion at 80^0C.

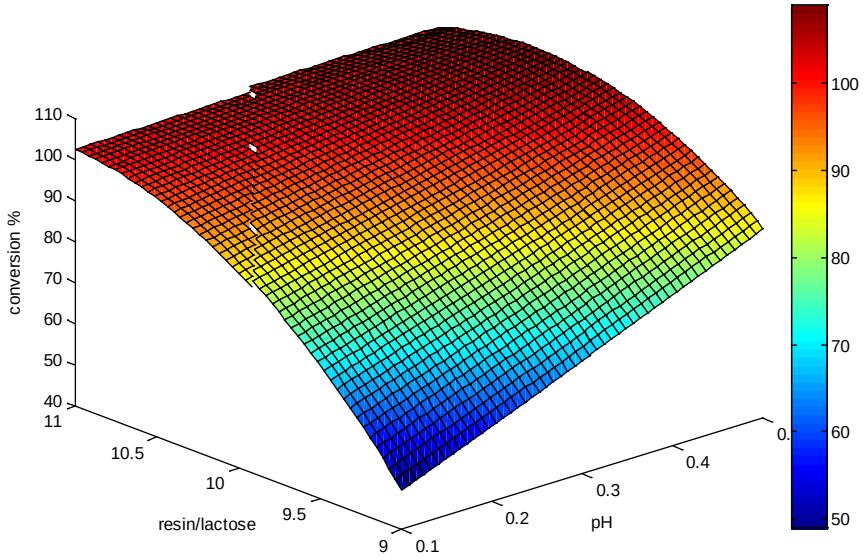

Figure 5.35. Response Surface for Conversion at 90^0C.

Equation (38), predicts the optimal operating conditions. The results from the canonical analysis of the response surface based on the coded data are shown in Table 5.4.

Table 5.4. Results of Canonical Analysis of the Response Surface Based on Coded Data.

Factor	Critical value	
	Coded	Un-Coded
Temperature	0.746590	87.465895
Resin/Lactose	1.322071	0.564414
pH	-1.763224	8.236776
Predicted value of response at stationary point: 98.088192 %		

Table 5.5 gives the critical values of the factors at the stationary point and also the predicted response at that point. Table 5.5 shows that the eigenvalues of the factors have different signs, which indicates that the stationary point is a saddle point.

Table 5.5. Eigenvalues Calculated by Canonical Analysis.

Eigenvalues	Eigenvectors		
	Temperature	Resin/Lactose	pH
0.708172	-0.195374	-0.304588	0.932231
-2.504000	0.968542	-0.209312	0.134595
-13.629922	0.154131	0.929201	0.335901

As the stationary point is a saddle point, the estimated surface does not have a unique optimum and a ridge analysis was carried out using SAS to find the optimum operating conditions yielding maximum response (conversion). Table 5.6 shows the estimated ridge of maximum response for variable conversion. The ridge analysis indicates that the conversion would reach maximum (100%) at approximately 80.8^0C, 0.37 resin/lactose mass ratio and a pH of 10.3 (values at coded radius 0.5 in Table 5.6). Figure 5.36, Figure 5.37 and Figure 5.38 show the contour plots. The values close to the optimum values attained in ridge analysis can be observed in Figure 5.37.

Table 5.6. Estimated Ridge of Maximum Conversion.

Coded radius	Estimated response %	Standard error %	Uncoded factor values		
			Temperature	Resin/Lactose	pH
0.0	93.7	1.60	80.0	0.30	10.0
0.1	95.6	1.63	80.2	0.32	10.0
0.2	97.3	1.62	80.3	0.33	10.1
0.3	98.7	1.59	80.5	0.35	10.2
0.4	99.9	1.57	80.7	0.36	10.2
0.5	100.9	1.54	80.8	0.37	10.3
0.6	101.7	1.52	80.8	0.38	10.4
0.7	102.3	1.51	80.8	0.38	10.6
0.8	102.9	1.53	80.7	0.37	10.7
0.9	103.5	1.60	80.6	0.37	10.8
1	104.1	1.73	80.4	0.36	10.9

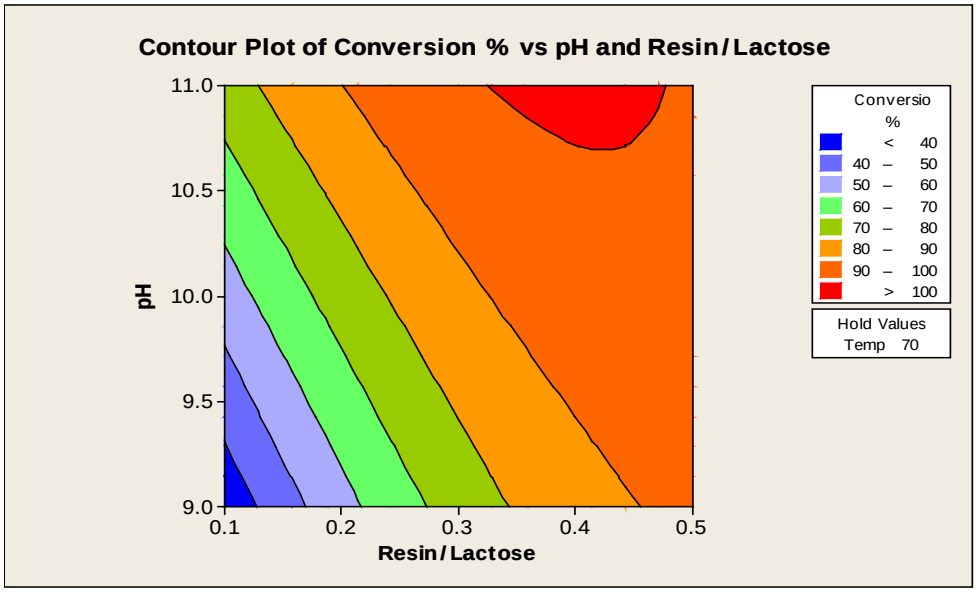

Figure 5.36. Contour Plot of Conversion of Lactose vs pH and Resin/Lactose Ratio at 70^0C.

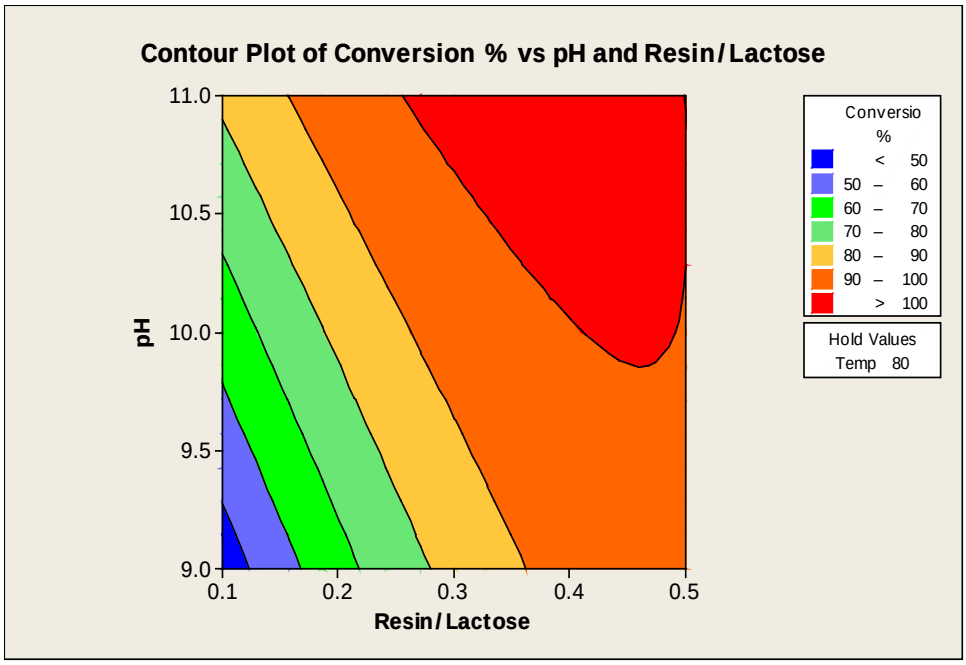

Figure 5.37. Contour Plot of Conversion of Lactose vs pH and Resin/Lactose Ratio at 80^0C.

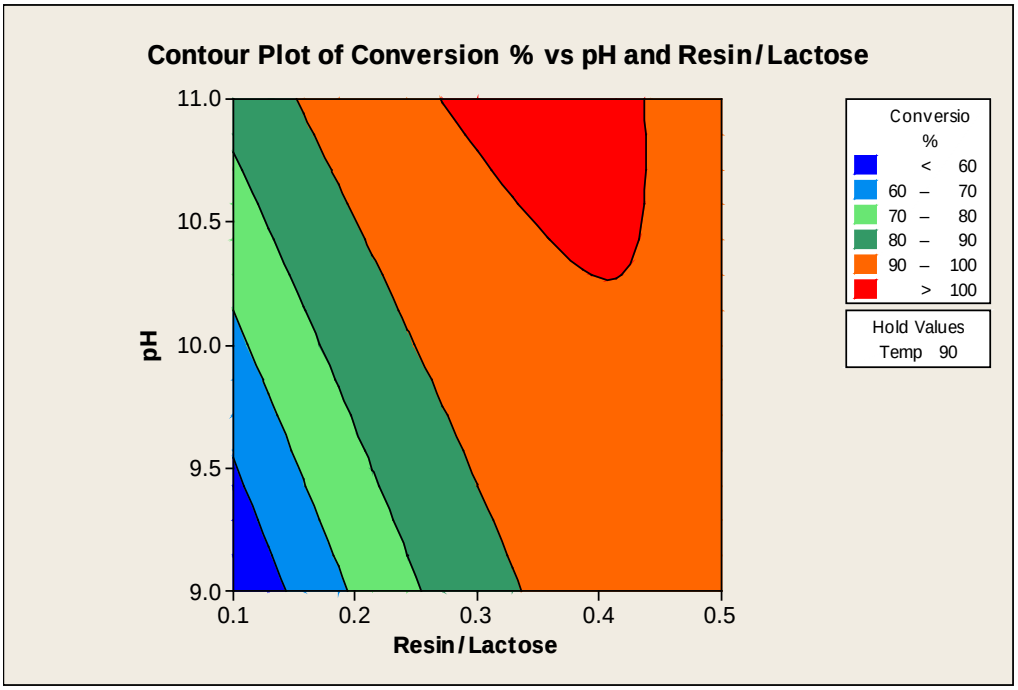

Figure 5.38. Contour Plot of Conversion of Lactose vs pH and Resin/Lactose Ratio at 90^0C.

The analysis uses the simplified LHHW model discussed in Section 2.3 as shown below.

$$r_{lu} = -r_L = \frac{k_1 k_2 R_0 w L}{(1 + k_1 L)} \tag{39}$$

The approach is to assume values for the equilibrium adsorption parameter, K_1, the pre-exponential factor, A_0 $\left(\frac{1}{\text{hr}}\right)$, and the activation energy, E_A $\left(\frac{\text{kJ}}{\text{mole of lactose}}\right)$; then compute the corresponding reaction time according to the integrated analytical expression shown below for each of the measured lactose concentrations.

$$\frac{1}{k_1 A_0 e^{\left(\frac{-E_a}{RT}\right)} R_0 w} \ln\left(\frac{L}{L_0}\right) + \frac{1}{k_1}(L - L_0) = -t \quad (40)$$

The sum of the squares of the residual between the computed reaction time and the sample time for each concentration is then computed. Values of the assumed parameters are then adjusted using the Excel SOLVER tool to minimize the sum of squared residuals. The experimental data at pH 10, which includes the center replicates of the design, were first used to determine regressed values of the parameters. The values of the activation energy (E_a=19.05$\frac{kJ}{\text{mole Lactose}}$), and of the adsorption coefficient (K_1= 6.47 x 10^{-5}) were fixed and the data at pH 9 and pH 11 were then used to regress values of the pre-exponential factor, A_0, at each pH respectively. The parameters estimated by least squares method at pH 9, 10 and 11 are shown in Table 5.7. The root mean square error (RMSE) and R-square values for nonlinear regression at each pH are shown in Table 5.8, Table 5.9 and Table 5.10.

Table 5.7. Parameters Estimated for an Activation Energy of 19.05$\frac{kJ}{\text{mole Lactose}}$ and an Adsorption Constant of 6.47 x 10^{-5} at Each Value of pH.

pH	Pre-exponential factor $\left(\frac{1}{hr}\right)$
9	4.91 x 10^7
10	7.699 x 10^7
11	13.349 x 10^7

Table 5.8. RMSE and R-Square Values of Regression at pH 9.

R-Square	0.999
RMSE	0.167

Table 5.9. RMSE and R-Square Values of Regression at pH 10.

R-Square	0.999
RMSE	0.0914

Table 5.10. RMSE and R-Square Values of Regression at pH 11.

R-Square	0.985
RMSE	0.886

The low RMSE values for each case indicate that the model has good prediction ability. Figure 5.39, Figure 5.40, Figure 5.41, Figure 5.42, Figure 5.43 and Figure 5.44 show the experimental data vs. predicted data plots for each pH level. It can be observed form these plots that the experimental data fits the kinetic model. The parameter estimation procedure determined the activation energy, E_a= 19.5 kJ/mole of lactose, the adsorption coefficient $K_1 = 6.47 \times 10^{-5}$ and pre-exponential factor of $A_0 = 4.91 \times 10^7 \frac{1}{\text{hr}}$ at pH = 9, $A_0 = 7.69 \times 10^7 \frac{1}{\text{hr}}$ at pH = 10 and $A_0 = 13.3 \times 10^7 \frac{1}{\text{hr}}$ at pH = 11. It is observed that the pre-exponential factor (A_0) increases with pH and Figure 5.45 illustrates the near linear a plot of $\ln(A_0)$ with pH. The plot gives equation of the regressed line as shown below.

$$\ln(A_0) = 0.5\,\text{pH} + 13.2 \tag{41}$$

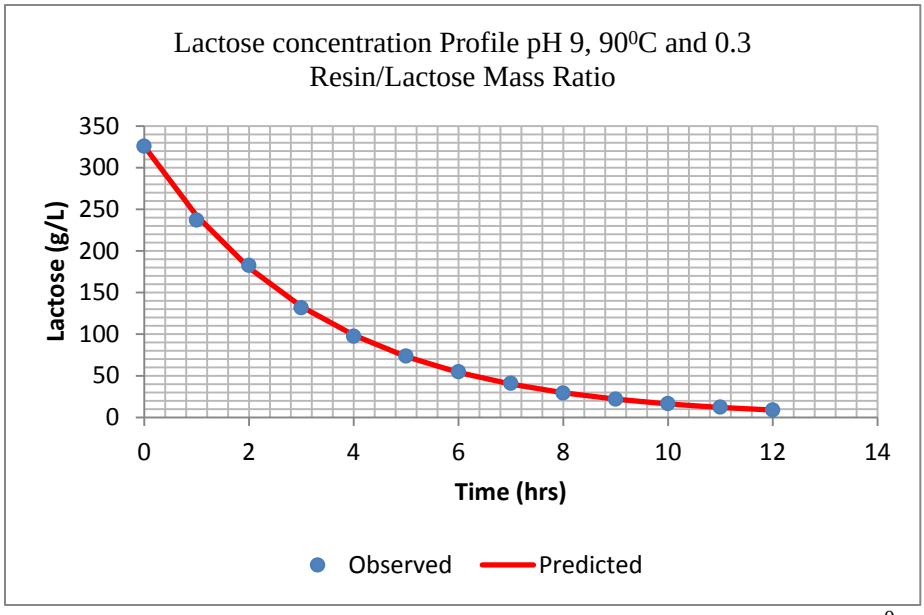

Figure 5.39. Observed vs Predicted Plot of Lactose Concentration at pH 9, 90^{0}C and 0.3 Resin/Lactose Ratio.

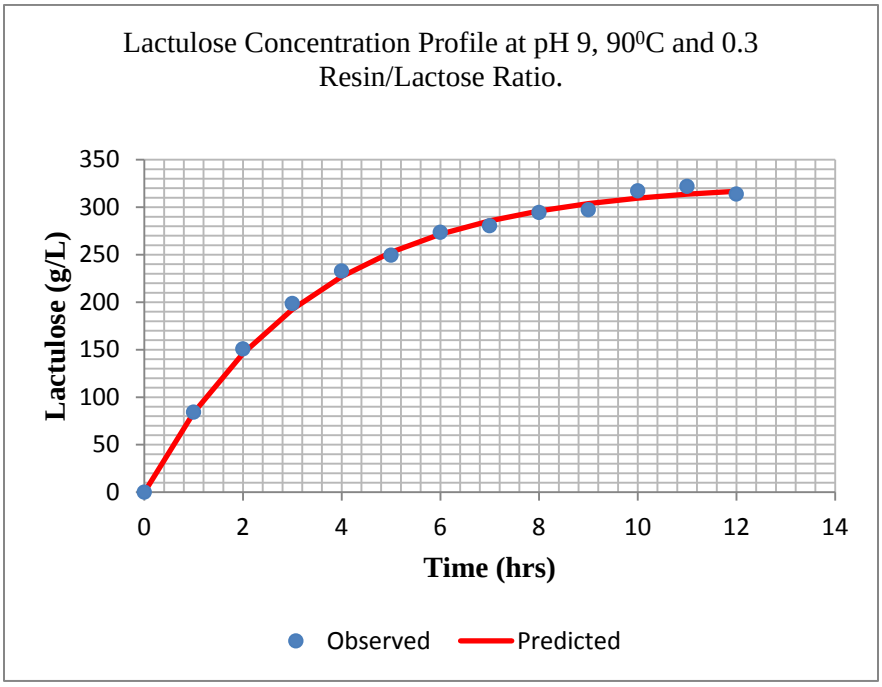

Figure 5.40. Observed vs Predicted Plot of Lactulose Concentration at pH 9, 90^{0}C and 0.3 Resin/Lactose Ratio.

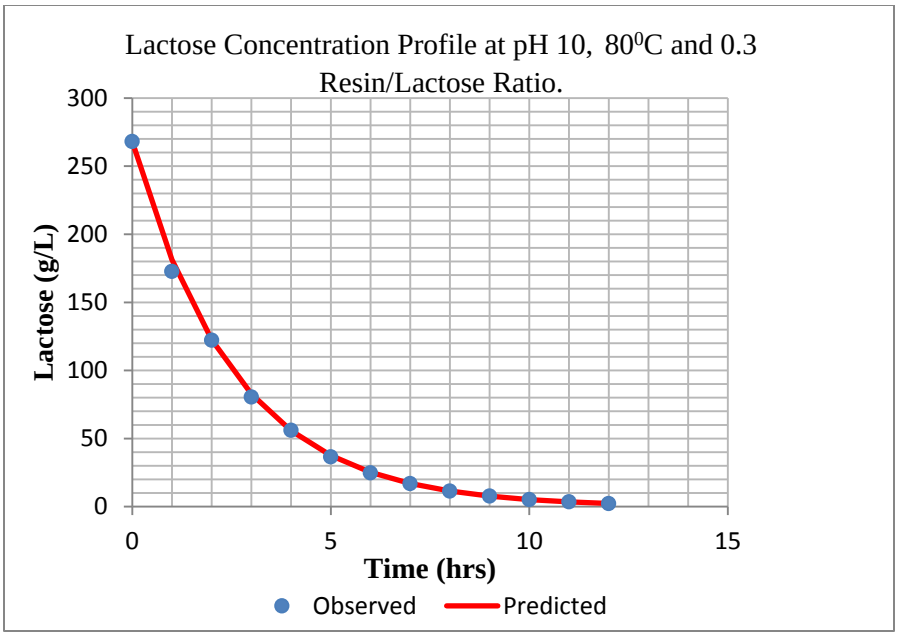

Figure 5.41. Observed vs Predicted Plot of Lactose Concentration at pH 10, 80^{0}C and 0.3 Resin/Lactose Ratio.

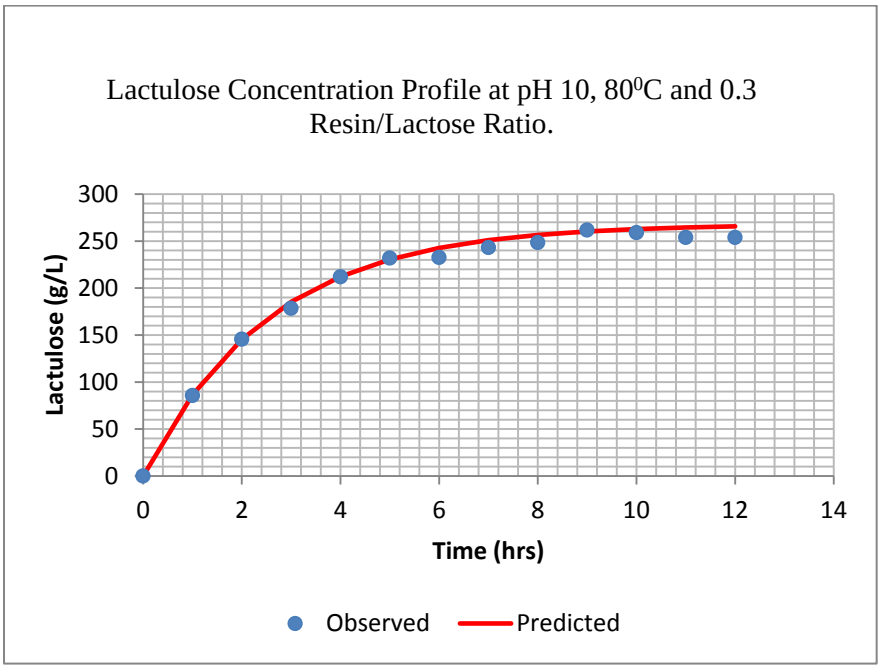

Figure 5.42. Observed vs Predicted Plot of Lactulose Concentration at pH 10, 80^{0}C and 0.3 Resin/Lactose Ratio.

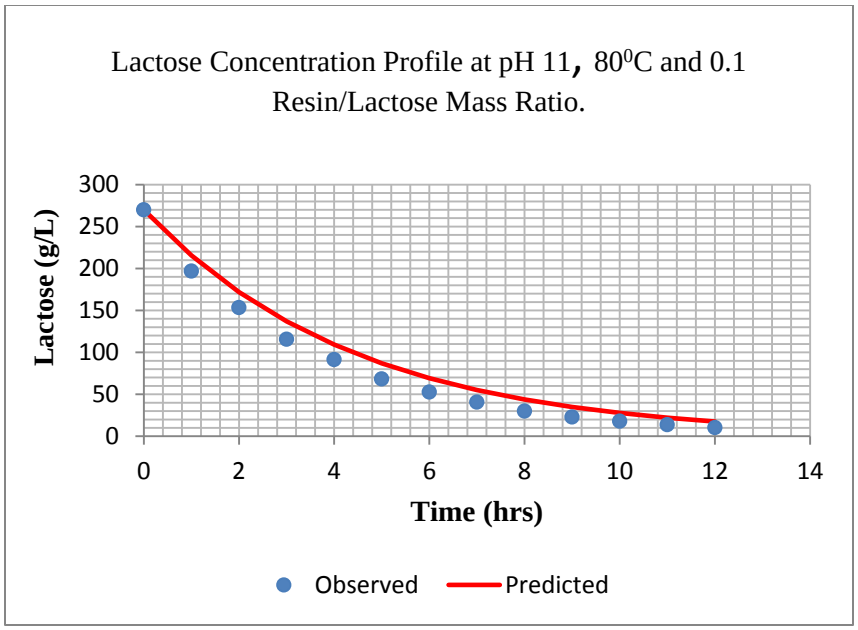

Figure 5.43. Observed vs Predicted Plot of Lactose Concentration at pH 11, 80^{0}C and 0.1 Resin/Lactose Ratio.

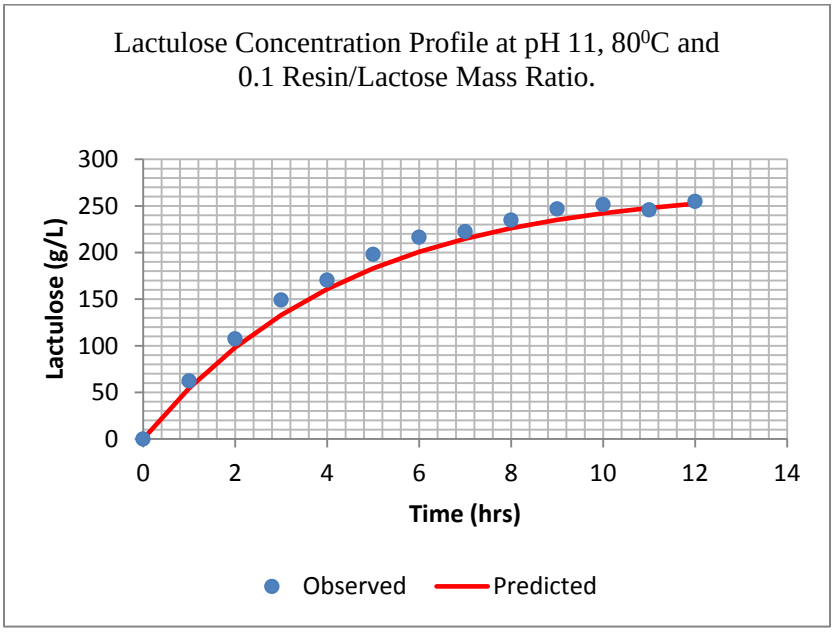

Figure 5.44. Observed vs Predicted Plot of Lactulose Concentration at pH 11, 80^{0}C and 0.1 Resin/Lactose Ratio.

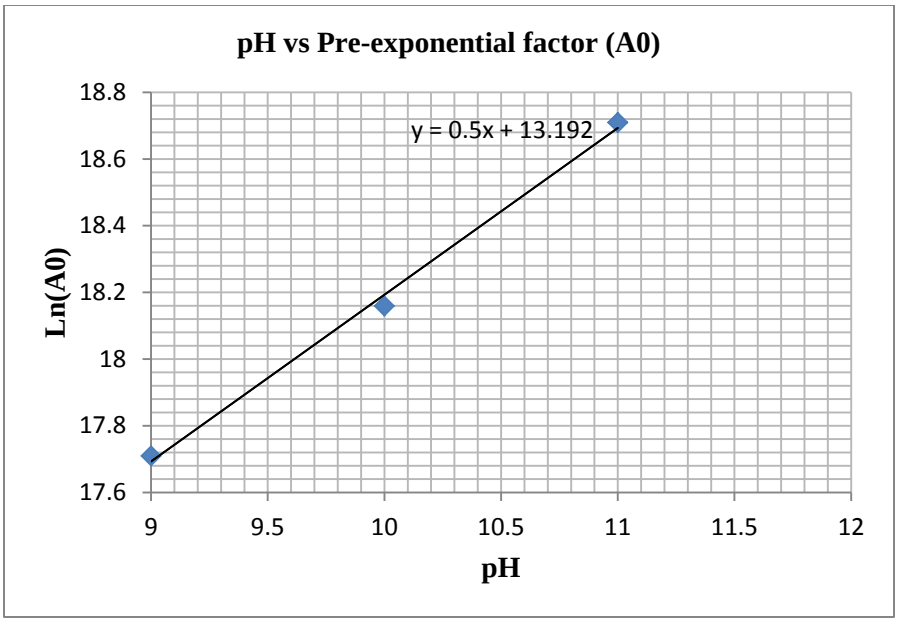

Figure 5.45. Plot of ln(A_0) with pH.

6 SUMMARY

The majority of Section 1 detailed the effects of internal and external diffusion resistances in heterogeneous catalytic reaction mediums, the ways of eliminating these resistances and the LHHW kinetic model based on a single site mechanism. The isomerization of lactose to lactulose follows a single site mechanism and a kinetic model was deduced. It was shown that the AMBERLITE-IRA 402 resin beads were in inactive state initially and had to be pretreated with NaOH solution to replace the chloride (Cl^-) ions with hydroxyl ions (OH^-). The resin bead diameter, effect of reaction volume on stirrer speed setting, the number of active sites in the resin and the total reaction time were studied in Section 2. It was shown that the internal diffusion resistance was eliminated as the resin beads were already small enough in as-received form and the stirrer speed setting of 7 with reaction volume of 5 mL eliminated the external diffusion resistance.

In Section 3, the Box-Behnken design and the treatment combinations were explained. The results obtained from the study revealed that the Box-Behnken design was a suitable design to optimize the operating conditions of the reaction. The second degree regression model was used to generate the response surface and the analysis of variance showed a low root mean square error (RMSE = 2.84), high coefficient of determination value (R^2 = 0.99077) and low pure error (0.08) ensuring a satisfactory prediction capability of the model. The canonical analysis revealed the stationary point to be a saddle point and the subsequent ridge analysis gave optimized operating conditions of temperature = 80.8^0C, resin/lactose mass ratio = 0.37 and pH = 10.3 for maximum

conversion of lactose. The parameters, activation energy (E_a), pre-exponential factor (A_0) and the adsorption coefficient (K_1) were estimated in chapter 4 by using least squares approximation method. The parameter estimation procedure determined the activation energy, E_a= 19.5 KJ/mole of lactose, the adsorption coefficient $K_1 = 6.47 \times 10^{-5}$ and pre-exponential factor of $A_0 = 4.91 \times 10^7 \frac{1}{\text{hr}}$ at pH = 9, $A_0 = 7.69 \times 10^7 \frac{1}{\text{hr}}$ at pH = 10 and $A_0 = 13.3 \times 10^7 \frac{1}{\text{hr}}$ at pH = 11.

The homogeneous catalysts like borates (Carubelli, 1970; Hicks, 1981; Kozempel and Kurantz,1994; Kozempel, McAloon, and Roth, 1997; Krumbbolz and Dorscheid, 1991; Mendicino, 1960; Zokaee et al., 2002a; Zokaee et al., 2002b) and calcium carbonate based catalysts (Tatdao, P., Darryl, M. S., and Frank, S, 2008) yield activation energy values of about $80\frac{\text{kJ}}{\text{mole of lactose}}$ as there would be a shift in rate control from a slow pathway to a faster pathway with change in the temperature. This is mainly due to the formation of by-products in the slow pathway. The activation energy for this reaction with AMBERLITE-IRA 402 resin is E_a=19.05 $\frac{\text{kJ}}{\text{mole of lactose}}$ and it is lower than the value for homogeneous catalysts indicating the formation of the enediol intermediate which lowers the activation energy of the reaction favoring the formation of lactulose.

7. CONCLUSION

The optimization of reaction conditions and development of akinetic model describing the isomerization reaction of lactose to lactulose with AMBERLITE-IRA 402 strong anion exchange resin were the main aims of the research. The conclusions of the research are briefed below.

7.1. OPTIMIZATION OF RESIN BEAD DIAMETER, STIRRER SPEED AND REACTION TIME

The resin bead diameter and the stirrer speed setting were studied to eliminate the internal and external diffusion resistances. The results for resin bead diameter optimization using the -20 +25 and -45 +100 size fractions are:

i) The same amount of lactulose was produced in the reaction by using the two resin sizes (the reaction conditions given in Table 3.7). Figure 3.12 in Section 3.3.3 shows the comparison of lactulose concentration profiles for the two resin sizes.

ii) The resin can be used in as-received form as there was no difference in the conversion of lactose for the different resin sizes. This proves the absence of internal diffusion resistance in the reaction.

The results for the stirrer speed test are:

i) The amount of lactulose produced was found to be essentially equal with reaction volumes of 5 mL and 3 mL at the stirrer speed setting of 7 (maximum) (the reaction conditions are given in Table 3.6). This shows that the external diffusion resistance was completely eliminated by using a 5 mL reaction volume and a stirrer speed

setting of 7. Figure 3.11 in section 3.3.3 shows the comparison of lactulose concentration profiles for the two reaction volumes.

The reaction time was optimized to achieve appreciable conversion. The results indicated that 12 hours of reaction time was enough to achieve near complete conversion. The reaction conditions and experimental data are given in Table 3.8 and Table 3.9. For the statistical analyses the conversion at 7 hours was used as the response variable.

7.2. EXPERIMENTAL DESIGN AND STATISTICAL ANALYSIS OF THE DATA

The Box-Behnken design was employed to optimize temperature (70-90^{0}C), resin/lactose mass ratio (0.1-0.5) and pH (9-11). The experimental results are given in Table 5.1. The stationary point of the response surface is a saddle point as the response surface does not have a global maximum. A ridge analysis indicates that the conversion would reach maximum (100%) at approximately 80.8^{0}C, 0.37 resin/lactose ratio and a pH of 10.3. The design shows that the following second order model is appropriate.

$$\%\,\text{Conversion} = 93.6894 + 3.5639X_1 + 17.86478X_2 + 9.914636X_3 - 8.769398X_2X_3 - 11.81228X_2^2$$

where X_1, X_2 and X_3 denote factors temperature, resin/lactose mass ratio and pH, respectively. The significant factors temperature (X_1), resin/lactose mass ratio (X_2), pH (X_3), and the resin/lactose*pH interaction effect (X_2*X_3) are included in the model and the other interaction and main effects were dropped.

7.3. REACTION KINETICS AND PARAMETER ESTIMATION

The kinetic model for the reaction derived in Section 1.4.1 was used to fit the experimental data to estimate the adsorption parameter, K_1, the pre-exponential factor, A_0, and the activation energy; E_a. The parameter estimation using the least squares approximation method resulted in activation energy, E_a, of 19.05 $\frac{\text{kJ}}{\text{mole of lactose}}$ and adsorption parameter, K_1, of 6.47 x 10^{-5}. The low RMSE values of regression at each pH indicate the good predictive nature of the kinetic model. The comparison of the experimental data and the data predicted by the kinetic model at each pH were shown in Figure 5.39, Figure 5.40, Figure 5.41, Figure 5.42, Figure 5.43 and Figure 5.44. These plots show that the experimental data fits the kinetic model deduced.

The measured data supports the following kinetic model for the reaction.

$$r_{Lu} = -r_L = \frac{K_1 k_2 R_a w L}{(1 + K_1 L)} = \frac{K_1 A_0 e^{\left(\frac{-E_a}{RT}\right)} R_a w L}{(1 + K_1 L)}$$

where

A_0: Pre-exponential constant = 4.91 x 10^7 $\frac{1}{\text{hr}}$ at pH = 9, 7.69 x 10^7 $\frac{1}{\text{hr}}$ at pH = 10 and 13.3 x 10^7 $\frac{1}{\text{hr}}$ at pH = 11,

E_A: Activation energy = 19.05$\frac{\text{kJ}}{\text{mole of lactose}}$,

R_0: Number of active sites on 1 g of -20+25 AMBERLITE IRA-402 resin = 0.116175 $\frac{\text{g equivalents}}{\text{g of resin}}$,

K_1: Adsorption constant = 6.47×10^{-5}.

The statistical analysis of the experimental design shows a root mean square error (RMSE) of the lactose conversion percentage data of 2.84.

APPENDIX A

SAMPLE CALCULATIONS FOR THE ACTIVE SITES IN AMBERLITE-IRA 402 RESIN

Sample calculations for the number of active sites in AMBERLITE-IRA 402 resin

From Table :

Molarity of the NaOH sample after pre-treatment = $m_2 = \frac{(v_1 * M_1)}{v_2} = 0.2125$ M

Weight of NaOH left in the solution after pre-treatment = $w_1 = \frac{(m_2 * 150 * 40)}{1000} = 1.275$ g

Weight of NaOH utilized by the resin = $w_2 = (\frac{M_2 * 150 * 40}{1000}) - w_1 = 4.647$ g

Number of Equivalents of NaOH used by the resin = $w_2/40 = 0.116175$ equivalents

Number of active sites on 1 g of -20+25 AMBERLITE IRA-402 resin $= 0.116175 \frac{\text{g equivalents}}{\text{g of resin}}$

APPENDIX B

HPLC CALIBRATION DATA, EXPERIMENTAL DATA FOR THE PRETREATMENT OF RESIN, STIRRER SPEED TEST AND OPTIMIZATION OF RESIN BEAD DIAMETER

Table B.1. HPLC Calibration Data.

Serial Dilution	Vial	Replicate #	Area of Lactose	Area of Lactulose
LACU-500	0	1	12.3	3831
LACU-450	1	1	409	3485
LACU-400	2	1	812	3165
LACU-350	3	1	1206	2803
LACU-300	4	1	1598	2456
LACU-250	5	1	1991	2057
LACU-200	6	1	2452	1705
LACU-150	7	1	2862	1334
LACU-100	8	1	3251	967
LACU-050	9	1	3687	553
LACU-000	10	1	4098	68.8
LACU-500	0	2	11.8	3818
LACU-450	1	2	407	3517
LACU-400	2	2	813	3167
LACU-350	3	2	1198	2793
LACU-300	4	2	1606	2468
LACU-250	5	2	1997	2060
LACU-200	6	2	2493	1736
LACU-150	7	2	2831	1317
LACU-100	8	2	3278	978
LACU-050	9	2	3615	238
LACU-000	10	2	4172	72.6
LACU-500	0	3	10.4	3902
LACU-450	1	3	411	3537
LACU-400	2	3	827	3224
LACU-350	3	3	1203	2847
LACU-300	4	3	1639	2524
LACU-250	5	3	1999	2059
LACU-200	6	3	2484	1733
LACU-150	7	3	2902	1370
LACU-100	8	3	3290	981
LACU-050	9	3	3718	555
LACU-000	10	3	4168	70.7

Table B.2. Experimental Data for the Pretreatment of Resin.

Pretreatment time (Hrs)	Lactulose (gm/L)
0	0
3	35.9
4	57.8
8	59.4

Table B.3. Experimental Data for Stirrer Speed Test.

Stirrer Speed	Injection #	Time (Hrs)	Lactulose
5	1	0	0
5	1	1	9.29
5	1	2	19.9
5	1	3	33.3
5	1	4	59.3
5	1	5	85.3
5	2	0	0
5	2	1	10.0
5	2	2	19.4
5	2	3	33.9
5	2	4	61.3
5	2	5	82.5
7	1	0	0
7	1	1	33.6
7	1	2	63.9
7	1	3	92.1
7	1	4	117.0

Table B.3 (Contd). Experimental Data for Stirrer Speed Test.

7	1	5	139
7	1	0	0
7	1	1	33.6
7	1	2	64.5
7	1	3	91.8
7	1	4	118
7	1	5	136

Table B.4. Experimental Data for Optimization of Resin Bead Diameter.

Injection	Resin size	Time (Hrs)	Lactulose
1	-20 +25'	0	0
1	-20 +25'	1	33.6
1	-20 +25'	2	63.9
1	-20 +25'	3	92.1
1	-20 +25'	4	117
1	-20 +25'	5	139
2	-20 +25'	0	0
2	-20 +25'	1	33.6
2	-20 +25'	2	64.5
2	-20 +25'	3	91.8
2	-20 +25'	4	118
2	-20 +25'	5	136
1	-45 +100'	0	0
1	-45 +100'	1	33.6
1	-45 +100'	2	64.1
1	-45 +100'	3	91.5
1	-45 +100'	4	113
1	-45 +100'	5	138
2	-45 +100'	0	0
2	-45 +100'	1	32.7
2	-45 +100'	2	65.5
2	-45 +100'	3	91.4
2	-45 +100'	4	113
2	-45 +100'	5	139

APPENDIX C

EXPERIMENTAL DATA OF MAIN RUNS

Table C.1. Experimental Data for Run Order 1 at pH 9, 90^0C and 0.3 Resin/Lactose Ratio.

Injection	Lactose (g/L)	Lactulose (g/L)	Conversion %
1	326	0	0
1	237	84.2	27.3
1	183	151	43.9
1	132	199	59.6
1	97.4	233	70.1
1	73.7	249	77.4
1	54.9	274	83.2
1	40.9	280	87.4
1	29.3	294	90.9
1	22.0	297	93.2
1	16.5	317	94.9
1	12.4	322	96.2
1	8.84	314	97.3
2	331	0	0
2	248	82.6	25.0
2	177	144	46.6
2	130	195	60.6
2	101	230	69.5
2	71.7	245	78.3
2	53.3	268	83.9
2	41.3	286	87.5
2	29.9	292	90.9
2	22.5	297	93.2
2	16.3	319	95.1
2	11.8	308	96.4
2	9.11	314	97.2

Table C.2. Experimental Data for Run Order 2 at pH 10, 80^0C and 0.3 Resin/Lactose Ratio.

Injection	Lactose (g/L)	Lactulose (g/L)	Conversion %
1	268	0	0
1	173	85.6	35.6
1	122	146	54.4
1	80.4	178	69.9
1	55.9	212	79.1
1	36.5	232	86.4
1	24.7	232	90.8
1	16.9	243	93.7
1	11.4	248	95.7
1	7.69	262	97.1
1	5.18	259	98.1
1	3.48	254	98.7
1	2.27	254	99.2
1	1.61	267	99.4
2	274	0	0
2	182	87.9	33.7
2	118	140	56.8
2	78.9	180	71.3
2	55.7	208	79.7
2	37.1	228	86.5
2	24.3	233	91.2
2	17.1	252	93.8
2	11.3	251	95.9
2	7.79	258	97.2
2	5.14	259	98.1
2	3.46	259	98.7
2	2.25	258	99.2
2	1.62	255	99.4

Table C.3. Experimental Data for Run Order 3 at pH 9, 70^0C and 0.3 Resin/Lactose Ratio.

Injection	Lactose (g/L)	Lactulose (g/L)	Conversion %
1	263	0	0
1	201	48.8	20.3
1	176	89.0	32.9
1	146	120	44.7
1	115	144	56.1
1	91.6	174	65.2
1	75.8	192	71.2
1	62.9	206	76.1
1	52.1	208	80.2
1	42.5	216	83.8
1	32.8	230	87.5
1	27.0	230	89.7
1	22.7	239	91.4
1	18.1	241	93.1
2	256	0	0
2	213	48.0	16.8
2	175	86.4	31.5
2	141	123	44.8
2	115	151	54.9
2	93.8	170	63.3
2	78.5	186	69.3
2	61.4	204	75.9
2	51.0	211	80.0
2	41.6	219	83.7
2	34.0	235	86.7
2	27.9	241	89.1
2	22.1	237	91.3
2	18.2	242	92.9

Table C.4. Experimental Data for Run Order 4 at pH 11, 80^0C and 0.1 Resin/Lactose Ratio.

Injection	Lactose	Lactulose	Conversion
1	270	0	0
1	197	62.2	27.1
1	153	107	43.2
1	116	149	57.2
1	91.4	170	66.1
1	68.3	198	74.7
1	52.6	216	80.5
1	40.5	222	84.9
1	29.9	235	88.9
1	22.8	247	91.6
1	17.9	251	93.4
1	13.7	246	94.9
1	10.2	255	96.2
2	267	0	0
2	201	61.5	24.9
2	158	107	40.8
2	117	142	56.3
2	91.3	169	65.8
2	68.6	189	74.3
2	50.6	211	81.0
2	40.6	227	84.8
2	30.5	237	88.6
2	22.7	240	91.5
2	18.1	239	93.2
2	13.9	254	94.8
2	10.2	255	96.2

Table C.5. Experimental Data for Run Order 5 at pH 11, 70^0C and 0.3 Resin/Lactose Ratio.

Injection	Lactose (g/L)	Lactulose (g/L)	Conversion %
1	267	0	0
1	159	106	40.5
1	96.2	169	63.9
1	56.3	206	78.9
1	33.1	235	87.6
1	19.8	245	92.6
1	12.3	258	95.4
1	7.13	258	97.3
1	4.26	254	98.4
1	2.64	257	99.0
1	1.58	268	99.4
1	0.914	259	99.7
1	0.541	256	99.8
2	272	0	0
2	159	106	41.7
2	94.9	173	65.1
2	56.2	204	79.3
2	33.3	228	87.7
2	19.9	245	92.7
2	11.7	250	95.7
2	7.32	253	97.3
2	4.23	263	98.4
2	2.53	268	99.1
2	1.55	269	99.4
2	0.913	261	99.7
2	0.545	266	99.8

Table C.6. Experimental Data for Rum Order 6 at pH 9, 80^0C and 0.1 Resin/Lactose Ratio.

Injection	Lactose (g/L)	Lactulose (g/L)	Conversion %
1	266	0	0
1	237	20.9	11.1
1	224	39.3	15.9
1	205	57.6	23.1
1	190	73.6	28.5
1	178	88.1	33.1
1	156	100	41.2
1	148	114	44.4
1	139	127	47.9
1	123	139	53.8
1	112	156	57.8
1	103	161	61.2
1	96.3	161	63.8
2	268	0	0
2	246	20.9	8.24
2	216	39.3	19.2
2	210	57.5	21.7
2	188	73.4	29.8
2	178	90.0	33.6
2	159	105	40.6
2	149	119	44.3
2	134	130	50.1
2	123	138	54.0
2	118	149	56.0
2	107	157	59.9
2	94.9	167	64.5

Table C.7. Experimental Data for Run Order 7 at pH 11, 90^0C and 0.3 Resin/Lactose Ratio.

Injection	Lactose (g/L)	Lactulose (g/L)	Conversion %
1	269	0	0
1	122	138	54.6
1	60.0	205	77.7
1	28.6	235	89.4
1	13.6	251	94.9
1	6.22	260	97.7
1	2.91	263	98.9
1	1.37	269	99.5
1	0.689	255	99.7
1	0.318	268	99.9
1	0.146	255	99.9
1	0.069	262	99.9
1	0.032	266	99.9
2	269	0	0
2	123	136	54.4
2	57.6	206	78.6
2	28.3	238	89.5
2	13.3	247	95.1
2	6.16	264	97.7
2	3.07	263	98.9
2	1.39	255	99.5
2	0.662	261	99.8
2	0.324	256	99.9
2	0.151	266	99.9
2	0.069	263	100.0
2	0.033	267	100.0

Table C.8. Experimental Data for Run Order 8 at pH 10, 70^0C and 0.5 Resin/Lactose Ratio.

Injection	Lactose (g/L)	Lactulose (g/L)	Conversion %
1	264	0	0
1	156	110	41.0
1	86.7	177	67.2
1	53.4	213	79.8
1	30.1	227	88.6
1	17.4	253	93.4
1	10.1	256	96.2
1	5.87	254	97.8
1	3.46	267	98.7
1	2.05	262	99.2
1	1.20	261	99.5
1	0.674	259	99.7
1	0.399	269	99.8
2	263	0	0
2	154	111	41.5
2	86.8	177	66.9
2	53.1	216	79.8
2	29.7	239	88.7
2	17.8	248	93.2
2	10.2	250	96.1
2	5.96	255	97.7
2	3.49	252	98.7
2	1.98	268	99.2
2	1.19	268	99.5
2	0.689	266	99.7
2	0.408	262	99.8

Table C.9. Experimental Data for Run Order 9 at pH 10, 90^0C and 0.1 Resin/Lactose Ratio.

Injection	Lactose (g/L)	Lactulose (g/L)	Conversion %
1	262	0	0
1	226	38.3	13.7
1	189	71.1	27.6
1	162	98.8	38.1
1	144	126	44.9
1	123	141	53.1
1	104	160	60.1
1	89.5	176	65.8
1	74.0	187	71.7
1	65.2	201	75.1
1	53.6	204	79.5
1	46.9	221	82.1
1	40.8	227	84.4
2	258	0	0
2	219	37.7	14.9
2	188	71.2	27.2
2	169	96.4	34.5
2	143	126	44.5
2	122	141	52.8
2	105	162	59.3
2	85.5	179	66.9
2	75.9	189	70.6
2	65.7	196	74.5
2	54.9	206	78.7
2	45.9	222	82.2
2	39.5	225	84.7

Table C.10. Experimental Data for Run Order 10 at pH 10, 90^0C and 0.5 Resin/Lactose Ratio.

Injection	Lactose (g/L)	Lactulose (g/L)	Conversion %
1	266	0	0
1	122	143	54.1
1	54.7	206	79.4
1	24.5	233	90.8
1	11.4	251	95.7
1	5.21	259	98.0
1	2.36	256	99.1
1	1.04	269	99.6
1	0.469	269	99.8
1	0.225	264	99.9
1	0.097	265	99.9
1	0.046	266	100.0
1	0.020	262	100.0
2	259	0	0
2	119	143	54.1
2	53.7	204	79.3
2	25.1	241	90.3
2	11.3	250	95.6
2	5.18	250	98.0
2	2.29	264	99.1
2	1.09	265	99.6
2	0.476	264	99.8
2	0.217	267	99.9
2	0.099	264	100.0
2	0.044	270	100.0
2	0.019	262	100.0

Table C.11. Experimental Data for Run Order 11 at pH 11, 80^0C and 0.5 Resin/Lactose Ratio.

Injection	Lactose (g/L)	Lactulose (g/L)	Conversion %
1	262	0	0
1	96.0	170	63.4
1	33.5	230	87.2
1	11.6	244	95.6
1	4.22	262	98.4
1	1.43	256	99.5
1	0.517	263	99.8
1	0.186	271	99.9
1	0.063	269	100.0
1	0.023	267	100.0
1	0.008	258	100.0
1	0.003	263	100.0
1	0.001	259	100.0
2	261	0	0
2	92.2	166	64.7
2	33.0	227	87.3
2	11.6	254	95.6
2	4.03	252	98.5
2	1.47	256	99.4
2	0.515	256	99.8
2	0.184	271	99.9
2	0.065	258	100.0
2	0.023	263	100.0
2	0.008	267	100.0
2	0.003	258	100.0
2	0.001	258	100.0

Table C.12. Experimental Data for Run Order 12 at pH 9, 80^0C and 0.5 Resin/Lactose Ratio.

Injection	Lactose (g/L)	Lactulose (g/L)	Conversion %
1	266	0	0
1	170	89.3	35.9
1	117	148	56.0
1	74.5	183	71.9
1	50.5	212	81.0
1	33.2	223	87.5
1	21.8	238	91.8
1	14.8	241	94.4
1	9.70	260	96.3
1	6.15	252	97.7
1	4.07	257	98.5
1	2.82	262	98.9
1	1.78	255	99.3
2	259	0	0
2	176	90.7	31.9
2	112	148	56.8
2	73.9	191	71.4
2	50.5	212	80.5
2	33.8	231	86.9
2	21.7	245	91.6
2	14.3	250	94.5
2	9.53	248	96.3
2	6.26	252	97.6
2	4.04	259	98.4
2	2.68	268	99.0
2	1.82	265	99.3

Table C.13. Experimental Data for Run Order 13 at pH 10, 80^0C and 0.3 Resin/Lactose Ratio.

Injection	Lactose (g/L)	Lactulose (g/L)	Conversion %
1	265	0	0
1	175	85.6	33.8
1	118	140	55.4
1	79.1	180	70.1
1	55.8	213	78.9
1	37.6	229	85.8
1	24.6	233	90.7
1	16.8	253	93.7
1	11.5	251	95.7
1	7.61	249	97.1
1	5.01	263	98.1
1	3.36	258	98.7
1	2.27	268	99.1
2	264	0	0
2	177	87.1	32.7
2	119	139	54.8
2	80.4	178	69.5
2	55.5	210	78.9
2	36.1	230	86.3
2	24.4	245	90.8
2	16.4	251	93.8
2	11.3	252	95.7
2	7.80	253	97.0
2	5.07	265	98.1
2	3.46	260	98.7
2	2.29	255	99.1

Table C.14. Experimental Data for Run Order 14 at pH 10, 70^0C and 0.1 Resin/Lactose Ratio.

Injection	Lactose (g/L)	Lactulose (g/L)	Conversion %
1	262	0	0
1	232	26.9	11.3
1	208	51.6	20.7
1	189	73.9	27.9
1	175	93.4	33.1
1	152	111	41.9
1	141	123	46.1
1	124	136	52.8
1	110	155	58.2
1	99.6	167	61.9
1	90.2	175	65.6
1	80.7	187	69.2
1	72.4	187	72.3
2	265	0	0
2	238	27.4	10.5
2	215	51.7	18.9
2	187	70.7	29.4
2	170	89.8	35.8
2	157	112	40.9
2	137	126	48.5
2	123	138	53.8
2	110	151	58.4
2	100.0	164	62.2
2	87.5	171	67.0
2	82.4	184	68.9
2	70.0	190	73.6

Table C.15. Experimental Data for Run Order 15 at pH 10, 80^0C and 0.3 Resin/Lactose Ratio.

Injection	Lactose (g/L)	Lactulose (g/L)	Conversion %
1	265	0	0
1	181	85.6	31.7
1	123	143	53.5
1	82.1	183	69.0
1	53.5	201	79.8
1	37.6	226	85.8
1	24.4	240	90.8
1	17.2	246	93.5
1	11.1	258	95.8
1	7.78	259	97.1
1	5.23	259	98.0
1	3.48	260	98.7
1	2.36	254	99.1
2	272	0	0
2	173	87.4	36.3
2	122	143	55.0
2	81.2	181	70.2
2	54.6	205	79.9
2	37.6	227	86.2
2	25.2	240	90.7
2	17.1	246	93.7
2	11.1	246	95.9
2	7.83	249	97.1
2	5.04	252	98.1
2	3.41	252.	98.7
2	2.37	266	99.1

APPENDIX D

MATLAB CODE OF SURFACE PLOT

```
clear all; close all; clc;

X_2=-1:(2)/50:1;

X_3=-1:(2)/50:1;

T=[-1,0,1];

k=1;

while (k<4)

for i=1:51

for j=1:51

Conversion(i,j) = 93.69+17.86*X_2(i)+3.56*T(k)+9.91*X_3(j)-8.77*X_2(i)*X_3(j)-
11.81*X_2(i)^2;

 if Conversion(i,j)<=100

Conv(i,j)=Conversion(i,j);

end

end

end

X2=0.1:(0.5-0.1)/50:0.5;

X3=9:2/50:11;

figure();

surface(X2,X3,Conversion)

k=k+1;

xlabel('pH','fontsize',10);

ylabel('resin/lactose','fontsize',10);

zlabel('conversion %','fontsize',10);

end
```

BIBLIOGRAPHY

Ahren, B., Havel, P. J., Pacini, G., & Cianflone, K. (2003). Acylation Stimulating Protein Stimulates Insulin Secretion. International Journal of Obesity , 27, 1037–1043.

Alan, B. B., & Charles, R. L. (2008). Protein Research Progress. Nova Science Publishers.

Carberry, J. J. (1976). Chemical and Catalytic Reaction Engineering. McGraw-Hill.

Carobbi, R., & Innocenti, F. (1990). Patent No. 0320670. European.

Carobbi, R., Miletti, S., & Franci, V. (1985). Patent No. 4536221. US.

Carubelli, R. (1970). Patent No. 3505309. US.

Dauglas, E. C., Christopher, W. F., & Mikhail, A. S. (2001). Lactose Processing Technology – Creating New Utilization Opportunities. 38th Annual Marschall Cheese Seminar, “Tools of the Trade".

De la Fuente, M. A., Juarez, M., De Rafael, D., Villamiel, M., & Olano, A. (1999). Isomerisation of Lactose Catalysed by Alkaline-Substituted Sepiolites. Food Chemistry , 66, 301-306.

Dendene, K., Guihard, L., Nicholas, S., & Bariou, B. (1994). Kinetics of Lactose Isomerization to Lactulose in Alkaline-Medium. Journal of Chemical Technology and Biotechnology , 61, 37-42.

Deya, E., & Takahashi, K. (1991). Patent No. 5034064. USA.

Dmitry Yu, M. (2005). On Surface Heterogeneity and Catalytic Kinetics. Industrial & Engineering Chemistry Research , 44, 1688-1697.

Fogler, S. H. (2001). Elements of Chemical Reaction Engineering (Second ed.). Prentice-Hall.

Guth, J. H., Prospect, M., & Tumerman, L. (1970). Patent No. 3546206. US.

Hicks, K. B. (1981). Patent No. 4273922. US.

Kozempel, M., & Kurantz, M. (1994). The Isomerisation Kinetics of Lactose to Lactulose in the Presence of Borate. Journal of ChemicalTechnology and Biotechnology , 54, 25–29.

Kozempel, M., McAloon, A., & Roth, L. (1997). Simulated Scale-up and Cost Estimate of a Process for Alkaline Isomerisation of Lactose to Lactulose using Boric Acid as Complexation. Journal of Chemical Technology and Biotechnology , 68, 229–235.

Krumbbolz, R. E., & Dorscheid, M. G. (1991). Patent No. 0375040. European.

Lodygin, S. V., Evdokimov, I. A., Ryabtseva, S. A., Abakumov, N. N., & Lodigina, S. V. (2005). Optimization of Parameters for Anion-Exchange Treatment of Whey. Proceedings of the NCSTU.

Malinda, G. (2010, May). *Cheese Industry Profile*. Retrieved from Agricultural Marketing Resource Center: http://www.agmrc.org/commodities__products/livestock/dairy/cheese_industry_profile.cfm

Mendicino, J. F. (1960). Effect of Borate on the Alkali-Catalyzed Isomerisation of Sugars. Journal of the American Chemical Society , 20, 4975–4979.

Mohammed, A., & Damien, d. H. (2007). Isomerization of Lactose and Lactulose Production: Review. Trends in Food Science & Technology , 18, 356-364.

Montgomery, E. M., & Hudson. (1930). Relation Between Rotary Power and Structure in the Sugar Group.XXVII. Synthesis of a New Disaccharide Ketose (Lactulose) from Lactose. Journal of America Chemical Society , 52, 2101-2106.

Nagasawa, T., Tomita, M., Tamura, Y., Obayashi, T., & Mizota, T. (1974). Patent No. 3814174. US.

Parrish, F. W. (1970). Patent No. 3514327. US.

Pluim, H., & De Haar, H. W. (1991). Patent No. 0339749. European.

Schumann, C. (2004). Medical, Nutritional and Technological Properties of Lactulose: An Update. European Journal of Nutrition , 41, 1436-6215.

Seungman, S., & Dongsu, K. (2005). Modification of Langmuir Isotherm in Solution Systems-Definition and Utilization of Concentration Dependent Factor. Chemosphere , 58, 115-123.

Shukula, R., Verykios, X. E., & Mutharasan, R. (1985). Isomerisation and Hydrolysis Reactions of Important Disaccharides over Inorganic Heterogeneous Catalyst. Carbohydrate Research , 143, 97-106.

Tapio, S., Esko, T., Juha, L., Erkki, P., & Daniel, V. (2003). Modeling of Complex Organic Solid-Liquid Reaction Systems in Stirred Tanks. Industrial & Engineering Chemistry Research , 42, 2516-2524.

Tatdao, P., Darryl, M. S., & Frank, S. (2008). Lactulose Production from Milk Concentration Permeate using Calicium Carbonate-Based Catalysts. Food Chemistry , 111, 283-290.

Troyano, E., de Rafael, D., Martinez-Castro, I., & Olano, A. (1996). Isomerisation of Lactose over Natural Sepiolite. Journal of Chemical Technology and Biotechnology , 65, 111–114.

Tumerman, L., & Guth, H. (1974). Patent No. *3822249*. US.

Villamiel, M., Corzo, N., Foda, M. I., Montes, F., & Olano, A. (2002). Lactulose Formation Catalysed by Alkaline-Substituted Sepiolites in Milk Permeate. Food Chemistry , 76, 7-11.

Zokaee, F., Kaghazchi, T., Soleimani, M., & Zare, A. (2002b). Isomerisation of Lactose to Lactulose – Study and Comparison. Process Biochemistry , *37*, 629–635.

Zokaee, F., Kaghazchi, T., Soleimani, M., & Zare, A. (2002a). Isomerisation of Lactose to Lactulose Using Sweet Cheese Whey Ultrafiltrate. Journal of the Chinese Institute of Chemical Engineers , *37*, 307–313.

VITA

Arvind Nanduri was born in Andhra Pradesh, India, on June 30, 1986. In May 2007, He received his B.Tech in Chemical Engineering from Jawaharlal Nehru Technological University, Hyderabad, India. In December 2010, he received his M.S degree in Chemical Engineering from Missouri University of Science and Technology, Rolla, Missouri, USA. In 2007, along with another colleague, he won the best project in the state at Shri Ramananda Institute of Science and Technology, India, for an innovative chemical waste treatment method using aerobic and an-aerobic treatments with dung and dry molasses cake.